Award Number: W81XWH-13-1-0016

TITLE: Underbody Blast Models of TBI Caused by Hyper- Acceleration and Secondary Head Impact

PRINCIPAL INVESTIGATOR: Dr. Gary Fiskum

CONTRACTING ORGANIZATION: University of Maryland
Baltimore, MD 21201

REPORT DATE: October 2017

TYPE OF REPORT: Final

PREPARED FOR: U.S. Army Medical Research and Materiel Command
Fort Detrick, Maryland 21702-5012

REPORT DOCUMENTATION PAGE

Form Approved
OMB No. 0704-0188

1. REPORT DATE October 2017

2. REPORT TYPE
Final

3. DATES COVERED
6Jan2013 - 5Jul2017

4. TITLE AND SUBTITLE
Underbody Blast Models of TBI Caused by Hyperacceleration and Secondary Head Impact

5a. CONTRACT NUMBER

5b. GRANT NUMBER
W81XWH-13-1-0016

5c. PROGRAM ELEMENT NUMBER

6. AUTHOR(S)
Gary Fiskum, PhD and William Fourney, PhD

E-Mail:gfiskum@anes.umm.edu and four@umd.edu

5d. PROJECT NUMBER

5e. TASK NUMBER

5f. WORK UNIT NUMBER

7. PERFORMING ORGANIZATION NAME(S) AND ADDRESS(ES)
University of Maryland, School of Medicine
220 Arch St RM 02148
Baltimore MD 21201-1531

8. PERFORMING ORGANIZATION REPORT NUMBER

9. SPONSORING / MONITORING AGENCY NAME(S) AND ADDRESS(ES)

U.S. Army Medical Research and Materiel Command
Fort Detrick, Maryland 21702-5012

10. SPONSOR/MONITOR'S ACRONYM(S)

11. SPONSOR/MONITOR'S REPORT NUMBER(S)

12. DISTRIBUTION / AVAILABILITY STATEMENT

Approved for Public Release; Distribution Unlimited

13. SUPPLEMENTARY NOTES

14. ABSTRACT

Most research on blast-induced traumatic brain injury (TBI) has focused on blast overpressure, as experienced by unmounted warfighters. We focused our efforts on an animal model of TBI caused by under-vehicle (underbody) blasts, relevant to injuries inflicted on occupants of vehicles targeted by IEDs. Our research was based on the central hypothesis that underbody blast induced acceleration alone, in the absence of exposure to significant ambient pressure changes, can cause brain injury at survivable G-forces relevant to those experienced by occupants of IED-targeted vehicles. Collaboration between the University of Maryland Schools of Engineering and Medicine has confirmed this hypothesis. Moreover, we described in detail the pathophysiology of underbody blast TBI, thus identifying targets for neuroprotection. Most importantly, we developed completely new military vehicle designs that dramatically reduce the acceleration (G force) experienced by the rats used as vehicle occupants in our small scale explosion experiments. The reduction in G force results in equally impressive reduction in mortality and protection against TBI. If these results are validated with full scale under-vehicle blast experiments, they may lead to the next generation of armor-protected military vehicles that will save lives and reduce traumatic injuries.

15. SUBJECT TERMS
blast, acceleration, traumatic brain injury, neuronal death, synapse, brain blood vessels, axon damage, inflammation, anxiety, vestibulomotor activity, improved vehicle design

16. SECURITY CLASSIFICATION OF:			17. LIMITATION OF ABSTRACT	18. NUMBER OF PAGES	19a. NAME OF RESPONSIBLE PERSON
a. REPORT	b. ABSTRACT	c. THIS PAGE			USAMRMC
Unclassified	Unclassified	Unclassified	Unclassified	93	19b. TELEPHONE NUMBER *(include area code)*

Standard Form 298 (Rev. 8-98)
Prescribed by ANSI Std. Z39.18

TABLE OF CONTENTS **PAGE**

1. **INTRODUCTION:** Narrative that briefly (one paragraph) describes the subject, purpose and scope of the research.

Approximately 25% of all combat casualties in recent US military conflicts have been caused by traumatic brain injury (TBI), with most of these head injuries caused by explosive munitions such as bombs, land mines, improvised explosive devices and missiles. The majority of experimental data from animal research on blast TBI has focused on blast overpressure. We focused our efforts on a model of TBI caused by under-vehicle (underbody) blasts, relevant to injuries inflicted on occupants of vehicles targeted by IEDs. Our research was based on the central hypothesis that underbody blast induced acceleration alone, in the absence of exposure to significant ambient pressure changes, can cause brain injury at survivable G-forces relevant to those experienced by occupants of IED-targeted vehicles. The collaborative efforts of Dr. William Fourney, Director of the Dynamic Effects Laboratory at University of Maryland School of Engineering, and Dr. Fiskum and Gullapalli from the School of Medicine have confirmed this hypothesis. Moreover, we have described in detail the pathophysiology of underbody blast TBI, thus identifying targets for neuroprotection. Most importantly, we have developed completely new military vehicle designs that dramatically reduce the acceleration (G force) experienced by the rats used as vehicle occupants in our small scale explosion experiments. The reduction in G force results in equally impressive reduction in mortality and protection against TBI.

2. **KEYWORDS:** Provide a brief list of keywords (limit to 20 words).

Warfighter, blast, acceleration, JERK, impact, elastomer, polyurea, neuronal death, synapse, cerebrovasculature, axon, inflammation, behavior, anxiety, memory, vestibulomotor activity

3. **ACCOMPLISHMENTS:** The PI is reminded that the recipient organization is required to obtain prior written approval from the awarding agency grants official whenever there are significant changes in the project or its direction.

1. Establish dose-dependent relationships between G-force/JERK, neuronal/axonal injury, neurochemical alterations, and inflammation in different brain regions at different times after the underbody blast in the absence and presence of secondary head impact. *24 months - completed*

2. Eludicate the neurobehavioral alterations that occur after underbody blasts and establish their temporal relationships with the nature and extent of neuropathology present in different brain regions. *36 months - completed*

3. Determine if alterations in vehicle hull design, particularly those that reduce both maximal G-force and JERK, reduce histologic, neurochemical, or behavioral indices of brain injury. *44 months – completed at 48 months with no cost extension*

What was accomplished under these goals?

A. Major activities: All small scale under-vehicle blast experiments were conducted at the University of Maryland School of Medicine. A large number of outcome measures were used to rigorously test the hypothesis that exposure to blast-induced acceleration alone, in the absence of significant exposure to blast overpressure, results in dose dependent TBI. These measures were performed as early as an hour after and as late as 30 days after blast exposure and included brain histology, brain magnetic resonance imaging (MRI) and magnetic resonance spectroscopy (MRS), and neurochemical measurements of changes in brain protein levels. All development of vehicle frame designs and tests conducted in the absence of animals were performed at the University of Maryland School of Engineering. Drs. Fourney and Leiste drove the 2 hr round-trip from College Park to Baltimore MD each time we conducted a test with animals. They typically transported the explosives, the detonation equipment, and the blast G force mitigation devices during each of these trips, which averaged 25/year for 4 years.

B. Specific objectives:

1. Establish dose-dependent relationships between G-force/JERK, neuronal/axonal injury, neurochemical alterations, and inflammation in different brain regions at different times after the underbody blast in the absence and presence of secondary head impact.
2. Eludicate the neurobehavioral alterations that occur after underbody blasts and establish their temporal relationships with the nature and extent of neuropathology present in different brain regions.
3. Determine if alterations in vehicle hull design, particularly those that reduce both maximal G-force and JERK, reduce histologic, neurochemical, or behavioral indices of brain injury.

C. Major Findings and Conclusions:

1. Development of the under-vehicle blast model and demonstration of TBI at low G forces (Objectives 1 and 2).

   Exposure of rats to underbody blast-induced accelerations at either 20 G or 50 G resulted in histopathologic evidence of diffuse axonal injury and astrocyte activation but no significant neuronal death (Appendix 1 Fig 2,3,4). The significance of these results is that they demonstrate that blast-induced vertical acceleration alone, in the absence of exposure to significant blast pressures, causes mild TBI. This unique animal model of TBI caused by underbody blasts may therefore be useful in understanding the pathophysiology of blast-induced mild TBI and for testing medical and engineering-based approaches toward mitigation. (Proctor et al., 2014; See Appendix 1)

2. Quantitative evidence for axonal injury and behavioral deficit using the under-vehicle blast TBI model. Both outcome measures are worsened by exposure of rats to hypobaria and hyperoxia simulating aeromedical evacuation (Objective 1).

   Exposure of rats to blast-induced acceleration of 100G increased cerebral axonal injury, which was significantly exacerbated by exposure to aeromedical evacuation-relevant hypobaria as early as 6 hours and as late as 6 days post-blas (Appendix 2, Fig 3). Rats exposed to underbody blasts and then to hypobaria under 100% O_2 exhibited increased axonal damage and impaired motor function compared to those subjected to blast and hypobaria under 21% O_2 (Appendix 2, Fig. 5 and 6). These findings raise concern about the effects of AE-related hypobaria on TBI victims, the timing of AE after TBI, and whether these effects can be mitigated by supplemental oxygen. (Proctor et al., 2017; See Appendix 2)

3. Effects of high blast-induced accelerations (1200 to 2800G) on neuronal cell death, neuro-inflammation, behavioral deficits and mortality (Objectives 1 and 2).

   Adult male rats were subjected to this range of accelerations, in the absence of exposure to blast overpressure, were evaluated over 28 days for working memory (Ymaze) and anxiety (elevated plus maze). In addition, brains obtained from rats at one and seven days post-injury were used for neuropathology and neurochemical assays. Sixty seven percent of rats died soon after being subjected to blasts resulting in 2800G acceleration. All rats exposed to 2400G acceleration survived and exhibited transient deficits in working memory and long-term anxiety like behaviors, while those exposed to 1200 acceleration G force only demonstrated increased anxiety (Appendix 4, Fig 2). Behavioral deficits were associated with acute microglia/macrophage activation, increased hippocampal neuronal death, and reduced levels of tight junction- and synapse- associated proteins (Appendix 4, Fig. 8). Taken together, these results suggest that exposure of rats to high underbody blast-induced G forces results in neurologic injury accompanied by neuronal apoptosis, neuroinflammation (Appendix 4, Figs. 3,6,7) and evidence for neurosynaptic alterations. (Tchantchou et al., 2017a; See Appendix 4)

4. Effects of under-vehicle blast-induced acceleration of 1700G on the biochemical and microstructural changes in the brain using diffusion tensor imaging (DTI) and magnetic resonance spectroscopy (MRS).

   Two groups of male rats were subjected to a sham procedure and under-vehicle blast, respectively. Axonal and neurochemical alterations were assessed using in vivo DTI and MRS at 2 h, 24 h, and 7 days after blast. Significant reductions in mean diffusivity, axial diffusivity, and radial diffusivity were observed in the hippocampus, thalamus, internal capsule, and corpus callosum as early as 2 h, and sustained up to 7 days post-blast (Appendix 3, Fig. 4). Total creatine and glutamine were reduced in the internal capsule at 24 h post-blast (Appendix 3, Fig. 5). The reductions in DTI parameters, creatine and glutamine in vivo suggest potential activation of astrocytes and diffuse axonal injury following a single under-vehicle blast, confirming previous histology reports. (Tang et al., 2017; See Appendix 3)

5. This study tested the hypothesis that the neuropathology and altered behavior that follow under-vehicle blast exposure are mitigated by vehicle frame designs that dramatically reduce blast-induced acceleration.

   Male rats were restrained on an aluminum platform that was accelerated vertically at up to 2850G, in response to detonation of an explosive positioned under a second platform in contact with the top via different structures. The presence of elastomeric, polyurea-coated aluminum cylinders between the platforms reduced acceleration by 80% to 550G compared to 2350G with uncoated cylinders. Moreover, 67% of rats exposed to 2850G, and 20% of those exposed to 2350G died immediately after blast, whereas all rats subjected to 550G-blast survived (Appendix 5, Table 1). Assays for working memory (Y maze) and anxiety (Plus maze) were conducted for up to 28 days. Rats were euthanized at 24 h or 29 days and their brains used for histopathology and neurochemical measurements. Rats exposed to 2350G-blasts exhibited increased cleaved caspase-3 immunoreactive neurons in the hippocampus. There was also increased vascular IgG effusion and F4/80 immunopositive macrophages/microglia. Blast exposure reduced hippocampal levels of synaptic proteins bassoon and homer-1, which were associated with impaired performance in the Y maze and the Plus maze tests. These changes observed after 2350G-blasts were reduced or eliminated with the use of polyurea coated cylinders Appendix 5, Figs. 2-9)

(Tchantchou et al., 2017b; See Appendix 5) Such advances in vehicle designs should aid in the development of the next generation of blast-resistant vehicles.

6. Mitigation of under-vehicle blast-induced traumatic injuries and death by advances in military vehicle designs

   As described under section 5 above, a major goal of our project was to develop military vehicle designs that mitigate the transduction of acceleration energy from the bottom of the vehicle to the passengers. While we have been very successful toward reaching this goal, there is still considerably additional testing that is necessary before these vehicle designs can be safely used. As described in the Appendix, in addition to reducing the maximum G force, we aim to increase the time taken to reach the maximum force, which is equivalent to decreasing JERK, defined as the first derivative of acceleration, or the second derivative of velocity. Our approaches toward these goals include the use of elastomeric polymers, e.g., polyurea, on the surface and within the core of aluminum cylinders located between the bottom and top frames of a vehicle. These structures allow for transient compression of the cylinders which dramatically reduces JERK experienced by the occupants and increases the possibility that the vehicle can continue to be functional following the blast. Any design that increases the height and therefore the center of gravity of the vehicle can potentially increase the risk of roll-overs. We are therefore working on elastomeric frame designs that will limit the increase in the height of the vehicle by a few inches, as described in Appendix 6.

7. Evidence that mortality is greater when rats are subjected to head impact following under-vehicle blast-induced acceleration compared to blast exposure alone.

   We performed a limited number of experiments (n=4-12 per group) comparing anxiety-like behavior and working memory for rats subjected to high G-force (2400G) underbody blast alone to that of rats exposed to 2400G acceleration followed immediately by the projectile concussive impact (PCI) model of closed head TBI developed by Dr. Frank Tortella. We did not observe any differences between the results obtained from the “one hit” and the “two hit” models using the elevated plus maze (anxiety) and working memory (Y maze) (See Appendix 7). We did, however, observe a 50% immediate mortality for rats exposed to the under-vehicle blast plus projectile concussive impact compared to no morality for rats exposed to blast-TBI alone. This more complex but very military relevant should be used further in the future to determine the cause of morality.

What opportunities for training and professional development has the project provided?

Dr. Flaubert Tchantchou was a postdoctoral fellow who worked part-time on this project for approximately 2 yr. During this period, his professional development flourished, as evidenced by the following publication which he authored: Tchantchou F, et al., Neuropathology and neurobehavioral alterations in a rat model of traumatic brain injury to occupants of vehicles targeted by underbody blasts. Exp Neurol. 2017, 289:9-20. He was then promoted to the faculty position of Research Associate and published the following article Tchantchou F, et al., Rat Model of Brain Injury to Occupants of Vehicles Targeted by Land Mines: Mitigation by Elastomeric Frame Designs. J Neurotrauma. 2017 Epub Nov 29.

How were the results disseminated to communities of interest?

The following invited oral presentations included results obtained from this project:

1. Military Health System Research Symposium, Ft. Lauderdale, FL (08/13) "Hypobaria Worsens Axonal Injury and Blood Brain Barrier Disruption Induced by Underbody Blast-Induced Hyperacceleration"
2. Fort Detrick US Army Medical Command (11/14) "Traumatic Brain Injury Caused by Underbody Blast"
3. International Anesthesiology Education and Research (IARS) society meeting, San Francisco, CA (05/16) "Translational Research in Traumatic Brain Injury: The Basic Scientist's Perspective"
4. Johns Hopkins University School of Medicine Department of Biological Chemistry (10/16) "Translational Research in Ischemic and Traumatic Brain Injury: The Basic Scientist's Perspective"
5. Aerospace Medical Association (AsMA) meeting, Denver, CO (05/17) "Aeromedical Evacuation-Relevant Hypobaria Worsens Traumatic Brain Injury Caused by Impact or Under-Vehicle Blast"
6. Military Health Services Research Symposium, Orlando, FL. (08/17) "TBI neuropathology and behavioral deficits in a rat model of brain injury to occupants of vehicles targeted by land mines: Mitigation by shock-absorbing hull designs"

What do you plan to do during the next reporting period to accomplish the goals?

Nothing to report since the project finished as of 07/05/17

4. IMPACT: Describe distinctive contributions, major accomplishments, innovations, successes, or any change in practice or behavior that has come about as a result of the project relative to:

What was the impact on the development of the principal discipline(s) of the project?

The results we obtained with the under-vehicle blast TBI model provide new and detailed insight into the causes of TBI experienced by occupants of vehicles targeted by land mines. Identification of these causes may lead to pharmacologic therapy specifically directed to victims of blast TBI who were in vehicles when the blast occurred.
Our demonstration that the blast force transmitted to occupants of vehicles targeted by land mines can be reduced by approximately 80% through the use of new, advanced vehicle frame designs may very well lead to the next generation of US military vehicles that better protect against trauma of all kinds, including traumatic brain injury.

What was the impact on other disciplines?

The devices we have developed the mitigate the G force transmitted to occupants in vehicles could be used in other ways, including improved automobile bumpers and more effective helmets for warfighters and athletes, e.g., football players.

What was the impact on technology transfer?

One intellectual property disclosure was filed at the University of Maryland College Park and is still active.

What was the impact on society beyond science and technology?

Nothing to report.

5. **CHANGES/PROBLEMS:** The PD/PI is reminded that the recipient organization is required to obtain prior written approval from the awarding agency grants official whenever there are significant changes in the project or its direction. If not previously reported in writing, provide the following additional information or state, "Nothing to Report," if applicable:

Changes in approach and reasons for change

There were no major changes in the experimental design. We submitted several animal use amendments related primarily to the G force levels used in the experiments. We also were approved to use fully conscious rats in the high G force blast experiments, which enhanced the relevance of our models to real combat zone scenarios.

Actual or anticipated problems or delays and actions or plans to resolve them

A postdoctoral fellow who worked on this project left on maternity leave for 3 months, returned for work for a few months, and then resigned to be a full-time mother. It then took several months to recruit a replacement, Dr. Tchantchou, who was very successful and more than made up for lost time. A one year no-cost extension was granted that enabled us to finish the project and publish several very important manuscripts.

Changes that had a significant impact on expenditures

No significant changes

Significant changes in use or care of human subjects, vertebrate animals, biohazards, and/or select agents

Significant changes in use or care of human subjects

Not applicable

Significant changes in use or care of vertebrate animals

Approximately 8 amendments were approved by both the Univ Maryland Sch Medicine and the US Army ACURO. The most significant of these was to test for the effects of blast-induced high G force on rats that were fully conscious during the blast. Unlike the earlier experiments where the rats were anesthetized with ketamine before, during and for an hour after the blast, the amended protocol used isoflurane to anesthetized the rats for 5 min prior to their placement in the restraints secured to the top of the model vehicle. At 5 min after the anesthesia was discontinued when the rats were fully conscious the explosive was detonated under the vehicle, resulting in a vertical acceleration of the rats ranging from 700 to 2500G.

Significant changes in use of biohazards and/or select agents

None

6. PRODUCTS: List any products resulting from the project during the reporting period. If there is nothing to report under a particular item, state "Nothing to Report."

- **Publications, conference papers, and presentations**
  Report only the major publication(s) resulting from the work under this award.

All of the following publications were peer-reviewed and are either in print or have been electronically published. All acknowledge support from this grant. Each of these are included in the Appendix.

1. Proctor JL, Fourney WL, Leiste UH, Fiskum G. Rat model of brain injury caused by under-vehicle blast-induced hyperacceleration. J Trauma Acute Care Surg. 2014 Sep;77(3 Suppl 2):S83-7. PMID: 25159367.
2. Tchantchou F, Fourney WL, Leiste UH, Vaughan J, Rangghran P, Puche A, Fiskum G. Neuropathology and neurobehavioral alterations in a rat model of traumatic brain injury to occupants of vehicles targeted by underbody blasts. Exp Neurol. 2017 Mar;289:9-20. PMID: 27923561.
3. Tang S, Xu S, Fourney WL, Leiste UH, Proctor JL, Fiskum G, Gullapalli RP. Central Nervous System Changes Induced by Underbody Blast-Induced Hyperacceleration: An in Vivo Diffusion Tensor Imaging and Magnetic Resonance Spectroscopy Study. J Neurotrauma. 2017 Jun 1;34(11):1972-1980. PMID: 28322622.
4. Proctor JL, Mello KT, Fang R, Puche AC, Rosenthal RE, Fourney WL, Leiste UH, Fiskum G. Aeromedical evacuation-relevant hypobaria worsens axonal and neurologic injury in rats after underbody blast-induced hyperacceleration. J Trauma Acute Care Surg. 2017 Jul;83(1 Suppl 1):S35-S42. PMID: 28452879.
5. Tchantchou F, Puche AC, Leiste U, Fourney W, Blanpied TA, Fiskum G. Rat Model of Brain Injury to Occupants of Vehicles Targeted by Land Mines: Mitigation by Elastomeric Frame Designs. J Neurotrauma. 2017 Epub Nov 29. PMID: 29187028.

Books or other non-periodical, one-time publications.

None

Other publications, conference papers and presentations (within last year).

Aerospace Medical Association (AsMA) meeting, Denver, CO (05/17) "Aeromedical Evacuation-Relevant Hypobaria Worsens Traumatic Brain Injury Caused by Impact or Under-Vehicle Blast" *

Military Health Services Research Symposium (MHSRS), Orlando, FL. (08/17) "TBI neuropathology and behavioral deficits in a rat model of brain injury to occupants of vehicles targeted by land mines: Mitigation by shock-absorbing hull designs" *

Association of Military Surgeons of the United States (AMSUS) meeting, Washington DC (11/17) "CSTARS Baltimore research on aeromedical evacuation-relevant hypobaria, traumatic brain injury, hemorrhagic shock, and sepsis *

Website(s) or other Internet site(s)

None

Technologies or techniques

The technology that resulted from this research is the devices that when incorporated into the frame of military vehicles can dramatically reduce the transduction of acceleration G force from an under-vehicle blast to occupants within the vehicles.

Inventions, patent applications, and/or licenses

Intellectual property disclosure
PS-2016-098/Energy Absorbing Devices for Highly Dynamic Loading

7. PARTICIPANTS & OTHER COLLABORATING ORGANIZATIONS

What individuals have worked on the project?

Name: Gary Fiskum
Project Role: PI
Researcher Identifier: Univ. of Maryland School of Medicine
Nearest person month worked: 1.8
Contribution to Project: Dr. Fiskum was the PI and oversaw all aspects of experimental design, data analysis, personnel management, progress reports, animal use protocols, peer-reviewed manuscripts, abstracts, and presentation at scientific meetings.
Funding Support: This project

Name: Flaubert Tchantchou
Project Role: Coinvestigator
Researcher Identifier: University of Maryland School of Medicine
Nearest person month worked: 8.0
Contribution to Project: Dr. Tchantchou worked first as a postdoctoral fellow and then as a Research Associate on this project. He performed most of the histologic, biochemical, and behavioral measurements. He is also the primary author on two of the manuscripts published on this research.
Funding Support: This project

Name: William Fourney and Ulrich Leist
Project Role: Subcontractors
Researcher Identifier: University of Maryland College Park
Nearest person month worked: 1.0 each
Contribution to Project: Drs. Fourney and Leist were subcontracted to conduct the blast tests both at UMSOM and UMCP and to develop vehicle frame devices that mitigate the force of under-vehicle blasts transmitted to the occupants of vehicles targeted by these blasts.
Funding Support: This project

Has there been a change in the active other support of the PD/PI(s) or senior/key personnel since the last reporting period?

Nothing to report

What other organizations were involved as partners?

Provide the following information for each partnership:
Organization Name: University of Maryland College Park
Location of Organization: (if foreign location list country)
Partner's contribution to the project (identify one or more)

- *Financial support;*$100,000 per year for 4 yr
- *In-kind support;* None
- *Facilities:* Blast lab at UMCP used to develop blast mitigation devices.
- *Collaboration (e.g., partner's staff work with project staff on the project);* Contributors to all blast experiments and coauthors on all published manuscripts.
- *Personnel exchanges;* Drs. Fourney and Leist traveled to and from UMSOM approximately 25 times per year to conduct blast TBI animal experiments.

8. SPECIAL REPORTING REQUIREMENTS

COLLABORATIVE AWARDS: For collaborative awards, independent reports are required from BOTH the Initiating Principal Investigator (PI) and the Collaborating/Partnering PI. A duplicative report is acceptable; however, tasks shall be clearly marked with the responsible PI and research site. A report shall be submitted to **https://ers.amedd.army.mil** for each unique award.

QUAD CHARTS: If applicable, the Quad Chart (available on https://www.usamraa.army.mil) should be updated and submitted with attachments.

See Appendix

9. APPENDICES: Attach all appendices that contain information that supplements, clarifies or supports the text. Examples include original copies of journal articles, reprints of manuscripts and abstracts, a curriculum vitae, patent applications, study questionnaires, and surveys, etc.

See the following Appendix

APPENDIX 1

Proctor JL, Fourney WL, Leiste UH, Fiskum G. Rat model of brain injury caused by under-vehicle blast-induced hyperacceleration. J Trauma Acute Care Surg. 2014 Sep;77(3 Suppl 2):S83-7. PMID: 25159367.

Rat model of brain injury caused by under-vehicle blast-induced hyperacceleration

Julie L. Proctor, MS, William L. Fourney, PhD, Ulrich H. Leiste, PhD, *and* **Gary Fiskum, PhD,** *Baltimore, Maryland*

BACKGROUND: More than 300,000 US war fighters in Operations Iraqi and Enduring Freedom have sustained some form of traumatic brain injury (TBI), caused primarily by exposure to blasts. Many victims are occupants in vehicles that are targets of improvised explosive devices. These underbody blasts expose the occupants to vertical acceleration that can range from several to more than 1,000 G; however, it is unknown if blast-induced acceleration alone, in the absence of exposure to blast waves and in the absence of secondary impacts, can cause even mild TBI.

METHODS: We approached this knowledge gap using rats secured to a metal platform that is accelerated vertically at either 20 G or 50 G in response to detonation of a small explosive (pentaerythritol tetranitrate) located at precise underbody standoff distances. All rats survived the blasts and were perfusion fixed for brain histology at 4 hours to 30 days later.

RESULTS: Robust silver staining indicative of axonal injury was apparent throughout the internal capsule, corpus callosum, and cerebellum within 24 hours after blast exposure and was sustained for at least 7 days. Astrocyte activation, as measured morphologically with brains immunostained for glial fibrillary acidic protein, was also apparent early after the blast and persisted for at least 30 days.

CONCLUSION: Exposure of rats to underbody blast-induced accelerations at either 20 G or 50 G results in histopathologic evidence of diffuse axonal injury and astrocyte activation but no significant neuronal death. The significance of these results is that they demonstrate that blast-induced vertical acceleration alone, in the absence of exposure to significant blast pressures, causes mild TBI. This unique animal model of TBI caused by underbody blasts may therefore be useful in understanding the pathophysiology of blast-induced mild TBI and for testing medical and engineering-based approaches toward mitigation. (*J Trauma Acute Care Surg*. 2014;77: S83–S87. Copyright © 2014 by Lippincott Williams & Wilkins)

KEY WORDS: Axonal injury; astrocyte; inflammation; internal capsule; cerebellum.

Approximately 25% of all US combat casualties in Operation Iraqi Freedom and Operation Enduring Freedom have been caused by traumatic brain injury (TBI), with most of these injuries caused by explosive munitions such as bombs, land mines, improvised explosive devices (IEDs), and missiles.[1,2] Little is known regarding the pathophysiology of "blast TBI." The majority of animal research on blast TBI has focused on one aspect of these explosions, the blast overpressure.[3–6] Most of these studies use a model in which a gas-driven pressure wave was delivered via a long shock tube, directly to the immobilized animal's head or body. A multitude of physical forces may play a role in blast TBI, including blast overpressure, thermal and chemical components, shockwave, and hyperacceleration of the brain. We hypothesize that this extreme hyperacceleration, with subsequent rapid deceleration, is responsible for many aspects of blast TBI.

Acceleration may be particularly important for the large number of soldiers and others injured while being occupants of armored vehicles targeted by IEDs. Such explosions result in a very short but very intense acceleration of the vehicle and its occupants. The Dynamic Effects Laboratory at the University of Maryland School of Engineering has used small-scale testing to evaluate the loads applied to personnel carriers when a buried explosive detonates beneath them.[7,8] Adaptation and scaling of this model to allow animal injury in a similar explosive environment could provide a completely new, clinically relevant model of blast TBI that encompasses many of the physical forces including the extreme hyperacceleration. As a first step toward this goal, this study tested the hypothesis that relatively low underbody blast-induced accelerations of 20 G and 50 G result in histologic evidence for mild TBI in the absence of obvious injury to other vital organs.

MATERIALS AND METHODS

Underbody Blast-Induced Hyperacceleration

The device used to induce underbody blast-induced acceleration consists of an aluminum water tank 3 ft long × 2 ft wide × 2 ft deep in which a platform is located that supports two thick aluminum plates, each 15 in square and 1.5 in thick (Fig. 1). The two plates are separated by a styrofoam pad of the same dimensions, which absorbs some of the force transmitted between the plates. The plates and pad travel vertically in response to a blast in the water tank, guided by poles located in

Submitted: December 13, 2013, Revised: March 6, 2014, Accepted: March 17, 2014.

From the Department of Anesthesiology (J.L.P., G.F.), and Shock, Trauma, and Anesthesiology Research Center (STAR) (J.L.P., G.F.), School of Medicine, and Department of Mechanical Engineering (W.L.F., U.H.L.), School of Engineering, and the Center of Energetics Concepts Development (W.L.F., U.H.L.), University of Maryland, Baltimore, Maryland.

This work was presented at the 2013 Military Health System Research Symposium, August 12–15, 2013, in Fort Lauderdale, Florida.

Address for reprints: Gary Fiskum, PhD, Department of Anesthesiology, School of Medicine, University of Maryland, 685 W Baltimore St, 534 MSTF, Baltimore, MD; email: gfiskum@anes.umm.edu.

DOI: 10.1097/TA.0000000000000340

holes in each corner of the plates and pad. The two cylinders secured to the top of the plate each house an anesthetized rat that is wrapped in a thick cotton "blanket" to minimize secondary movement within the cylinders. An explosive charge of 0.75-g pentaerythritol tetranitrate is placed in the water precisely under the center of the plate at distances that generate precise, maximal G forces in these experiments of between 20 G and 50 G. Standoff distances were determined previously at the Dynamics Effects Laboratory and measured during the animal experiments, using accelerometers. When detonated, the explosion causes the plate containing the two rats to accelerate upward extremely rapidly to heights of less than 4 in, followed by a return down to the original location. Pressure sensors located immediately next to the rat heads indicated that they were exposed to less than 1-psi increase in pressure following the explosion. Figure 1 provides examples of the accelerometer measurements performed during these tests, demonstrating reproducibility between two different blasts at both 20 G and 40 G and differences observed at 20, 40, and 60 G, with peak accelerations occurring at 5, 4, and 3 milliseconds, respectively.

Animal Experiments

All animal procedures were performed in accordance with the University of Maryland School of Medicine Institutional Animal Care and Use Committee, the US Army Animal Care and Use Review Office, and the US Air Force Animal Use Program Office of Research Oversight and Compliance. At approximately 10 minutes before each blast, two adult male Sprague-Dawley rats (300–350 g) were deeply anesthetized by intraperitoneal injection of ketamine (80 mg/kg) and xylazine (10 mg/kg). Immediately following the underbody blast, the rats were removed from the cylinders, and their respiratory rates were compared with those recorded before the blast. No changes in respiration were observed. All animals were fully conscious within 90 minutes after the blast and appeared unharmed. In addition to the 25 anesthetized rats subjected to blast-induced hyperacceleration, 10 sham rats were anesthetized but not used in blast experiments.

Tissue Preparation

At different times following the blasts or sham anesthetization, rats were heavily reanesthetized by intraperitoneal injection of ketamine (160 mg/kg) and xylazine (20 mg/kg) and transcardially perfused with 4% paraformaldehyde plus 2.5% acrolein.[9] Brains were removed from the skull and transferred into 30% sucrose. Once brains sunk to the bottom of the container, they were cut (40 μm) on a freezing sliding microtome, yielding 12 series per animal, and were kept in cryoprotectant (−20°C) until further processing was initiated.

Pathology

None of the 25 rats used in the blast experiments exhibited any evidence of injury to the lungs, heart, liver, or spleen upon inspection following thoracotomy during perfusion fixation.

Staining of brain sections with Fluoro-Jade B (FJB) was used to detect dead or dying neurons.[9,10] Free floating brain sections were rinsed free of cryoprotectant with KPBS, mounted on Vectabond-treated PLUS superfrost glass slides and dried overnight at 50°C. Slides were sequentially dipped in the following: 100% EtOH (3 minutes), 70% EtOH (1 minute), deionized H_2O (1 minute), 0.06% $KMnO_4$ (15 minutes), H_2O (2 minutes), and 0.0005% solution of FJB (30 minutes). Slides were then dipped in H_2O four times to five times and were allowed to dry for 30 minutes at 50°C before being cleared in xylene and coverslipped with DPX mounting media.

The amino cupric silver method of de Olmos was used to stain free-floating 40-μm tissue for the identification of damaged and degenerating axons. Our staining procedure closely followed the detailed protocol described by Tenkova and Goldberg.[11] Before staining, all glassware was cleaned in 50% nitric acid. Sections were rinsed free from cryoprotectant and incubated in 4% paraformaldehyde (4°C) for 1 week before staining to block nonspecific labeling of neurons. Sections were then rinsed with deionized H_2O and incubated in preimpregnation buffer (cupric silver) for 1 hour at 50°C then at room temperature overnight. The next day, sections were exposed to the following solutions at room temperature: 100% acetone (30 seconds), impregnation buffer (silver diamine) solution for 35 minutes, reduction agent (formaldehyde with citric acid) for 2 minutes, bleaching solution (potassium ferricyanide) for 20 minutes, deionized H_2O for 3 minutes, and stabilization buffer (thiosulfate solution) for 10 minutes. All solutions were made fresh immediately before use, and sections were carefully shielded from direct light during all staining procedures. After staining, sections were mounted in

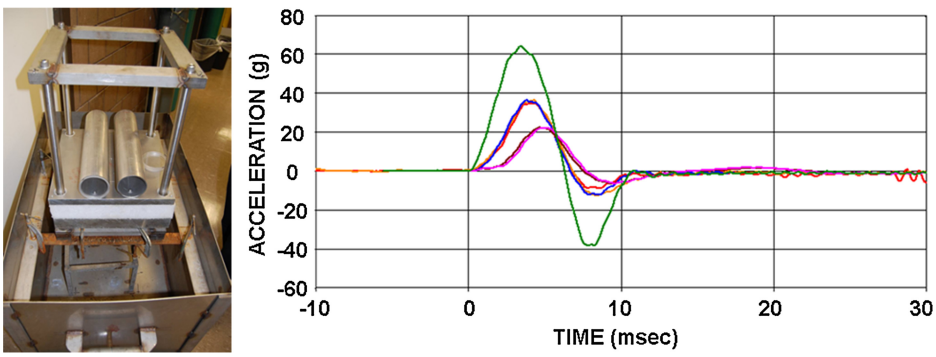

Figure 1. Device used for underbody blast-induced hyperacceleration experiments and accelerometer recordings obtained during the blasts. Tracings show highly reproducible accelerations generated by duplicate blasts at both 20 G and 40 G as well as a single blast at 60 G.

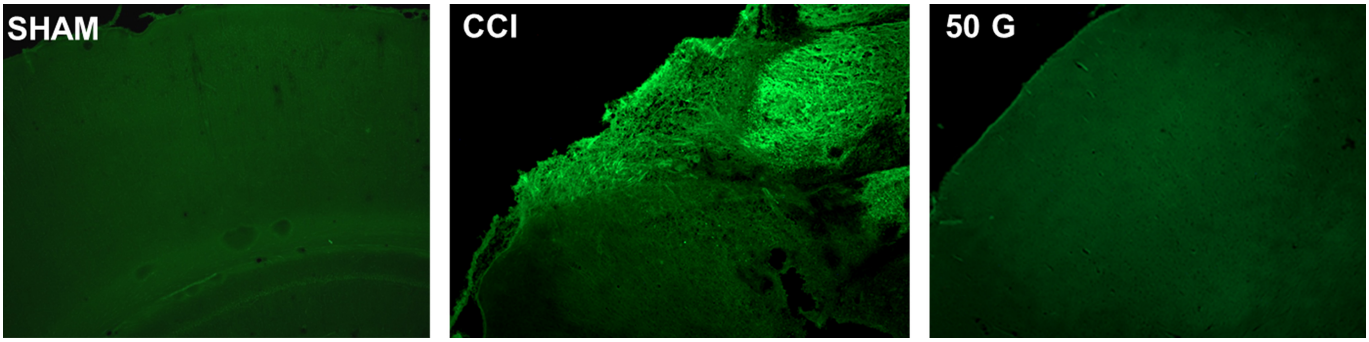

Figure 2. FJB staining for dead or dying cortical neurons after exposure of rats to head impact or underbody blast. Sham animal was anesthetized with ketamine and perfusion fixed 7 days later. One rat was used in a CCI model of moderate TBI and perfused 7 days later. One ketamine-anesthetized rat was subjected to a 50-G underbody blast and perfused 7 days later.

50% ethanol onto subbed PLUS slides, dehydrated with ethanol and xylene, and subsequently coverslipped with DPX mounting media.

Immunohistochemistry

Free-floating sections were single labeled with antibodies against the astrocyte marker, glial fibrillary acidic protein (GFAP),[9] by rinsing multiple times in 0.05-M KPBS buffer before and after exposure to the following: 1% solution of sodium borohydride for 20 minutes; primary antibody diluted in 0.05-M KPBS + 0.4% Triton-X for 48 hours (Dako Anti-GFAP; 1:150K); biotinylated secondary antibody diluted in 0.05-M KPBS + 0.4% Triton-X 1:600 for 1 hour; and incubation in Vectastain A/B solution (1:222) for 1 hour. Tissue was then rinsed before and after 12-minute incubation in Ni-DAB solution with 0.175-M sodium acetate buffer. After a final rinse in KPBS buffer, slices were mounted on slides, dehydrated, and coverslipped with DPX mounting media. The sections were examined with Nikon Eclipse E800 microscope and captured using StereoInvestigator software.

RESULTS

Neuronal death is typically observed within 1 week of injury in most rodent TBI models. Neuronal death or degeneration that occurs in this period is often detected histologically, using a FJB stain, which selectively labels dead or dying neurons.[9,10] Figure 2 compares FJB staining present in the frontal cerebral cortex of a sham rat, perfusion fixed 7 days after ketamine anesthesia, to that observed 7 days following moderate injury induced using a controlled cortical impact (CCI) model, which uses a pneumatic device to directly impact the cortical surface.[12] Representative tissue from the CCI model was obtained from our rodent brain bank and not generated as part of this study. Extensive staining was apparent in the brain from the rat that underwent the CCI, whereas virtually no staining was detectable in the sham rat. In contrast to the staining exhibited by the positive control animal that was previously subjected to cortical impact, no FJB staining was observed at 7 days in a rat subjected to a 50-G underbody blast. Examination of 12 coronal sections representing the entire brain detected no FJB-stained neurons in 23 rats used in the 50-G underbody blast experiments or in 2 rats used in 20-G underbody blast experiments.

Diffuse axonal injury is often observed in rodent brain injury models and can be detected by staining of axons with silver-containing reagents.[10,13] With the use of the de Olmos silver staining method, widespread staining was evident at 7 days after 50-G blasts. Staining was most striking in the internal capsule, corpus callosum, and cerebellum (Fig. 3). Abnormal axon morphologic finding was represented by undulations and bulb-like swellings (Fig. 3, bottom panels). Additional axonal staining was observed in tracts serving the thalamus, while very few fibers in the olfactory bulb or anterior commissures showed evidence of axonopathy. Where silver staining was observed in superficial layers of the brain, it occurred more commonly in the ventral rather than dorsal cortical regions. Relatively little axonal silver staining was observed in noninjured sham animals.

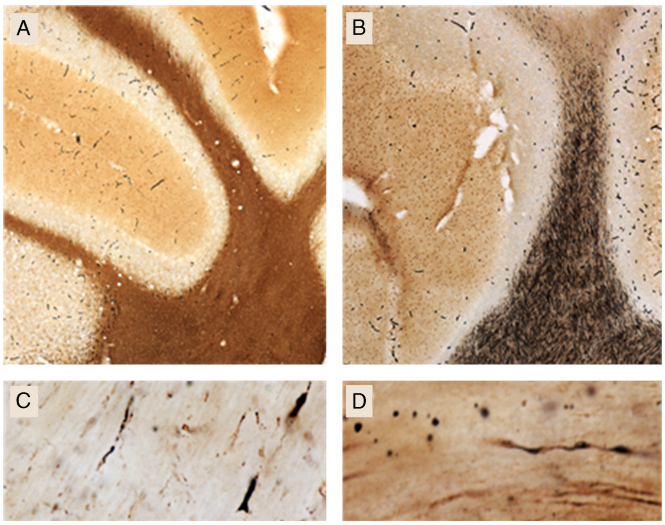

Figure 3. de Olmos silver staining of rat brain 7 days following a 50-G underbody blast. Widespread staining demonstrates axonopathy in white matter structures of the cerebellum in rats exposed to underbody blast (*B*) as compared with sham controls (*A*). High magnification confirms the presence of abnormal swellings and varicosities present in silver-stained axons within the internal capsule (*C* and *D*) following blast exposure.

Axonal silver staining was detectable in the internal capsule of animals subjected to 20-G underbody blasts and perfusion fixed at either 24 hours or 7 days. Evidence for even earlier axonal injury was obtained with brains fixed 3 hours after 50-G blasts (Fig. 4). In contrast, silver staining was much less obvious at 30 days after blast than at 3 hours or 7 days (Fig. 4).

Cellular inflammatory responses are another hallmark of TBI. These responses are characterized by proliferation, migration, and morphologic transformation of astrocytes and microglia, which constitute approximately 50% of the mass of the human brain.[14] Surprisingly, we obtained no convincing evidence for microglial activation following 20-G or 50-G blasts at any outcome times (not shown). Nevertheless, we consistently observed astrocyte accumulation near ventral cortical surfaces, hypothalamic regions, and the internal capsule (Fig. 5). In addition, many astrocytes present in different brain regions exhibited large cell bodies, indicative of activation. Unlike the silver staining of axons, which declined between 7 days and 30 days after the blast, these cellular inflammatory reactions persisted and possibly increased during this period.

DISCUSSION

To the best of our knowledge, these experiments represent the first to test for the effects of specifically underbody blast-induced hyperacceleration on the brains of laboratory animals. The blast paradigm was designed to test for the effects of this form of acceleration on the brains of rats in the absence of exposure to any significant blast overpressure. Several conclusions can be made. (1) Adult rats can be subjected to blast-induced hyperacceleration at maximal G forces of at least 50 G with a 100% survival rate, provided they are protected against secondary impact injuries. (2) FJB-detectable neuronal death does not occur following exposure of rats to either 20-G or 50-G underbody blasts. (3) Diffuse axonal injury occurs in several brain regions, as early as 4 hours after 20-G or 50-G underbody blasts and is still evident at 7 days, based on silver staining of axonal fibers. (4) Despite the lack of evidence for substantial microglial activation, astrocyte activation occurs within 7 days and persists for 30 days following 20-G or 50-G underbody blasts. 5. Based on these qualitative histologic findings, we conclude that rats subjected to 50-G blasts and possibly even 20-G blasts experience mild TBI.

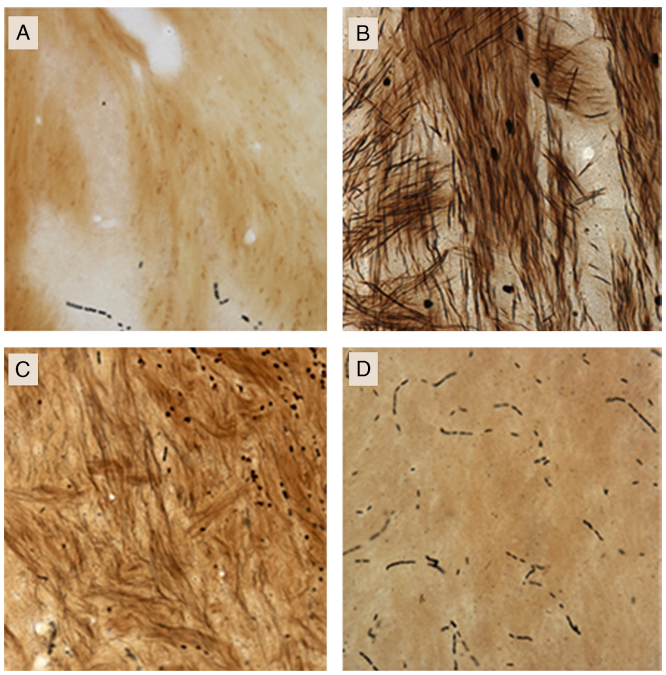

Figure 4. de Olmos silver staining of rat brain internal capsule at early and late time points following 50-G generated blasts. Intense internal capsule staining is induced with 50-G forces (*B–D*), which appears to dissipate with time as compared with ketamine-anesthetized sham controls (*A*). *A*, Sham; *B*, 50 G at 3 hours after blast; *C*, 50 G at 7 days after blast; *D*, 50 G at 30 days after blast.

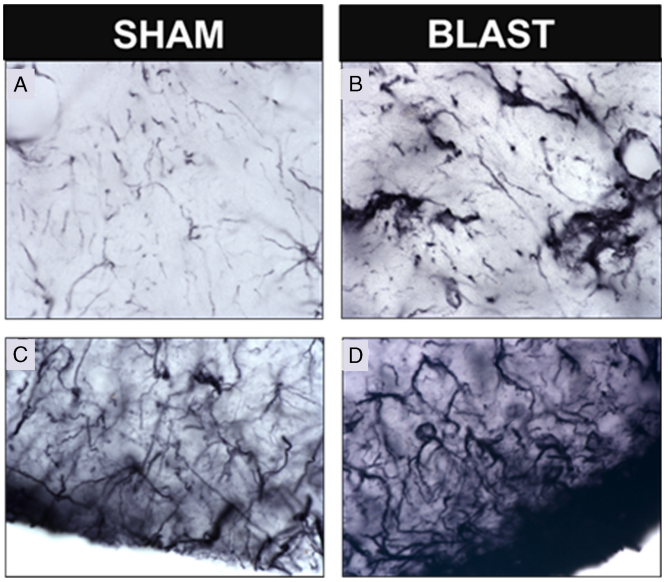

Figure 5. Astrocyte activation near hypothalamic regions at 7 days after a 50-G underbody blast. Intensities of GFAP-stained astrocytes were greater in animals exposed to underbody blasts compared with sham-treated rats. Astrocyte activation was observed in the internal capsule (*B*) and regions of the hypothalamus (*D*) as compared with these regions in shams (*A* and *C*).

This unique initial approach to understanding the effects of underbody blasts on the brain has several limitations. (1) We specifically designed the device for exposing rats to underbody blasts to test specifically for the effects of acceleration, without secondary effects of potential head impact. Clearly, many victims of TBI who are occupants of vehicles targeted by IEDs detonated underneath the vehicles are subjected to both acceleration, head impact, and other injuries. Therefore, polytrauma animal models may be more clinically relevant.[5,15] (2) Only two maximal G forces were used, which are much lower than maximum survivable G forces experienced by occupants within targeted vehicles. We purposely used relatively low loads in this initial study to avoid mortality and injury to other vital organs. Studies are in progress exposing rats to underbody blasts at much higher G forces in the range of 100 G to 2,000 G. Recently, one study published evidence of head acceleration exceeding 3,000 G in a

blast tube, porcine model of survivable free field blast exposure.[16] (3) Neuronal death was only measured using one method, that is, FJB tissue staining. It is therefore possible that other methods, such as active caspase 3 immunostaining, could detect neuronal death not detected by FJB. (4) Diffuse axonal injury was only evaluated using the de Olmos silver staining method. Although this approach is used extensively, additional procedures, for example, immunohistochemical detection of phosphorylated tau protein and beta-amyloid precursor protein, could provide helpful validation.[17,18] 5. The results obtained from the silver staining of degenerative neurons and the GFAP immunostaining of astrocytes demonstrating activated morphology are at this juncture purely qualitative. Studies are in progress to obtain quantitative results for these and other histologic outcome measures. (6) No quantitative assessment of behavior was performed. Now that we have obtained histologic evidence for mild TBI following low-G underbody blasts, we are developing neurobehavioral tests sensitive enough to detect neurologic alterations at these and higher G forces.

AUTHORSHIP

J.L.P. performed all of the histology and generated all of the results presented in the article. W.L.F. and U.H.L. designed and built the device used for the underbody blast TBI model, were present at every experiment, and conducted the blasts and performed the accelerometer measurements. G.F. is the principal investigator of the grants that supported the work and conceived the study design. He was also present at every experiment. All authors contributed to the writing of this manuscript.

DISCLOSURE

There are no financial, consultant, institutional, or relationship conflicts declared by any author. This work was supported in part by US Air Force grant FA8650-11-2-6D04 and the US Army grant W81XWH-13-1-0016.

REFERENCES

1. Okie S. Traumatic brain injury in the war zone. *N Engl J Med*. 2005;352:2043–2047.
2. Hoge CW, McGurk D, Thomas JL, Cox AL, Engel CC, Castro CA. Mild traumatic brain injury in U.S. Soldiers returning from Iraq. *N Engl J Med*. 2008;358:453–463.
3. Magnuson J, Leonessa F, Ling GS. Neuropathology of explosive blast traumatic brain injury. *Curr Neurol Neurosci Rep*. 2012;12:570–579.
4. Cernak I, Radosevic P, Malicevic Z, Savic J. Experimental magnesium depletion in adult rabbits caused by blast overpressure. *Magnes Res*. 1995; 8:249–259.
5. Garman RH, Jenkins LW, Switzer RC 3rd, Bauman RA, Tong LC, Swauger PV, Parks SA, Ritzel DV, Dixon CE, Clark RS, et al. Blast exposure in rats with body shielding is characterized primarily by diffuse axonal injury. *J Neurotrauma*. 2011;28:947–959.
6. Long JB, Bentley TL, Wessner KA, Cerone C, Sweeney S, Bauman RA. Blast overpressure in rats: recreating a battlefield injury in the laboratory. *J Neurotrauma*. 2009;26:827–840.
7. Fourney WL, Leiste U, Bonenberger R, Goodings D. Explosive impulse on plates. *FRAGBLAST*. 2005;9:1–17.
8. Fourney WL, Leiste U, Bonenberger RJ, Goodings D. Mechanism of loading on plates due to explosive detonation. *FRAGBLAST*. 2005;9:205–217.
9. Hazelton JL, Balan I, Elmer GI, Kristian T, Rosenthal RE, Krause G, Sanderson TH, Fiskum G. Hyperoxic reperfusion after global cerebral ischemia promotes inflammation and long-term hippocampal neuronal death. *J Neurotrauma*. 2010;27:753–762.
10. Hall ED, Bryant YD, Cho W, Sullivan PG. Evolution of post-traumatic neurodegeneration after controlled cortical impact traumatic brain injury in mice and rats as assessed by the de Olmos silver and fluorojade staining methods. *J Neurotrauma*. 2008;25:235–247.
11. Tenkova TI, Goldberg MP. A modified silver technique (de Olmos stain) for assessment of neuronal and axonal degeneration. *Methods Mol Biol*. 2007;399:31–39.
12. Robertson CL, Puskar A, Hoffman GE, Murphy AZ, Saraswati M, Fiskum G. Physiologic progesterone reduces mitochondrial dysfunction and hippocampal cell loss after traumatic brain injury in female rats. *Exp Neurol*. 2006;97:235–243.
13. Kochanek PM, Dixon CE, Shellington DK, Shin SS, Bayır H, Jackson EK, Kagan VE, Yan HQ, Swauger PV, Parks SA, et al. Screening of biochemical and molecular mechanisms of secondary injury and repair in the brain after experimental blast-induced traumatic brain injury in rats. *J Neurotrauma*. 2013;30:920–937.
14. Kumar A, Loane DJ. Neuroinflammation after traumatic brain injury: opportunities for therapeutic intervention. *Brain Behav Immun*. 2012;26:1191–1201.
15. Hicks RR, Fertig SJ, Desrocher RE, Koroshetz WJ, Pancrazio JJ. Neurological effects of blast injury. *J Trauma*. 2010;68:1257–1263.
16. Shridharani JK, Wood GW, Panzer MB, Capehart BP, Nyein MK, Radovitzky RA, Bass CR. Porcine head response to blast. *Front Neurol*. 2012;3:70.
17. Goldstein LE, Fisher AM, Tagge CA, Zhang XL, Velisek L, Sullivan JA, Upreti C, Kracht JM, Ericsson M, Wojnarowicz MW, et al. Chronic traumatic encephalopathy in blast-exposed military veterans and a blast neurotrauma mouse model. *Sci Transl Med*. 2012;4(134):134ra60.
18. Risling M, Plantman S, Angeria M, Rostami E, Bellander BM, Kirkegaard M, Arborelius U, Davidsson J. Mechanisms of blast induced brain injuries. Experimental studies in rats. *Neuroimage*. 2011;54(Suppl 1):S89–S97.

APPENDIX 2

Proctor JL, Mello KT, Fang R, Puche AC, Rosenthal RE, Fourney WL, Leiste UH, Fiskum G. Aeromedical evacuation-relevant hypobaria worsens axonal and neurologic injury in rats after underbody blast-induced hyperacceleration. J Trauma Acute Care Surg. 2017 Jul;83(1 Suppl 1):S35-S42. PMID: 28452879.

Aeromedical evacuation-relevant hypobaria worsens axonal and neurologic injury in rats after underbody blast-induced hyperacceleration

Julie L. Proctor, Kaitlin T. Mello, Raymond Fang, MD, Adam C. Puche, PhD, Robert E. Rosenthal, MD, William L. Fourney, PhD, Ulrich H. Leiste, PhD, *and* **Gary Fiskum, PhD***, Baltimore, Maryland*

BACKGROUND: Occupants of military vehicles targeted by explosive devices often suffer from traumatic brain injury (TBI) and are typically transported by the aeromedical evacuation (AE) system to a military medical center within a few days. This study tested the hypothesis that exposure of rats to AE-relevant hypobaria worsens cerebral axonal injury and neurologic impairment caused by underbody blasts.

METHODS: Anesthetized adult male rats were secured within cylinders attached to a metal plate, simulating the hull of an armored vehicle. An explosive located under the plate was detonated, resulting in a peak vertical acceleration force on the plate and occupant rats of 100G. Rats remained under normobaria or were exposed to hypobaria equal to 8,000 feet in an altitude chamber for 6 hours, starting at 6 hours to 6 days after blast. At 7 days, rats were tested for vestibulomotor function using the balance beam walking task and euthanized by perfusion. The brains were then analyzed for axonal fiber injury.

RESULTS: The number of internal capsule silver-stained axonal fibers was greater in animals exposed to 100G blast than in shams. Animals exposed to hypobaria starting at 6 hours to 6 days after blast exhibited more silver-stained fibers than those not exposed to hypobaria. Rats exposed to 100% oxygen (O_2) during hypobaria at 24 hours postblast displayed greater silver staining and more balance beam foot-faults, in comparison with rats exposed to hypobaria under 21% O_2.

CONCLUSION: Exposure of rats to blast-induced acceleration of 100G increases cerebral axonal injury, which is significantly exacerbated by exposure to hypobaria as early as 6 hours and as late as 6 days postblast. Rats exposed to underbody blasts and then to hypobaria under 100% O_2 exhibit increased axonal damage and impaired motor function compared to those subjected to blast and hypobaria under 21% O_2. These findings raise concern about the effects of AE-related hypobaria on TBI victims, the timing of AE after TBI, and whether these effects can be mitigated by supplemental oxygen. (*J Trauma Acute Care Surg.* 2017;83: S35–S42.

KEY WORDS: Axonopathy; balance beam; hypoxia; hyperoxia; normoxia.

During Operations IRAQI FREEDOM and ENDURING FREEDOM, the U.S. Air Force aeromedical evacuation (AE) system moved more than 100,000 casualties globally. Modern capability to safely transport critically ill and injured casualties early after injury enabled a doctrinal revolution in the military medical system. Although movement to advanced medical care is advantageous, the potentially negative physiologic impacts of the flight environment, to include hypobaria, are incompletely understood, and much of the patient flight validation practice is based on historical and anecdotal observations.[1] Considering that approximately 16% of military AE patients are victims of traumatic brain injury (TBI)[2] and that supplemental oxygen (O_2) is commonly provided during transport, it is particularly important to determine what effects flight-associated variables, for example, temperature, vibration, barometric pressure, and O_2, have on TBI.

Studies using animal models of impact-induced moderate to severe TBI provide evidence that exposure to AE-relevant hypobaria within a few days after injury worsens outcomes, including brain oxygenation, neuroinflammation, neuronal death, and behavior deficits.[3–5] However, no studies have reported the effects of flight-relevant hypobaria on mild TBI caused by exposure to blasts. The vast majority of the over 300,000 US warfighters who suffered TBI during the last 15 years are victims of blast-induced, mild TBI. Many of these injuries are primarily the result of hyperacceleration of the armored vehicle by the blast, with most of the barometric pressure wave deflected by sloped armored hull designs. Thus, further insight into the interactions between AE and blast-induced acceleration TBI is sorely needed.[6]

This study used our unique undervehicle blast rat model of mild TBI to test the hypothesis that a single or double exposure to hypobaria, equivalent to one or two AE flights, within a few days after injury worsens either histologic and/or neurologic outcomes. The effects of different levels of O_2 present

Submitted: January 4, 2017, Revised: February 27, 2017, Accepted: March 2, 2017. Published online: April 27, 2017.

From the Department of Anesthesiology (J.L.P., K.T.M., GF.), University of Maryland School of Medicine, Program in Trauma (R.F., R.E.R.), R. Adams Cowley Shock Trauma Center, University of Maryland Medical Center; U.S. Air Force Center for the Sustainment of Trauma and Readiness Skills (R.F.); Department of Anatomy and Neurobiology (A.C.P.), Department of Emergency Medicine (R.E.R.), University of Maryland School of Medicine, Baltimore; and School of Engineering (W.L.F., U.L.H.), University of Maryland College Park, College Park, Maryland.

This study was presented at the 2016 annual meeting of the Military Health Sciences Research Symposium, August 15–17, 2016, in Kissimmee, Florida.

Supplemental digital content is available for this article. Direct URL citations appear in the printed text, and links to the digital files are provided in the HTML text of this article on the journal's Web site (www.jtrauma.com).

Address for reprints: Gary Fiskum, PhD, Department of Anesthesiology, University of Maryland School of Medicine, 685W. Baltimore St., 5.34 MSTF Baltimore, MD 21201; email: gfiskum@anes.umm.edu.

DOI: 10.1097/TA.0000000000001478

during the hypobaria exposure were also tested to determine if the deleterious effects of hypobaria after TBI are mitigated or amplified by inspiration of supplemental O_2.

MATERIALS AND METHODS

Underbody Blast-Induced Hyperacceleration

The device used to induce underbody blast-induced acceleration consists of an aluminum water tank in which a platform is located that supports two thick aluminum plates, each 15 in square and 1.5 in thick. The two plates are separated by styrofoam of the same dimensions. A small explosion detonated in the water tank causes the plates to travel vertically, guided by poles (Fig. 1A). Upon this "vehicle," two cylinders are secured horizontally to the top plate with accelerometers located near the cylinders. Two male Sprague-Dawley rats (300–350 g) were wrapped in several layers of 100% cotton batting and placed in the prone position inside the cylinders.

An explosive charge of 0.75 g pentaerythritol tetranitrate was placed in the water under the center of the plate at a stand-off distance that generated a reproducible G-force of 100 ± 2.6G (SEM) (n = 20 blasts). The explosion caused the plate, and the cylinders containing the two rats, to accelerate vertically approximately 6 inches, followed by return down to the original location. Figure 1B provides an example of an accelerometer measurement performed under these conditions, demonstrating a peak acceleration of 100G occurring approximately 2.0 ms after detonation. Measurements of barometric pressure at the head-end of the cylindrical restraints indicated that the rats were exposed to a negligible barometric shockwave (<1 psi).

Animal Exposure to Underbody Blasts

All animal procedures were performed in accordance with the University of Maryland School of Medicine and the US Army and Air Force Institutional Animal Care and Use Committees and Federal regulations. At approximately 10 minutes before each blast, rats (300–350 g) were deeply anesthetized by intraperitoneal injection of ketamine (80 mg/kg), xylazine (10 mg/kg), and acepromazine (2 mg/kg). Six rats were excluded rfrom the study. Two rats died within 5 minutes after anesthesia. One rat died during exposure to the blast. Another rat died at approximately 1 day after blast exposure. In addition, two rats were excluded because the accelerometers failed during the blast. Immediately after the blast, the rats were removed from the cylinders and appeared normal. All animals were fully conscious within 90 minutes. Sham rats were anesthetized and transiently placed into the cylinders in the absence of a blast. Before blast or sham procedures, rats were randomized into one of nine treatment groups (n = 8–10/group), where onset of hypobaric exposure(s) and oxygenation level during a 6-hour exposure were varied (as below).

Exposure to Hypobaria

Rats were randomized into groups representing various chamber pressures (normobaria, equivalent to 80 feet altitude, or hypobaria, equivalent to 8,000 feet altitude), chamber O_2 perfusion levels (21% O_2 normoxic or 100% O_2 hyperoxic), and timing conditions (6, 24, 72 hours, or 6 days after blast exposure) as shown in Table 1 (see Table, Supplemental Digital Content 1, http://links.lww.com/TA/A938). Up to four cages containing double-housed rats with food and water were placed in a large steel cylindrical chamber that was fitted with a pressure gauge and air intake port and connected to a vacuum pump. Immediately after the chamber was closed, the vacuum pump was adjusted every 5 minutes until the pressure in the chamber reached 568 mm Hg over 30 minutes, which is equivalent to the ambient pressure present at 8,000 feet altitude. This altitude was maintained for 5 hours, followed by 30 minutes of gradual repressurization to 757 mm Hg. During these exposures, the chamber gas intake port was connected to a tank containing either air (21% O_2) or 100% O_2.

Brain Tissue Preparation

At 7 days after exposure to blast or sham, rats were deeply anesthetized and then transcardially perfused with oxygenated, artificial cerebrospinal fluid solution for 5 minutes, followed

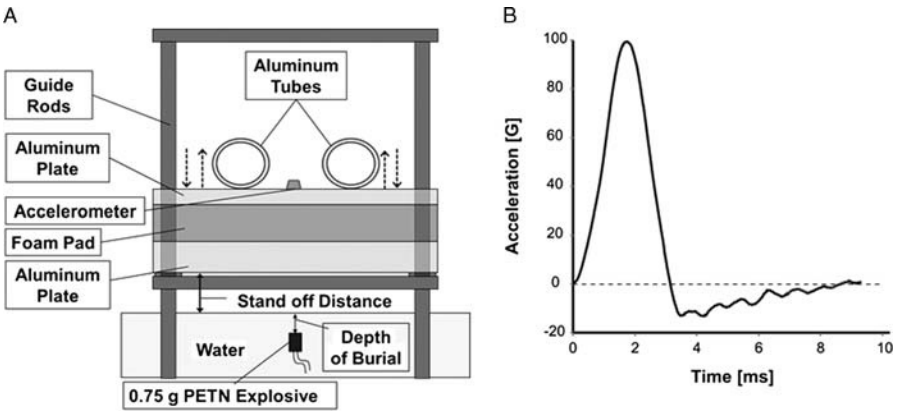

Figure 1. Vertical acceleration loading on rats modeling what occurs to occupants of vehicles targeted by land mines. (*A*) For each experiment, ketamine-anesthetized rats were placed prone within two tubes bolted to the top of a platform. Specific maximal vertical acceleration of the rats was achieved by detonation of polyerythritol tetranitrate located at a specific depth of burial in water where the surface is located at a specific stand-off distance under the bottom of two plates. (*B*) An accelerometer located immediately next to the heads of both rats provided filtered recordings indicating a maximal acceleration of 100G ± 12G (SEM; n = 20 blasts), occurring at slightly less than 2 ms after detonation.

by perfusion with 4% paraformaldehyde solution for 20 minutes, as described previously.[7] Brains were removed from the skulls and postfixed in 4% paraformaldehyde for 48 hours and then transferred into a 30% sucrose solution. Once brains had sunk to the bottom of the container, they were cut (40 μm) on a freezing sliding microtome, yielding 24 series per animal and kept in cryoprotectant (−20°C).

Amino Cupric Silver Staining of Damaged Axons

The amino cupric silver method of de Olmos was used to stain free-floating 40-μm tissue for the identification of damaged and degenerating axons.[8] Sections were rinsed free from cryoprotectant and incubated in 4% paraformaldehyde (4°C) for 1 week before staining to block nonspecific labeling of neurons. Sections were then rinsed with deionized water and incubated in preimpregnation buffer (cupric-silver) for 1 hour at 50°C and then at room temperature overnight. The next day, sections were exposed to the following solutions at room temperature: 100% acetone (30 seconds), impregnation buffer (silver-diamine) solution for 35 minutes, reduction agent (formaldehyde with citric acid) for 2 minutes, bleaching solution (potassium ferricyanide) for 20 minutes, deionized water for 3 minutes, and stabilization buffer (thiosulfate solution) for 10 minutes. After staining, sections were mounted in 50% ethanol onto subbed PLUS slides, dehydrated with ethanol and xylene, and subsequently coverslipped with DPX mounting media.

Sections containing the internal capsule (corresponding to bregma, −1.80 mm) were examined using bright field illumination at 100× magnification. A 25 × 25-μm grid was randomly superimposed over the tissue using the StereoInvestigator software (Fig. 2A). In total, five lines (25 μm each) within that field of view were randomly chosen for counting (Fig. 2A). The total number of axons crossing each of the five lines throughout the entire 40-μm tissue depth was counted. In the example shown in Figure 2B, 10 silver-stained axons crossed one such line. The data were expressed as number of crossings per cross-sectional 5,000-micron squared. These data were acquired by a microscopist blinded to the animal group identification.

Balance Beam Tests

Gross vestibulomotor function was assessed using a beam balance test. A rat was placed on one end of a narrow wooden beam (1 inch wide × 48 inches long) and the number of

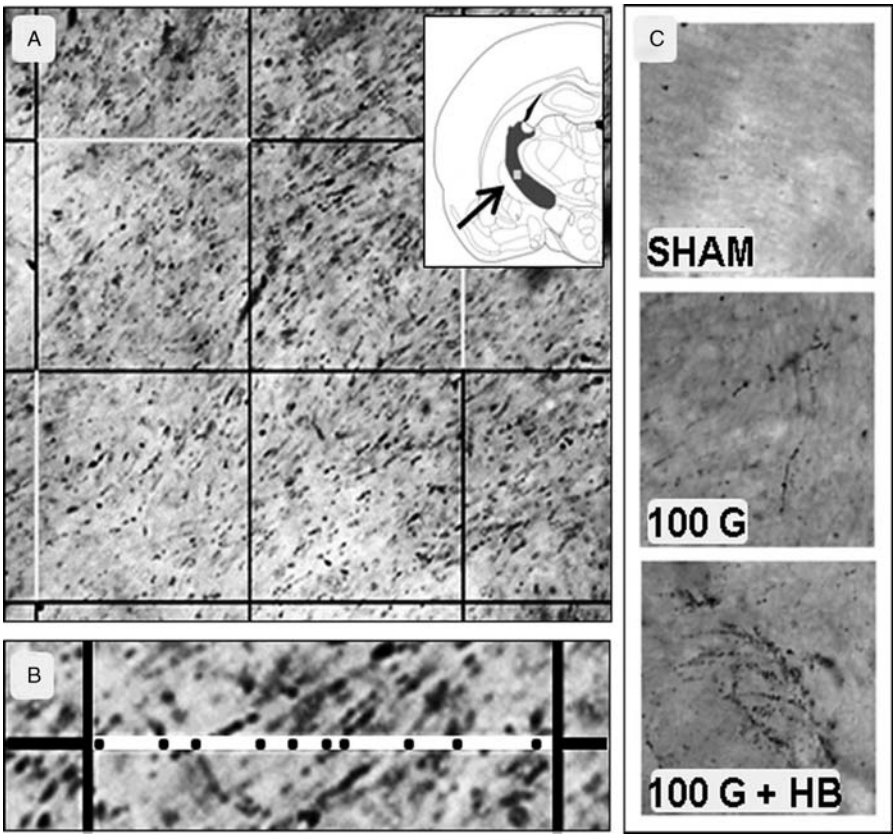

Figure 2. Appearance of axonal injury in the internal capsule using amino cupric silver staining of rat brains at 7 days postblast. The internal capsule was located in the sections obtained from bregma level –2.30. (*A*) The 25 × 25-μm grid overlay was then placed over the reference point under 100× magnification, using StereoInvestigator software. The arrow shown in the inset indicates the location used for quantification. (*B*) The number of silver-stained axons crossing five random 25-μm lines present within a given field of view was counted throughout the 40-micron-thick section, yielding a total number of axonal crossings per 5,000 μm^2. Each point on the superimposed white line represents a crossing. (*C*) Representative images of silver-stained internal capsule from a sham rat and rats subjected to underbody blast in the absence and presence of exposure to 6 hours hypobaria (under 100% O_2) initiated at 24 hours postblast.

foot-faults and the amount of time taken to traverse the length of the beam were recorded. The test consisted of training, baseline, and postinjury phases, occurring at 1 week prior, 24 hours prior, and 7 days postinjury, respectively. Each phase consisted of three separate crossings. Data are expressed as the total number of foot-faults recorded while crossing the beam over three trials comparing baseline to postinjury. These data were acquired by an examiner blinded to the animal group identification.

Data Analysis

Sample sizes (n = 8–10) in this study were selected based on a power analysis to provide greater than 80% power to detect a 25% difference in indices of axon injury between experimental and control groups. Significance was set at 0.05 and within-group standard deviations were estimated at 15% of the mean. Results from measurements of silver-stained axons are presented as group means ± standard error of the mean. Data were compared with one-way analysis of variance with Fisher's least significant difference *post hoc* analysis. Balance beam foot-faults were analyzed using a repeated measures two-way analysis of variance with Fisher's least significant difference *post hoc* test. Significance was defined as p less than 0.05.

RESULTS

Animals were exposed to hyperacceleration induced by explosive blast in an undervehicle blast model, using parameters that generated a mean peak acceleration of 100 ± 2.6G SEM, measured during 20 blasts. The change in barometric pressure on the platform during the blast was negligible (<1 psi) compared with the survivable increases in pressure of at least 20 psi generated by compressed gas-driven shock tube models of exposure to open field blasts.[9] One rat died during the blast and one died within 24 hours later, due to unknown causes. All other rats used in the underbody blast experiments survived and exhibited normal weight gain during the ensuing 7 days.

Axonal injury in white matter neuronal fiber tracts is often observed in impact models of TBI.[10] At 7 days postblast, we observed an increase in de Olmos silver-stained fibers in the internal capsule, consistent with the directional pattern of axonal fiber tracts present within the internal capsule (Fig. 2A). Sparse silver staining was observed in the brains of sham rats exposed to ketamine anesthetization alone, whereas higher staining levels were found in brains after blast-induced 100G acceleration (Fig. 2C). The mean axonal crossings at 7 days after 100G blast were approximately twice as great as those observed in sham animals (Fig. 3; $p < 0.05$; n = 10). These observations indicate mild axonal injury is induced by acceleration in the underbody blast model.

Military casualties injured by vehicle underbody blast events are commonly transported by the AE system from current combat zones shortly after injury (hours to days) in flights with approximately 8,000 feet cabin pressures lasting for approximately 4 hours to 8 hours. We tested the effect of 6 hours of hypobaric exposure on rats experiencing an underbody blast 6 hours, 24 hours, 72 hours, and 6 days before hypobaria. At all postblast interval points examined, there were nearly twice as many silver-stained damaged axons in the internal capsule in animals undergoing 6 hours of hypobaria compared with blast alone (Fig. 3; $p < 0.05$; n = 10). These data suggest that hypobaric exposure at any interval out to 6 days can worsen axonal injury in the brain.

AE of injured soldiers often occurs in two flights, when they are evacuated from combat zones to a regional AE hub in an allied country (e.g., Germany) and from there in a second flight back to the United States. Because we observed elevated axonal injury in rodents experiencing one "flight," we tested whether two exposures to hypobaria, the first at 24 hours and the second at 72 hours postblast, results in greater axonal injury than that observed after one flight at either of the two times alone. Single hypobaria exposure at either 24 hours or 72 hours resulted in significantly higher axonal injury compared with sham (as described above and in Fig. 4). However, the level of axonal injury from sequential hypobaria at 24 hours and again at 72 hours postinjury was not significantly different from a single exposure at either 24 hours or 72 hours.

One possible mechanism by which exposure to hypobaria during AE could worsen TBI is cerebral hypoxia, due to a reduced ambient O_2. At a cabin pressure equivalent to 8,000 feet, the ambient O_2 concentration is reduced from normobaric 21% O_2 by approximately a quarter to 16% O_2. Although some mild TBI victims during AE may not require any supplemental O_2 to maintain normal blood hemoglobin saturation, many mild and most moderate-to-severe TBI patients should receive O_2 ranging from approximately 50% to 100%[11] We therefore tested for any

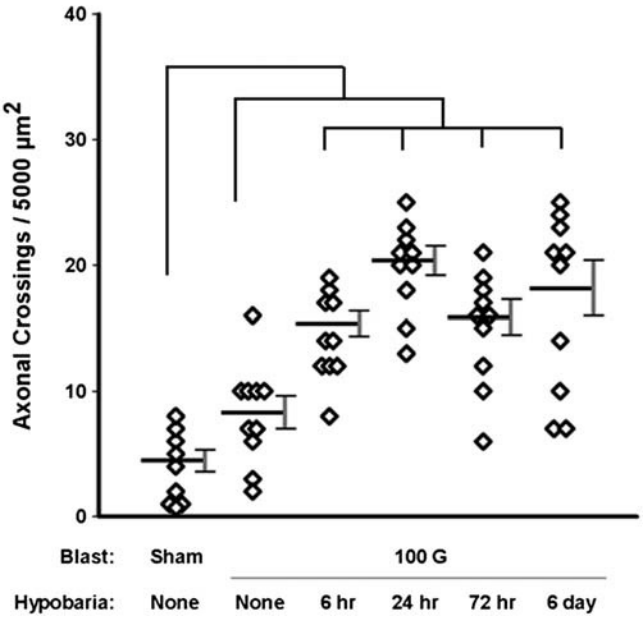

Figure 3. Hypobaria exposure increases the number of silver-stained axonal fibers present in the internal capsule at 7 days after underbody blast. The number of silver-stained axon fibers in all 100G blast groups was significantly greater than that observed with brains from sham animals (n = 9–10/group; $p < 0.05$). 100G blast groups exposed to hypobaria initiated at 6 hours, and 1 day, 3 days, or 6 days, were significantly greater than after blast exposure without subsequent hypobaria (n = 9–10/group; $p < 0.05$). The number of silver-stained axonal crossings present in the 24 hour group is greater than either the 6 hour or 72 hour hypobaria group ($p < 0.05$).

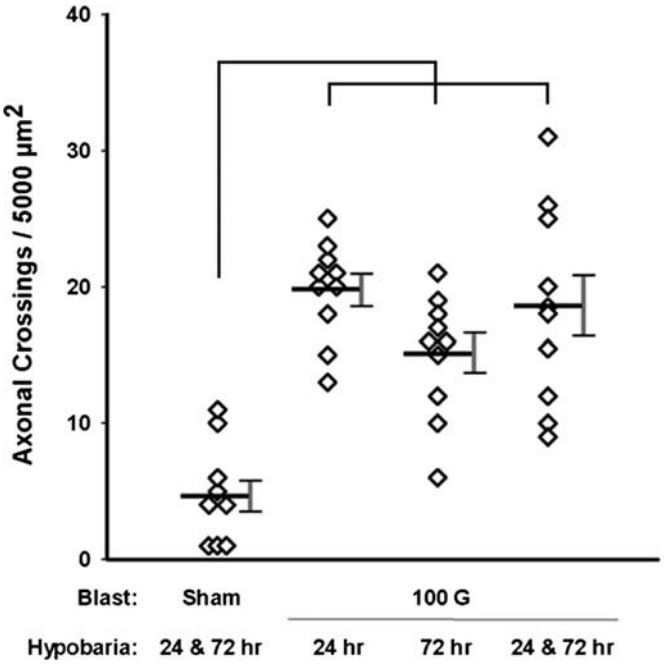

Figure 4. Exposure to hypobaria at 24 hours and 72 hours after blast exposure does not worsen axonal injury that occurs after a single hypobaria exposure at either time postblast. All 100G blast groups exposed to single or double hypobaria exhibited greater axonal injury at 7 days, in comparison with shams (n = 9–10/group; $p < 0.001$). These shams were ketamine anesthetized on day 0, not exposed to blast, and then exposed to hypobaria at both 1 day and 3 days later.

differences in white matter damage in 24 hours after blast animals exposed during 6 hours hypobaric exposure with room air (16% O_2 at hypobaria) or 100% O_2. The number of silver-stained axonal fibers was nearly twofold higher in the brains of rats subjected to 100% O_2 compared with those exposed to room air (Fig. 5; $p < 0.001$; n = 9–10). Thus, the combination of hypobaria and hyperoxia dramatically increased the number of silver-stained injured axons.

Mild neural injury may be fully compensated at the gross functional level, such that the increased numbers of damaged axons observed in this study do not cause apparent functional impairment. Several behavior tests that are often used in rat models of impact-induced TBI were used to assess neurologic impairment at up to 7 days after underbody blast exposure. The general tests of composite neuroscore, open field, and novel object recognition showed no differences between rats exposed to blasts and sham rats exposed only to ketamine (not shown), suggesting that the observed mild blast TBI does not reach the threshold for general cognitive impairment. However, the balance beam test of vestibulomotor activity that we have used successfully in other rat TBI models is quite sensitive to even mild deficits.[12,13] In this behavior sham animals and those exposed to hypobaria with room air after blast showed no differences between baseline measured 1 day before blast and postinjury performance at 7 days. However, animals in the blast TBI group that were exposed to hypobaria under 100% O_2 exhibited threefold greater foot-faults at 7 days postblast compared with baseline measurements or to those observed after blast alone or blast plus hypobaria under 21% O_2 (Fig. 6; $p < 0.01$; n = 8–9). Thus, although overall cognitive/behavioral metrics of composite neuroscore and open field were not affected by the elevated white matter axonal injury, fine motor performance in the beam crossing detected impaired function with hypobaria/hyperoxic treatment.

DISCUSSION

Explosive blasts account for 81% of injuries sustained in Operations IRAQI FREEDOM and ENDURING FREEDOM.[14] Blast-induced TBI has been called a "signature" injury of these conflicts, with the standard of care treatment involving AE of TBI patients from the combat theatre as soon as feasible.[2] The present rodent study was used to model the potential effects of AE-relevant hypobaria after mild TBI generated by exposure to undervehicle blasts. Four main conclusions can be reached from our results. First, rats exposed to an underbody blast generating a peak vertical acceleration equal to 100G in the absence of exposure to significant blast-induced pressure changes exhibited a quantitatively significant increase in damaged internal capsule axonal fibers, as measured by de Olmos silver staining. Second,

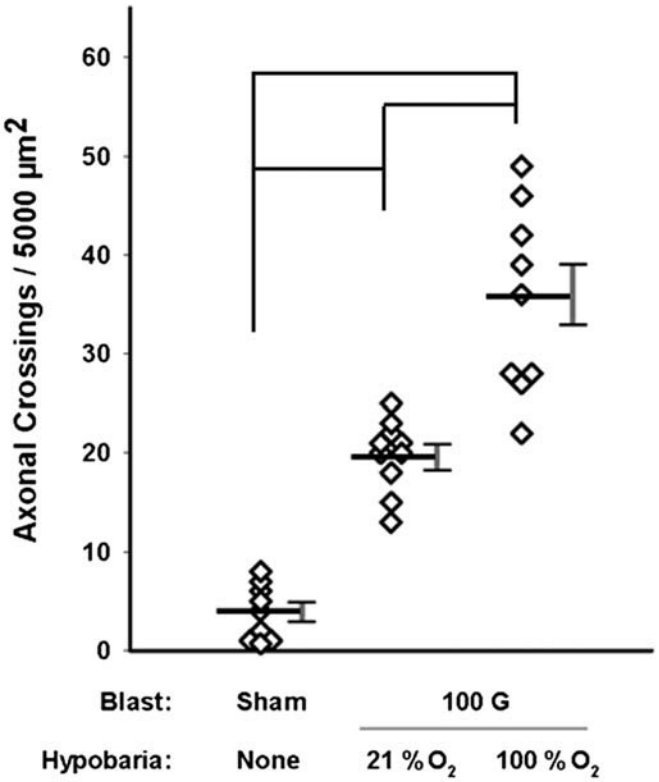

Figure 5. Exposure of rats to 100% O_2 during hypobaria at 24 hours postblast worsens axonal injury compared to that observed with rats exposed to room air during hypobaria. Both 100G blast TBI groups exposed to 21% or 100% inspired O_2 during hypobaria displayed significantly more injured neurons than shams (n = 9–10/group; $p < 0.001$). The number of axonal crossings present in the 100% O_2 group was greater than in the 21% O_2 hypobaric group ($p < 0.001$).

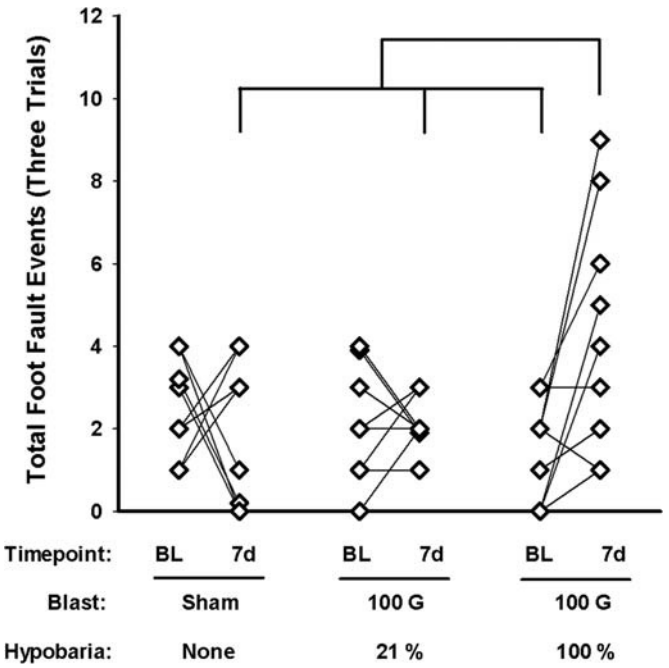

Figure 6. Hyperoxic hypobaria after underbody blast exposure impairs balance beam performance. Individual data points on scatterplot represent the sum foot faults of three crossings recorded for each animal on a given day. Lines connect baseline to postinjury counts for individual animals. Exposure to blast and hyperoxic but not normoxic hypobaria increased the total number of foot faults at 7 days postinjury compared with own baseline (n = 9/group; $p < 0.002$). At 7 days post-100G blast, rats subjected to hyperoxic hypobaria had significantly more foot faults than their normoxic counterparts and shams (n = 8–9/group; $p < 0.01$).

exposure of rats to 6 hours of flight-relevant hypobaria equivalent to 8,000 feet initiated at 6 hours, 24 hours, 72 hours, and 6 days postinjury resulted in a greater number of damaged axon fibers than those maintained under normobaric conditions. Third, rats exposed to "dual flight" hypobaria under 21% O_2 at both 24 hours and 72 hours postblast did not exhibit greater axonal silver staining than that observed after "single flight" hypobaria after one flight at either 24 hours or 72 hours. Fourth, exposure to hypobaria under 100% O_2 at 24 hours after the blast resulted in greater silver staining in the internal capsule and a higher number of foot-faults on the balance beam than either sham or blast-exposed rats that underwent the same hypobaria under 21% O_2. Together, these data highlight the need for additional studies on when it is safest to conduct AE of mild underbody blast patients and under what supplemental O_2 conditions.

The rat model of TBI induced by undervehicle, blast-induced acceleration was similar to the model we reported earlier,[15] except that the standoff distance between the explosive and the bottom plate (hull) was calibrated to result in 100G peak acceleration rather than 30G to 50G. The less than 1-psi change in barometric pressure to which the rats were exposed during blasts that generated 100G was negligible compared with the survivable increases in pressure of at least 20 psi generated by compressed gas-driven shock tube models of exposure to open field blast.[9] Thus, the main force experienced by the rats in this underbody blast model is acceleration, modeling undervehicle blasts, whereas the main force in effect during most of the blast tube experiments is rapid changes in barometric pressure, also known as blast overpressure, modeling open field blast exposure.

All rats except for two that were exposed to 100G acceleration survived and appeared completely normal during the 7 days after the blast or sham blast anesthesia. One of the two rats died during the blast procedure and the other died within 24 hours later. The scaling of acceleration injury between human and rodent is incompletely characterized. A 100G impulse shock in humans results in severe injury, most likely due to the larger absolute mass of each internal organ, whereas the same 100G absolute acceleration in rats results in injuries at the mild end of the survival scale. The 100G acceleration force in the rodent model enabled us to quantify damage to white matter from mild TBI, using the de Olmos silver staining method for identifying degenerating axons present at 7 days postinjury. Additional evidence that diffuse axonal injury occurs in response to the underbody blast-induced acceleration comes from diffusion tensor magnetic resonance imaging. Recent magnetic resonance imaging measurements demonstrated a reduction in mean water diffusivity, axial diffusivity, and radial diffusivity in the internal capsule and corpus callosum at 1 day to 7 days after exposure of rats to 700G underbody blasts.[16] After exposure to a 100G blast alone in the absence of hypobaria, there was an approximate doubling of silver-stained neurons in the internal capsule compared to the background observed in sham animals. Strikingly, this elevated injury induced by hypobaria was present whether the simulated AE "flight" occurred at 6 hours postinjury or at 6 days. This observation suggests that there is a window of sensitivity to further injury from hypobaria in mild TBI that exists for at least 6 days. This "second hit" hypothesis is consistent with the literature on concussion injury that has identified a prolonged window of sensitivity to additional stressors,[17,18] of which hypobaria may be one such stressor, as shown in the present study.

Qualitatively, similar sensitization of the injured brain to secondary damage caused by exposure to hypobaria is observed after moderate TBI in rats using a lateral fluid compression model.[4] In this model, exposure to hypobaria at 6 hours, 24 hours, and 72 hours postinjury resulted in elevated neuron loss in CA1, CA2/3, and dentate gyrus hippocampal neurons measured at 30 days. In addition, the number of activated microglia present in the ipsilateral cortex was elevated by exposure to hypobaria out to 1 month. Animals injured by the lateral fluid percussion (LFP) model exhibited worse spatial memory after two 8,000-feet hypobaria exposures compared to one.[4] This finding is in contrast to the present study, which did not provide evidence for greater diffuse axonal injury when rats were exposed to hypobaria at 24 hours followed 2 days later by another exposure, in comparison with the injury observed after a single flight at either 24 hours or 72 hours. This difference could be attributed to the more mild TBI induced by acceleration compared to LFP, consistent with our observations of little to no detectable neuronal cell death after 30G to 100G blasts,[15] whereas substantial cortical and hippocampal death accompanies the LFP TBI model.[4]

Deleterious effects of exposure to hyperoxia during hypobaria were observed both with the underbody blast and

the LFP models. In the present blast TBI study, the presence of 100% O_2 in the flight chamber during hypobaria at 24 hours postinjury significantly increased the number of silver-stained axons in the internal capsule, in comparison with the number observed after hypobaria in the chamber flushed with 21% O_2 (room air). Hyperoxic hypobaria also resulted in significant impairment in balance beam performance under conditions where no deficit was observed after exposure to hypobaria in the chamber flushed with 21% O_2. In the LFP study, Morris water maze measurements of cognition were also worse after exposure to hyperoxic hypobaria compared with normoxic hypobaria.[4] Based on previous findings with animal models of both traumatic and global ischemic brain injury, the most likely explanation for the deleterious effects of hyperoxia during hypobaria is exacerbation of reactive oxygen species generation, neuroinflammation, oxidative modification of macromolecules, and impaired cerebral energy metabolism.[19–21]

The worsening of neuropathology and neurologic outcomes observed when rats were exposed to 100% O_2 during hypobaria does not necessarily contraindicate the use of more modest supplemental O_2 levels during aeromedical transport. For instance, inspired O_2 in the range of 40% to 60% might be sufficient to counteract any potential cerebral hypoxia that can occur under hypobaric conditions in injured patients,[5] without resulting in systemic and cerebral hyperoxia. As we have shown with animal models of resuscitation after cardiac arrest,[22] the use of pulse oximetry measurements of hemoglobin O_2 saturation may be the most practical and safe approach to titration of supplemental O_2, with the goal of avoiding both hyperoxia and hypoxia. Further study is needed to determine if a similar oximetry-titrated oxygen therapy can balance the competing needs of reduced oxidative hyperoxic stress on TBI with providing sufficient oxygen to limit any potential hypobaric hypoxia.

The results of this study taken together with others using different species (mice and swine) and different TBI models (weight drop, LFP, and controlled cortical impact) indicate that exposure to AE-relevant hypobaria as early as 3 hours and as late as 6 days can worsen a variety of neurooutcomes.[4,5,23] These findings clearly raise concern about the rapid air transport of both military and civilian TBI victims. There are, however, several limitations to these studies that should be recognized. In particular, all of the animal studies to date have used models of isolated TBI. Many moderate to severe TBI victims suffer from additional trauma and related disorders, for example, pulmonary atelectasis, coagulopathies, systemic inflammatory response syndrome, infectious and noninfectious sepsis, and others. These comorbidities can result in systemic conditions that could have a major impact on the effects of hypobaria on the brain and other vital organs. Often times, tactical considerations mandate AE of these casualties so if the risks cannot be avoided, they should be minimized if possible. The increasingly rapid throughput of military trauma casualties from combat zones to top-level military medical centers with subspecialty expertise unavailable in the deployed theatre has likely reduced the overall morbidity and mortality after TBI and other traumatic injuries.[24] Nevertheless, hypobaria associated with AE may exacerbate many common combat injuries, and further study into mitigation of the hypobaria effect is critically needed. One study found that the complication rates for patients after AE when the cabin pressure altitude was restricted to between 4,000 feet and 6,000 feet were lower than in the absence of such restriction, when the cabin pressure is approximately 8,000 feet.[25] Thus, some combination of optimizing supplemental O_2 levels and other critical care variables, together with restricting the degree of hypobaria that patients experience during flights, may reduce medical complications.

Mitigating any lifelong impact of neurologic morbidity, in particular, is important to consider for long-term veteran care. One limitation of the present study is that outcome measures were restricted to a relatively short period of seven days after blast exposure. Our previous qualitative measurements of silver-stained axon fibers after underbody blasts that generated lower, 50G accelerations indicated a dramatic reduction in staining at 30 days compared with 7 days postblast.[15] This observation suggests reversibility of axon injury; however, quantitative measurements of normal axon density and function are needed to test this hypothesis. Moreover, neurobehavioral tests should be conducted for at least several months after a broad range of blast-induced G forces to determine if underbody blasts result in prolonged or secondary neuropsychologic aberrations relevant to the clinical diagnosis of chronic traumatic encephalopathy. Therefore, although the results of this study and others are cautionary, it should be stressed that additional translational preclinical and clinical research is necessary before changes in aeromedical transport guidelines should be made.

AUTHORSHIP

J.L.P. acquired the data and interpreted the results from the histology measurements. K.T.M. acquired the data and analyzed the results from the behavior measurements. R.F. assisted in the experimental design, based on his extensive experience with AE of military trauma victims. A.P. assisted with the data analysis and interpretation for the histology measurements. R.E.R. designed the hypobaria experiments. W.F. and U.L. designed and conducted the blast experiments. G.F. served as principal investigator and was involved with all aspects of study design, performance, and data analysis and interpretation. All authors also contributed to writing and editing the article.

DISCLOSURE

There are no financial, consultant, institutional, or relationship conflicts declared by any author. This work was supported by U.S. Air Force grant FA8650-11-2-6D04 and U.S. Army grant U.S. Army W81XWH-13-1-0016. The views expressed in this article are those of the authors and do not necessarily reflect the official policy or position of the Air Force, the Department of Defense, or the U.S. Government.

REFERENCES

1. Goodman MD, Makley AT, Lentsch AB, Barnes SL, Dorlac GR, Dorlac WC, Johannigman JA, Pritts TA. Traumatic brain injury and aeromedical evacuation: when is the brain fit to fly? *J Surg Res*. 2010;164:286–293.
2. Galvagno SM, Dubose JJ, Grissom TE, Fang R, Smith R, Bebarta VS, Shackelford S, Scalea TM. The epidemiology of Critical Care Air Transport Team operations in contemporary warfare. *Mil Med*. 2014;179:612–618.
3. Goodman MD, Makley AT, Huber NL, Clarke CN, Friend LA, Schuster RM, Bailey SR, Barnes SL, Dorlac WC, Johannigman JA, et al. Hypobaric hypoxia exacerbates the neuroinflammatory response to traumatic brain injury. *J Surg Res*. 2011;165:30–37.
4. Skovira JW, Kabadi SV, Wu J, Zhao Z, DuBose J, Rosenthal R, Fiskum G, Faden AI. Simulated aeromedical evacuation exacerbates experimental brain injury. *J Neurotrauma*. 2016;33:1292–1302.
5. Scultetus AH, Haque A, Chun SJ, Hazzard B, Mahon RT, Harssema MJ, Auker CR, Moon-Massat P, Malone DL, McCarron RM. Brain hypoxia is

exacerbated in hypobaria during aeromedical evacuation in swine with traumatic brain injury. *J Trauma Acute Care Surg*. 2016;81:101–107.
6. Helmick KM, Spells CA, Malik SZ, Davies CA, Marion DW, Hinds SR. Traumatic brain injury in the US military: epidemiology and key clinical and research programs. *Brain Imaging Behav*. 2015;9:358–366.
7. Tchantchou F, Fourney WL, Leiste UH, Vaughan J, Rangghran P, Puche A, Fiskum G. Neuropathology and neurobehavioral alterations in a rat model of traumatic brain injury to occupants of vehicles targeted by underbody blasts. *Exp Neurol*. 2017;289:9–20.
8. Tenkova TI, Goldberg MP. A modified silver technique (de Olmos stain) for assessment of neuronal and axonal degeneration. *Methods Mol Biol*. 2007;399: 31–39.
9. Wang Y, Wei Y, Oguntayo S, Wilder D, Tong L, Su Y, Gist I, Arun P, Long JB. Cerebrospinal fluid chemokine (C-C Motif) ligand 2 is an early-response biomarker for blast-overpressure-wave-induced neurotrauma in rats. *J Neurotrauma*. 2017;34:952–962.
10. McGinn MJ, Povlishock JT. Pathophysiology of traumatic brain injury. *Neurosurg Clin N Am*. 2016;27:397–407.
11. Johannigman J, Gerlach T, Cox D, Juhasz J, Britton T, Elterman J, Rodriquez D Jr, Blakeman T, Branson R. Hypoxemia during aeromedical evacuation of the walking wounded. *J Trauma Acute Care Surg*. 2015;79:S216–S220.
12. Proctor JL, Scutella D, Pan Y, Vaughan J, Rosenthal RE, Puche A, Fiskum G. Hyperoxic resuscitation improves survival but worsens neurologic outcome in a rat polytrauma model of traumatic brain injury plus hemorrhagic shock. *J Trauma Acute Care Surg*. 2015;79:S101–S109.
13. Scafidi S, Racz J, Hazelton J, McKenna MC, Fiskum G. Neuroprotection by acetyl-L-carnitine after traumatic injury to the immature rat brain. *Dev Neurosci*. 2011;32:480–487.
14. Owens BD, Kragh JF Jr, Wenke JC, Macaitis J, Wade CE, Holcomb JB. Combat wounds in operation Iraqi Freedom and operation enduring freedom. *J Trauma*. 2008;64:295–299.
15. Proctor JL, Fourney WL, Leiste UH, Fiskum G. Rat model of brain injury caused by under-vehicle blast-induced hyperacceleration. *J Trauma Acute Care Surg*. 2014;77:S83–S87.
16. Tang S, Xu S, Fourney WL, Leiste UH, Proctor JL, Fiskum G, Gullapalli RP. Central nervous system changes induced by underbody blast-induced hyperacceleration: an *in vivo* diffusion tensor imaging and magnetic resonance spectroscopy study. *J Neurotrauma*. Epub March 17, 2017.
17. Corrigan F, Mander KA, Leonard AV, Vink R. Neurogenic inflammation after traumatic brain injury and its potentiation of classical inflammation. *J Neuroinflammation*. 2016;13:264.
18. Hovda DA. The neurophysiology of concussion. *Prog Neurol Surg*. 2014;28: 28–37.
19. Hazelton JL, Balan I, Elmer GI, Kristian T, Rosenthal RE, Krause G, Sanderson TH, Fiskum G. Hyperoxic reperfusion after global cerebral ischemia promotes inflammation and long-term hippocampal neuronal death. *J Neurotrauma*. 2010;27:753–762.
20. Ahn ES, Robertson CL, Vereczki V, Hoffman GE, Fiskum G. Normoxic ventilatory resuscitation following controlled cortical impact reduces peroxynitrite-mediated protein nitration in the hippocampus. *J Neurosurg*. 2008;108: 124–131.
21. Richards EM, Fiskum G, Rosenthal RE, Hopkins I, McKenna MC. Hyperoxic reperfusion after global ischemia decreases hippocampal energy metabolism. *Stroke*. 2007;38:1578–1584.
22. Balan IS, Fiskum G, Hazelton J, Cotto-Cumba C, Rosenthal RE. Oximetry-guided reoxygenation improves neurological outcome after experimental cardiac arrest. *Stroke*. 2006;37:3008–3013.
23. Yang SH, Gustafson J, Gangidine M, Stepien D, Schuster R, Pritts TA, Goodman MD, Remick DG, Lentsch AB. A murine model of mild traumatic brain injury exhibiting cognitive and motor deficits. *J Surg Res*. 2013;184: 981–988.
24. Blackbourne LH, Baer DG, Eastridge BJ, Renz EM, Chung KK, DuBose J, Wenke JC, Cap AP, Biever KA, Mabry RL, et al. Military medical revolution: deployed hospital and en route care. *J Trauma Acute Care Surg*. 2012;73:S378–S387.
25. Butler WP, Steinkraus LW, Burlingame EE, Fouts BL, Serres JL. Complication rates in altitude restricted patients following aeromedical evacuation. *Aerosp Med Hum Perform*. 2016;87:352–359.

APPENDIX 3

Tang S, Xu S, Fourney WL, Leiste UH, Proctor JL, Fiskum G, Gullapalli RP. Central Nervous System Changes Induced by Underbody Blast-Induced Hyperacceleration: An in Vivo Diffusion Tensor Imaging and Magnetic Resonance Spectroscopy Study. J Neurotrauma. 2017 Jun 1;34(11):1972-1980. PMID: 28322622.

JOURNAL OF NEUROTRAUMA 34:1972–1980 (June 1, 2017)

DOI: 10.1089/neu.2016.4650

Central Nervous System Changes Induced by Underbody Blast-Induced Hyperacceleration: An *in Vivo* Diffusion Tensor Imaging and Magnetic Resonance Spectroscopy Study

Shiyu Tang,[1,2] Su Xu,[1,2] William L. Fourney,[3,4] Ulrich H. Leiste,[3,4] Julie L. Proctor,[5,6] Gary Fiskum,[5,6] and Rao P. Gullapalli[1,2]

Abstract

Blast-related traumatic brain injury (bTBI) resulting from improvised explosive devices is the hallmark injury of recent wars, and affects many returning veterans who experienced either direct or indirect exposure. Many of these veterans have long-term neurocognitive symptoms. However, there is very little evidence to show whether blast-induced acceleration alone, in the absence of secondary impacts, can cause mild TBI. In this study, we examine the effect of under-vehicle blast-induced hyperacceleration (uBIH) of ~1700 g on the biochemical and microstrucutral changes in the brain using diffusion tensor imaging (DTI) and magnetic resonance spectroscopy (MRS). Two groups of adult male Sprague–Dawley (SD) rats were subjected to a sham procedure and uBIH, respectively. Axonal and neurochemical alterations were assessed using *in vivo* DTI and MRS at 2 h, 24 h, and 7 days after uBIH. Significant reduction in mean diffusivity, axial diffusivity, and radial diffusivity were observed in the hippocampus, thalamus, internal capsule, and corpus callosum as early as 2 h, and sustained up to 7 days post-uBIH. Total creatine (Cr) and glutamine (Gln) were reduced in the internal capsule at 24 h post-uBIH. The reductions in DTI parameters, Cr and Gln *in vivo* suggest potential activation of astrocytes and diffuse axonal injury following a single underbody blast, confirming previous histology reports.

Keywords: DTI; hyperacceleration; MRS; underbody blast

Introduction

Accumulating clinical evidence, as well as experience from contemporary military operations, suggests that substantial short- and long-term neurological deficits can result from blast exposure in the absence of a mechanical hit to the head. [1–5] Although the biological mechanisms underlying blast-induced traumatic brain injury (bTBI) are not completely understood, interaction with a fast-moving, transient pressure wave is generally accepted as the primary cause of brain injury that results from blast exposure.[3,6–8] Over the last few decades, a number of experimental blast models have been implemented to study the mechanisms of blast overpressure impact in rodents and larger animals such as sheep. [9–11] A common methodology is to use a shock tube where a gas-driven pressure wave is delivered directly to the immobilized animal's head or body. Experimental studies in rodents have demonstrated a correlation between memory dysfunction and distribution of neuropathological damage in the brain after exposure to blast overpressure.[12,13] However, in addition to blast overpressure, a multitude of other physical forces may play a role in bTBI, including thermal components and hyperacceleration. Recently, we described the development of a new device[14] that can be used to induce underbody blast-induced hyperacceleration (uBIH) in rodents. Our uBIH paradigm models what occurs to occupants of vehicles targeted by land mines, rather than what occurs when an explosion occurs in the vicinity of an unmounted soldier. Using this device, we demonstrated that exposure of rats to uBIH results in histopathological evidence of diffuse axonal injury and potential astrocyte activation under conditions resulting in an accelerative load of 50 g, indicating that hyperacceleration alone in the absence of significant blast pressure can cause mild TBI. Whether these subtle changes are discernible *in vivo* through advanced imaging has not been examined. The ability to accurately diagnose changes in the brain *in vivo* can have a profound impact on the appropriate therapeutic management of the patient.

[1]Department of Diagnostic Radiology and Nuclear Medicine, [2]Core for Translational Research in Imaging at Maryland, [5]Department of Anesthesiology, and [6]Shock, Trauma, and Anesthesiology Research Center, University of Maryland, Baltimore, Maryland.
[3]Department of Mechanical Engineering, and [4]Center of Energetics Concepts Development, University of Maryland, College Park, Maryland.

Several advanced *in vivo* imaging techniques, including diffusion tensor imaging (DTI) and proton magnetic resonance spectroscopy (MRS), have been explored to study TBI in pre-clinical animal models, to better understand the temporal microstructural and biochemical changes following TBI.[15–21] Commonly used DTI parameters include mean diffusivity (MD) and fractional anisotropy (FA). MD measures the average water diffusion within the brain tissue, whereas FA measures the degree of diffusion anisotropy present within a voxel, as would be in the case of axons where water diffuses preferentially along the axon. Alterations in MD reflect pathological changes in the brain tissue caused by changes in the diffusion characteristics of the intra- and extracellular water compartments, including restricted diffusion (cytotoxic edema) and water exchange across permeable boundaries.[22] Changes in the FA, on the other hand, are indicative of the structural integrity of the tissue. The sub-parameters of FA include axial diffusivity (AD) and radial diffusivity (RD). Diffusion along the axon is measured by AD, and is a measure of axonal integrity, whereas RD measures diffusion across the axon and is reflective of myelin integrity.[23] Previous TBI studies on both humans and animals have shown altered MD[24–27] and FA in white matter regions [19,28–33] anywhere from 24 h to several days following injury, reflecting pathological conditions such as edema, fiber degeneration, cellular membrane disruption, and cell death.[20,32,34,35] High-resolution *in vivo* MRS provides complementary information and assesses metabolic irregularities following injury. Several metabolites such as *N*-acetylaspartate (NAA), choline (Cho), and lactate (Lac) are highly sensitive to the pathology that contributes to TBI. Reduction in concentration of NAA, glutamate (Glu), creatine (Cr), myo-inositol (Ins), and taurine (Tau) in tissues and increased concentrations of lactate, phosphocholine (PCho), and glutamine (Gln) at either acute or subacute stages have been reported, indicating conditions including ischemia, mitochondrial dysfunction, and imbalance of excitatory/inhibitory and astrocyte activation.[20,21,36,37] In this study, we use both *in vivo* DTI and MRS to evaluate early microstructural and biochemical alterations caused by uBIH in the rat brain.

Methods

Animal preparation

Six adult male Sprague–Dawley (SD) rats weighing 300–350 g underwent the uBIH procedure as described by Proctor and coworkers,[14] and another group of six male SD rats in the same weight range were assigned to be the sham group.[14] Briefly, all rats were initially anesthetized with ketamine (80 mg/kg) and xylazine (10 mg/kg). Each of two rats belonging to the uBIH group was wrapped in 2 cm thick cotton blankets to minimize movement, and placed in the prone position in one of two aluminum cylinders, 37 cm long by 3 cm wide, which was bolted onto a 38 cm^2 and 5 cm thick aluminum platform. This platform was located immediately above a second 38 cm^2 aluminum platform that was 2.5 cm thick. A 0.6 cm thick hard rubber pad was placed between the two platforms to dampen oscillatory accelerations. Both platforms had 2.5 cm wide holes located inside each of the four corners. Aluminum rods 90 cm high were inserted through each of the holes and secured to a steel base on which the platforms rested, thus allowing for only direct movement of the platforms vertically following the blasts. The steel base was bolted to the edges of a steel tank filled with water to a standoff distance of from the bottom platform of 0.25 cm. An explosive charge of 1.5 g pentaerythritol tetranitrate was placed in the water 5 cm under the center of the plate, which when detonated, generated maximal *g* forces of $1734 \pm 90g$ (mean ± SEM; $n = 6$) as measured by an accelerometer attached to the top plate near the head ends of the cylinders. The explosion caused the plate to accelerate vertically to heights of ~70 cm and then drop back down to the original location. During two experiments, we also attached pressure sensors to the top plate near the accelerometer. An increase of <1 psi was observed. Following the uBIH exposure, the rats were removed from the assembly and allowed to recover from the anesthesia. All animals recovered normal activity within 1 h and exhibited no signs of distress. Following the imaging measurements performed on day 7 after sham or blast exposure, the rats were euthanized.

In vivo *DTI and ^{1}H MRS*

MR experiments were performed prior to the uBIH/sham procedure (baseline), 2 h, 24 h, and 7 days post-uBIH on a BrukerBioSpec 7.0 Tesla 30 cm horizontal bore scanner (Bruker Corporation, Ettlingen, Germany) equipped with a BGA12S gradient system and interfaced to a BrukerParaVision 5.1 console. A Bruker 72 mm linear-volume coil was used as the transmitter, and a Bruker ^{1}H four channel surface coil array was used as the receiver. The rat was under 2–3% isoflurane anesthesia and 1 L/min oxygen administration during the MR experiment. An MR compatible small-animal monitoring and gating system (SA Instruments, Inc., New York, NY) was used to monitor the animal's respiration rate and body temperature. The animal's body temperature was maintained at 35–37°C using a warm water bath circulation. Ear pins and bite bars were used to fix the animal's head to minimize head motion.

A three slice (axial, midsagittal, and coronal) scout image using rapid acquisition with fast low angle shot (FLASH) [38,39] was used to localize the rat brain. A fast shimming procedure (FASTMAP) was used to improve the B_0 homogeneity covering the brain.[40] Both proton density (PD) and T2-weighted images were obtained for anatomic reference using a two-dimensional rapid acquisition with relaxation enhancement (RARE) sequence covering the entire brain. [41] Imaging was performed over a 3.5 cm field of view (FOV) in the coronal plane with an in-plane resolution of 137 μm using 24 slices at 1 mm thickness, at an effective echo time (TE) of 18.94 ms for the PD-weighted images and an effective TE of 56.82 ms for the T2-weighted images. The repeat time (TR) was 3500 ms.

Diffusion tensor images were acquired with a single shot, spin-echo echo-planar imaging sequence. An encoding scheme of 30 gradient directions was used with the duration of each of the diffusion gradients being 4 ms with a temporal spacing of 20 ms between the two diffusion gradients. Three b-values (1000 sec/mm^2, 1500 sec/mm^2, and 2000 sec/mm^2) were acquired for each direction following the acquisition of five images acquired at $b = 0$ sec/mm^2. The diffusion tensor images were obtained using a single average over the same FOV as the coronal PD/T2 images, but at an in-plane resolution of 0.273 mm at a TR/TE of 6000/49.90 ms respectively.

^{1}H MRS data were obtained from voxels that covered the left internal capsule ($3 \times 3 \times 3$ mm^3), left hippocampus ($1.5 \times 3.5 \times 3$ mm^3), and left cortex ($1.5 \times 4 \times 3$ mm^3) respectively. These regions were chosen because they were implicated in a previous study using the same injury model and also based on reports using other TBI models.[14,36] Prior to acquiring the spectra, adjustments of all first- and second-order shims over the voxel of interest were accomplished with the FASTMAP procedure. A custom modified short-echo-time PointRESolved Spectroscopy (PRESS) pulse sequence (TR/TE = 2500/10 ms, number of averages = 360)[42] was used for MRS data acquisition covering the three regions of interest (ROI). The unsuppressed water signal from each of the prescribed voxels was obtained to serve as a reference for determining the specific metabolite concentrations. The total duration of the entire imaging experiment was ~2.5 h. All animal procedures were approved by the University of Maryland, Baltimore, Animal Care and Use Committee, and by the United States Army Medical Research and Materiel Command Animal Care and Use Review Office.

Data processing and analysis

DTI reconstruction was performed on each voxel using in-house MATLAB program (Mathworks, Natick, MA) to generate MD, FA, AD, and RD maps. ROIs for each rat were manually drawn on the FA map within the cortex (left, right), hippocampus (left, right), thalamus (left, right), internal capsule (left, right), and corpus callosum (genu, trunk, splenium), respectively, as shown in Figure 1A. ^{1}H MRS data were fitted using the LCModel package.[43] Representative *in vivo* high resolution ^{1}H MRS from the internal capsule from one uBIH rat at its baseline is shown in Figure 1B. The Cramer-Rao lower bounds were estimated by the LCModel to assess the reliability of the reported metabolite concentration, and only metabolites with standard deviations (SD) <20 were included for further analysis.

DTI and MRS data from each region were normalized to its own baseline level (pre-uBIH). The ratio of post to pre-uBIH level was used to capture changes between the two time points. Statistical analysis was performed using SigmaPlot version 12.5 (Systat Software, Inc., San Jose, CA). Both DTI and MRS data of sham and uBIH rats at four time points were analyzed using a two way repeated measures ANOVA to examine temporal changes in each region, and group comparisons were made at each observation point. Statistical significance was defined as $p < 0.05$.

Results

Microstructural alterations after uBIH

Six rats were exposed to uBIH that generated maximal *g* forces ranging from 1500 to 1900*g*, with a mean value of $1734 \pm 90g$. All of these rats and the six sham rats that were similarly anesthetized but not subjected to uBIH survived to 7 days, at which time they were euthanized. No animal demonstrated any visible changes on T2-weighted brain images at 2 h, 24 h, and 7 days post-blast or post-sham blast. However, broad reductions of DTI parameters were observed in the hippocampus, thalamus, and internal capsule of rats in the uBIH group compared with the sham group. Significant alterations of MD were observed in the hippocampus (right: $F = 2.44$, $p = 0.017$), and the thalamus (left: $F = 7.092$, $p = 0.024$; right: $F = 5.257$, $p = 0.045$) (Table 1) in the uBIH rats compared with the sham group. The reductions of MD were significant at 2 h ($p = 0.044$) and 7 days ($p = 0.025$) in the hippocampus (Fig. 2A) and at 24 h in the thalamus (left: $p = 0.008$; right: $p = 0.018$) (Fig. 2B, C) in the uBIH cohort compared with the sham cohort. AD was significantly reduced in the hippocampus (right: $F = 7.208$, $p = 0.023$) (Table 1) at 24 h ($p = 0.006$) and 7 days ($p = 0.008$) (Fig. 3A) and in the internal capsule (right: $F = 5.222$, $p = 0.045$) at 24 h ($p = 0.006$) (Fig. 3B) in the uBIH group compared with the sham group. RD was significantly reduced in the thalamus (left: $F = 14.291$, $p = 0.004$; right: $F = 7.861$, $p = 0.019$) (Table 1) at 2 h (left: $p < 0.001$; right: $p = 0.001$), 7 days (left: $p = 0.013$; right: $p = 0.041$) (Fig. 4A,B) and in the genu of the corpus callosum ($F = 8.407$, $p = 0.016$) at 2 h ($p = 0.031$) and 7 days ($p = 0.004$) (Fig. 4C) after uBIH.

Biochemical alterations after uBIH

Biochemical alterations were observed in the internal capsule where changes in the levels of Cr ($F = 5.844$, $p = 0.036$) were substantial, and marginal Gln ($F = 3.877$, $p = 0.077$) changes were also observed in the uBIH group compared with the sham group (Table 1). Both Cr ($p = 0.005$) and Gln ($p = 0.021$) levels were significantly reduced at 24 h in the uBIH group compared with the sham group (Fig. 5). No other significant biochemical alterations were detected in any other regions at any time points in the uBIH rats compared with the sham rats.

Discussion

To the best of our knowledge, this is the first *in vivo* study to apply a combination of DTI and MRS to detect biochemical and microstructural changes following hyperacceleration from a blast in isolation from the overpressure from the blast (primary impact) or other secondary impact-related injuries. We demonstrate early metabolic alterations and tissue microstructure following hyperacceleration, which persist until 7 days following the exposure. Our study reveals three main findings: 1) no visible brain injuries were observed on conventional T2-weighted imaging, even when the animals were exposed to an average of 1700*g*; 2) Cr and Gln levels

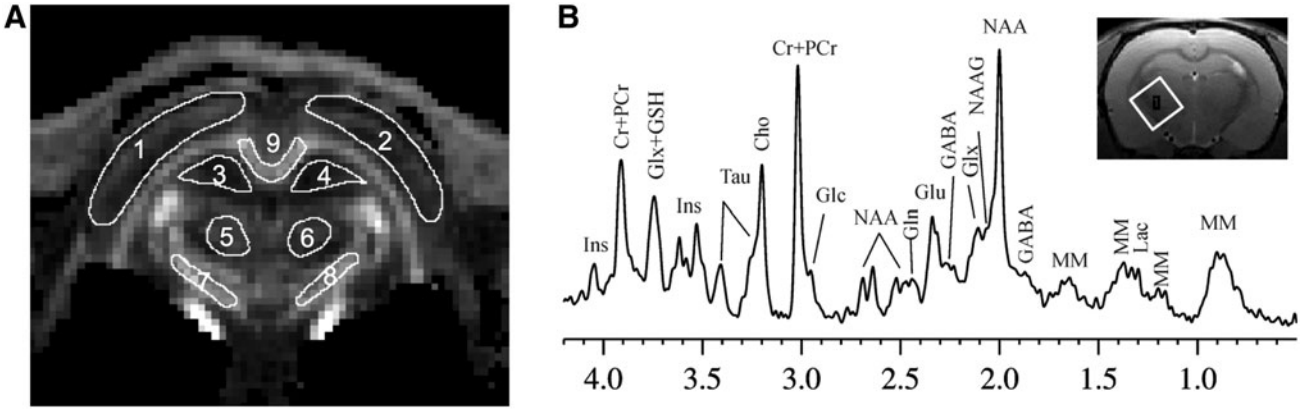

FIG. 1. **(A)** Placement of diffusion tensor imaging (DTI) regions of interest (ROIs) (white contours) on coronal fractional anisotropy (FA) maps. 1. left cortex; 2. right cortex; 3. left hippocampus; 4. right hippocampus; 5. left thalamus; 6. right thalamus; 7. left internal capsule; 8. right internal capsule; 9. corpus callosum (genu and splenium corpus callosum are on the most anterior and posterior slices respectively; corpus callosum on other slices are grouped to trunk corpus callosum). **(B)** Representative *in vivo* high resolution ^{1}H magnetic resonance spectroscopy (MRS) from the internal capsule (white box) from one under-vehicle blast-induced hyperacceleration (uBIH) rat at its baseline. creatine+phospocreatine (Cr+PCr); γ aminobutyric acid (GABA); glucose (Glc); glutamine (Gln); glutamate (Glu); Glu+Gln (Glx); myo-inositol (Ins); lactate (Lac); macromolecules (MM); *N*-acetylaspartate (NAA); *N*-acetylaspartyl glutamic acid (NAAG); taurine (Tau).

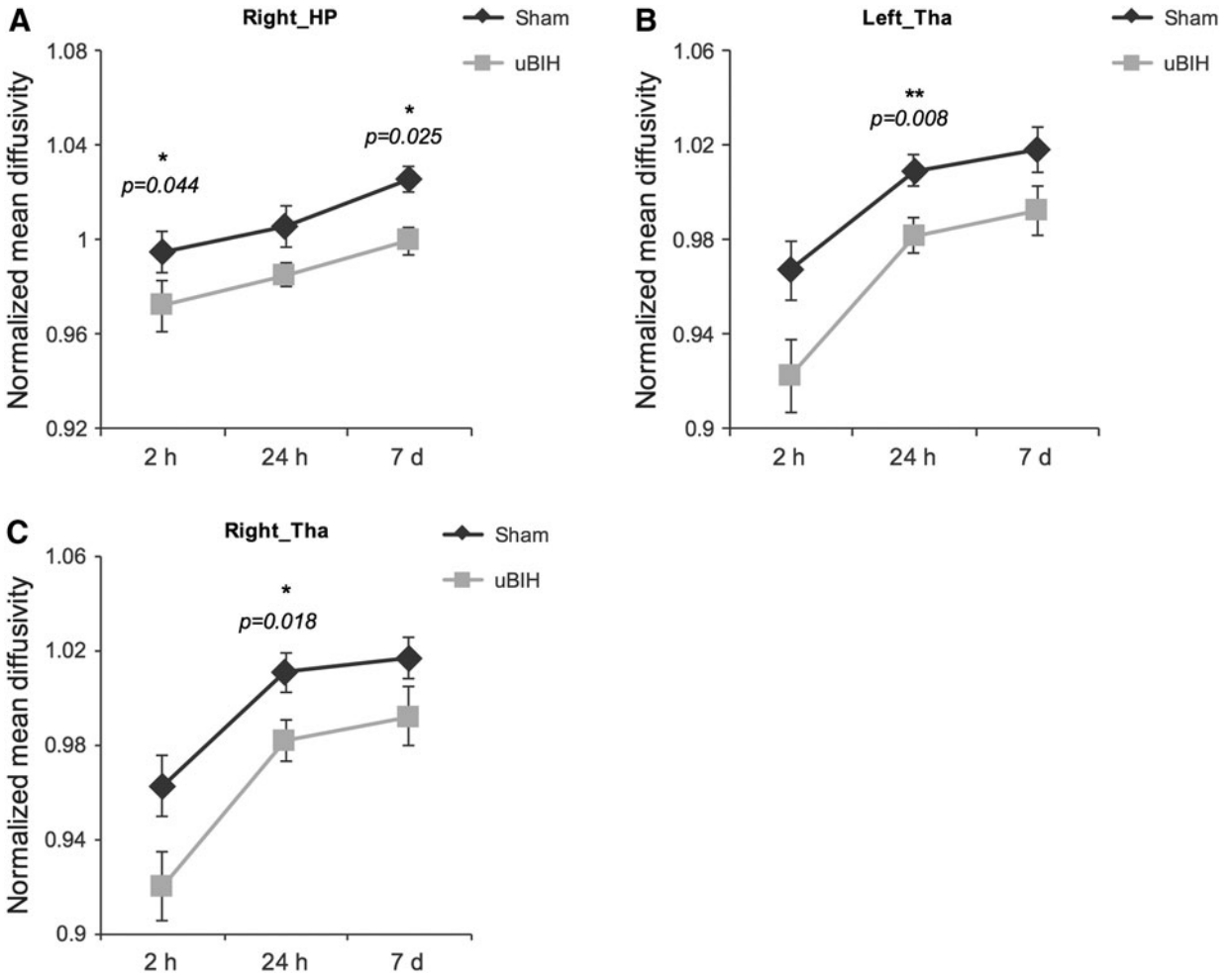

FIG. 2. Mean diffusivity alterations (ratio to baseline level) in right hippocampus (HP) **(A)**, and left **(B)** and right **(C)** thalamus (Tha) from 2 h to 7 days post- under-vehicle blast-induced hyperacceleration (uBIH). $*p<0.05$, $**p<0.01$.

decreased in the internal capsule at 24 h post-uBIH, and returned to baseline values by 7 days; and 3) shearing injuries as observed by changes in diffusion tensor parameters were observed in the internal capsule corpus callosum, hippocampus, and thalamus as late as 7 days following injury. When compared with the histological findings from our previous study performed under conditions that generated much lower *g* forces (50*g*), and that resulted in diffuse axonal injury and astrocyte activation,[14] the present study not only confirms these findings, but also provides further evidence that neuropathology changes can be detected *in vivo* using DTI and MRS techniques.

In the present study, decreased AD level in the internal capsule at 24 h, decreased RD to the corpus callosum, and decreased MD and AD levels in the hippocampus at both 2 h and 7 days post-uBIH are indicative of mild diffuse axonal injuries, which agrees with the histology findings using the same uBIH model.[14] In addition to these changes, we also observed a decreased MD at 24 h and decreased RD at 2 h and 7 days post-uBIH in the thalamus, indicating cell swelling. These results indicate that the sequelae of pathological events occur at a different rate in each vulnerable brain, which is well captured noninvasively from the longitudinal DTI data. The low Cr and Gln levels found in the uBIH rats at 24 h in the internal capsule may indicate an imbalance in astrocytic function after exposure to uBIH. Synthesized in the liver and transported to the brain,

Table 1. Brain Regions with Significant Changes in Diffusion and Spectroscopy Parameters

DTI	*Right_HP*	*Left_Tha*	*Right_Tha*	*Right_IC*	*CC_gn*
Mean diffusivity	$F=8.244$ $p=0.017$	$F=7.029$ $p=0.024$	$F=5.257$ $p=0.045$		
Axial diffusivity	$F=7.208$ $p=0.023$			$F=5.222$ $p=0.045$	
Radial diffusivity		$F=14.291$ $p=0.004$	$F=7.861$ $p=0.019$		$F=8.407$ $P=0.016$

MRS	*Left_IC*
Creatine	*$F=5.844$* *$p=0.036$*
Glutamine	*$F=3.877$* *$p=0.077$*

DTI, diffusion tensor imaging; MRS, magnetic resonance spectroscopy; HP, hippocampus; Tha, thalamus; IC, internal capsule; CC_gn, genu of corpus callosum).

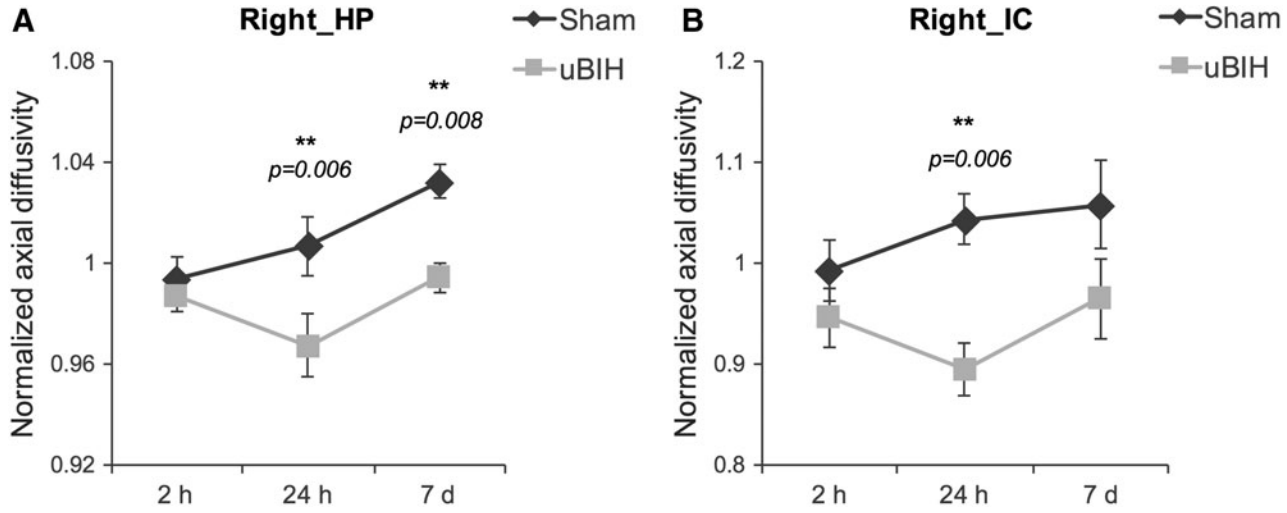

FIG. 3. Axial diffusivity alterations (ratio to baseline level) in right hippocampus (HP) **(A)** and right internal capsule (IC) **(B)** across three time points. $^{**}p < 0.01$.

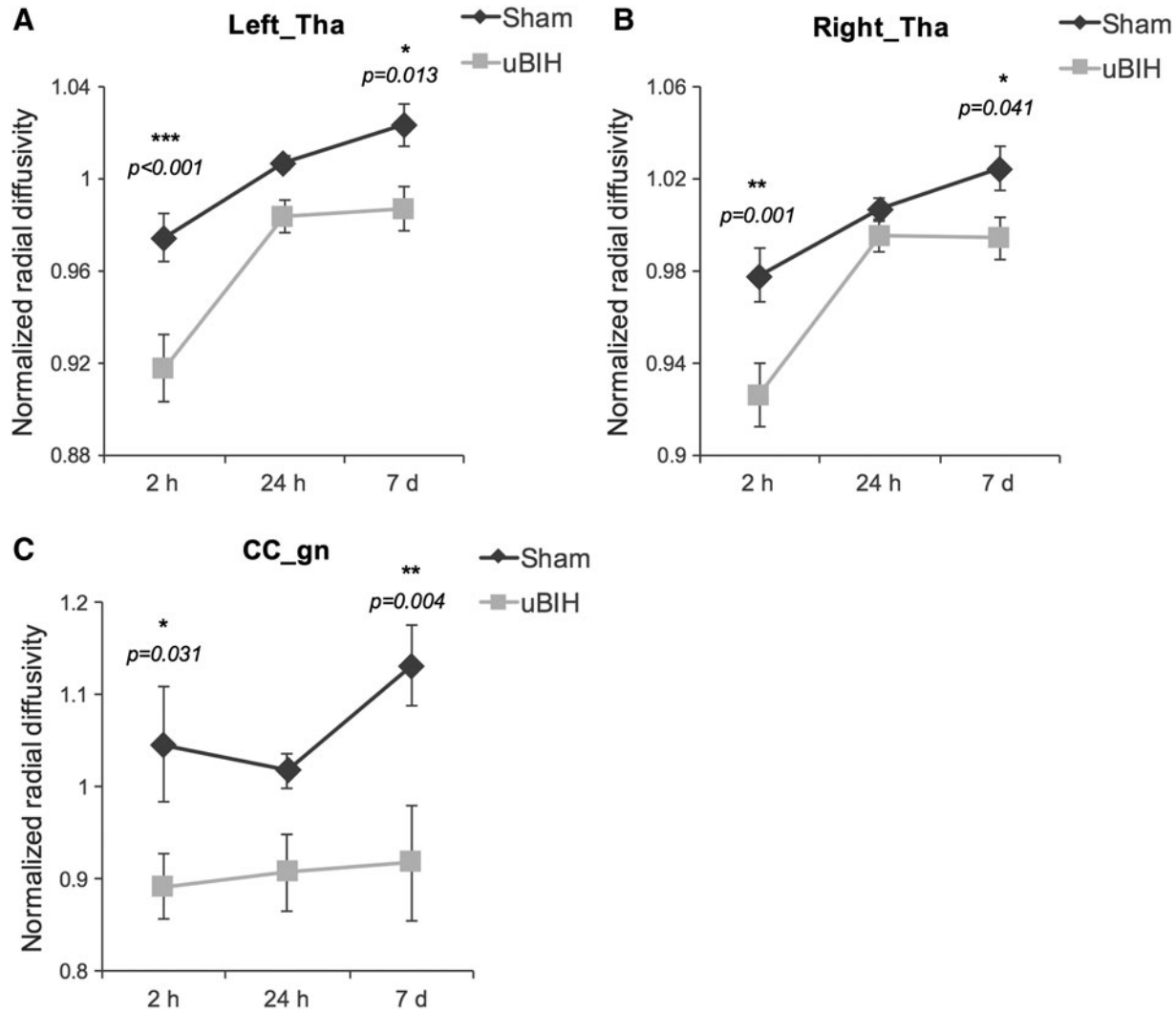

FIG. 4. Radial diffusivity alterations (ratio to baseline level) in left **(A)** and right **(B)** thalamus (Tha), and genu of corpus callosum (CC_gn) **(C)** across three time points. $^{*}p < 0.05$, $^{**}p < 0.01$, $^{***}p \leq 0.001$

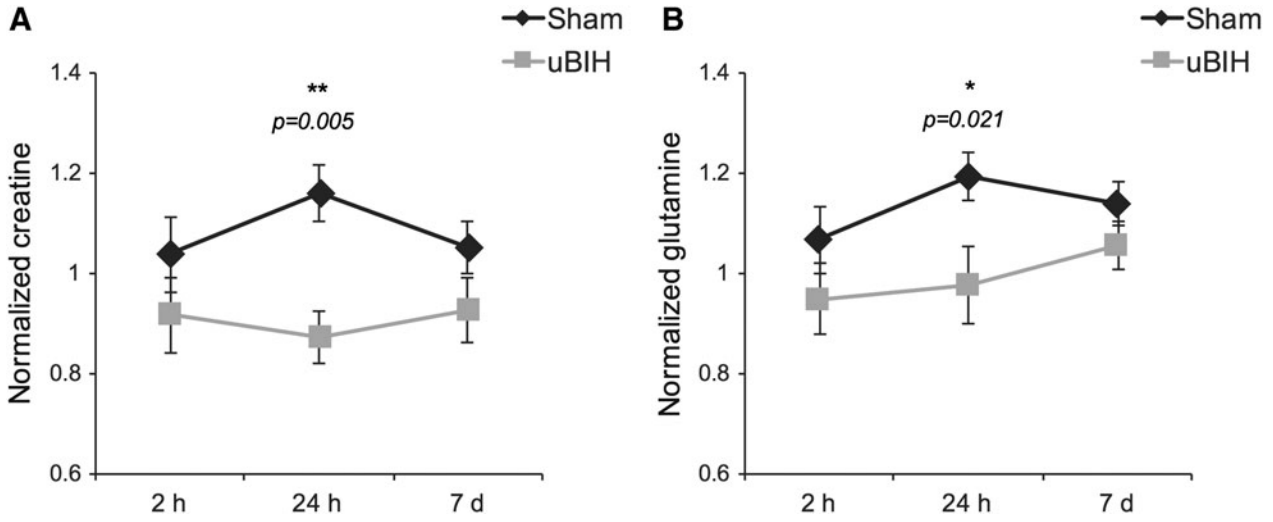

FIG. 5. Changes in creatine **(A)** and glutamine **(B)** relative to baseline in the internal capsule across three time points. $*p < 0.05$, $**p < 0.01$.

it has been shown that Cr is two- to four-fold more concentrated in glial cells than in neurons,[44] with quite large regional variations. Astroglial cells are virtually the sole site for Gln synthetase activity in the brain to convert Glu to Gln.[45] A prior study using this injury model demonstrated astrocyte activation in the internal capsule at 7 days post-uBIH.[14] It is, therefore, likely that the depletions of Cr and Gln are related to this astrocyte activation. The *in vivo* longitudinal localized MRS findings in this study provide further evidence that gliosis in the internal capsule is a prominent pathology following uBIH.[14,36] Quantitative analyses of cellular inflammatory responses, axonal injury, and behavorial alterations are in progress to further characterize the pathophysiology of uBIH.

Various animal models have been developed to replicate different aspects of human TBI over the past several decades. The most widely used ones are the controlled cortical impact (CCI) model,[46] the fluid percussion injury (FPI) model,[47] and blast tube bTBI models.[48,49] CCI and FPI models result in direct brain deformation and neuronal cell death, which we have not detected in the uBIH model (not shown). Depending on the severity of injury, tissue damage from CCI and FPI is focal, and may be directly visible even with conventional MRI. Studies have shown that the changes from these focal injuries lead to various changes in local conditions including ischemia, mitochondrial dysfunction, and imbalance of excitatory/inhibitory and astrocyte activation.[15,20,37,50]

Studies using blast overpressure primary bTBI models are more comparable to our uBIH model because they do not introduce direct impact on the brain, and they result in relatively mild injuries without severe tissue damage and broad biochemical disturbances. In primary bTBI models, injury is generated by blast overpressure waves or shock waves to the head, and often to the chest and abdomen. Previous *in vivo* or *in vitro* primary bTBI studies using shock tube or direct cranial blast reported increased mean kurtosis (MK), Gln levels, and expression of glial fibrillary acidic protein (GFAP), indicating astrocyte and microglial activation in subcortical regions such as the internal capsule, hippocampus, and hypothalamus at the subacute stage following injury.[36,51,52] Diffuse axonal injury was also observed as increased FA in the internal capsule and decreased MD in the hippocampus up to 14 days post-blast, indicating axonal swelling or a disruption of ionic homeostasis resulting in an imbalance in intra- and extracellular water.[18,19,36] A more recent study assessed the value of manganese-enhanced magnetic resonance imaging (MEMRI) using manganese chloride ($MnCl_2$) at various time points following a 30 psig blast in a shock tube, and found manganese uptake to be a promising biomarker of TBI.[53] Although future preclinical studies on hyperacceleration may benefit form MEMRI, the use of manganese in humans has been shown to be neurotoxic, and the translation of such studies may take some time, as research continues to make less toxic manganese-based chelates.

The clinical relevance of results obtained using this small scale underbody blast model depend to some degree on the scaling of the *g* force and its relationship with the *g* forces experienced by individuals present within vehicles targeted by land mines and improvised explosive devices. The issue of scaling is important but not straightforward. To our knowledge, there are no empirical data from comparisons obtained with small or large animals exposed to small- and large-scale explosions relevant to under-vehicle blasts. The closest estimate is a scaling factor of 10, based on buried explosions of different intensities.[54] Experiments with full scale models of military vehicles indicate that land mines generate *g* force loads of between 200 and 4000*g* at floor level,[55] which would be somewhat lower at the level of the passenger. If indeed the *g* force scaling factor is close to 10, our explosions generating 1700*g* would be equivalent to a full-scale under-vehicle blast generating 170*g*, which is close to the measured level of 200*g* load on full- scale vehicles generated by commonly used explosives.

The present study demonstrates that in uBIH, the changes are localized primarily to the internal capsule and the hippocampus, with changes occurring at different time points, depending on the parameter measured and the brain location. The results show some consistency with previous primary bTBI reports. In a previous study on a direct cranium only blast traumatic brain injury (dc-bTBI) rat model that was silent on conventional T2-weighted imaging, diffusion kurtosis imaging (DKI), and proton MRSalso demonstrated impairments in the internal capsule and the hippocampus, with peak changes observed at $\sim$21 days after dc-bTBI.[36] Significant microglial activation and neurodegeneration were observed even at 28 days in the hippocampus.

It is generally accepted that TBI without physical signs of brain injury can potentially contribute to post-traumatic stress disorder (PTSD).[5,56] The hippocampus and the internal capsule are reported to play a role in triggering the typical symptoms of PTSD.[57–64] PTSD patients with a history of combat trauma show a considerable reduction in the volume of the hippocampus, and hippocampal dysfunction.[58–60] Treatments that resulted in neurogenesis in the hippocampus or increased hippocampal volume were shown to improve PTSD symptoms.[61,63,64] PTSD symptoms induced by mTBI are also associated with white matter damage to the internal capsule and uncinate fasciculus, inducing a loss of inhibitory control of the autonomic nervous system (ANS), which results in alterations in ANS-driven defense and socially adaptive physiological states.[57] Significantly reduced FA in the internal capsule was also reported to be closely related to major depressive disorder (MDD) after mTBI.[62] Although the present study did not assess the long-term behavioral outcome on the rats, given the spatial locations that are implicated in this study and the dc-bTBImodel, the results suggest the possibility of vestibular dysfunction and memory impairment.[34] Our findings also suggest that both the cranium-only blast injury and the hyperacceleration-associated injury may combine synergistically, resulting in comorbidities that are worse than from a single type of injury. This is a more likely scenario, in which a person exposed to blast injury may also be exposed to a certain amount of hyperacceleration.

This study on microstructural and biochemical alterations after uBIH should be viewed in the context of certain limitations. First, no studies were performed to assess the long-term behavioral outcomes of these animals. Although we expect similar behavior changes as in the dc-bTBI model, given the similarity in the regions affected, future studies should include comprehensive behavioral testing and correlate with *in vivo* findings. Second, histological confirmation was not possible on these animals at this time. However, histology results from the previous study using the same uBIH model are supportive of the observed results in this study.[12] Third, this study only used male rats, and, therefore, the results cannot be generalized across the sexes. The effect of sex on the outcomes and recovery of TBI has been emphasized in multiple clinical and animal studies.[65–68] Given the limitation of this pilot study, future longitudinal studies should incorporate behavioral testing of the animals and histological confirmation incorporating both sexes.

Conclusion

In this study, we demonstrate for the first time that uBIH alone in the absence of the blast overpressure component results in acute mild TBI that continues to persist up to 7 days post-uBIH. These findings offer useful information in understanding the pathophysiology of uBIH-induced mild TBI. uBIH induces diffuse axonal injury and astrogliosis in the internal capsule and hippocampus. Given that similar regions were implicated in dc-bTBI, it is likely that the hyperacceleration along with the ensuing blast may synergistically lead to more comorbidities in the long term. The internal capsule and hippocampus may be potential therapeutic targets for treating bTBI and preventing delayed mental health problems.

Acknowledgments

This material is based on research sponsored by the United States Army grant W81XWH-13-1-0016 and by the United States Air Force grant 711HPW/XPT under Cooperative Agreement numbers FA8650-11-2-6142 and FA8650-11-2-6D04. The United States government is authorized to reproduce and distribute reprints for governmental purposes notwithstanding any copyright notation thereon. The views expressed in this article are those of the authors and do not necessarily reflect the official policy or position of the Air Force, the Department of Defense, or the United States government.

Author Disclosure Statement

No competing financial interests exist.

References

1. Trudeau, D.L., Anderson, J., Hansen, L.M., Shagalov, D.N., Schmoller J., Nugent S., and Barton S. (1998). Findings of mild traumatic brain injury in combat veterans with PTSD and a history of blast concussion. J. Neuropsychiatry Clin. Neurosci. 10, 308–313.
2. Cernak, I., Savic, J., Ignjatovic, D., and Jevtic, M. (1999). Blast injury from explosive munitions. J. Trauma 47, 96–104.
3. DePalma, R.G., Burris, D.G., Champion, H.R., and Hodgson, M.J. (2005). Blast injuries. N. Engl J. Med 352, 1335–1342.
4. Ling, G., Bandak, F., Armonda, R., Grant, G., and Ecklund, J. (2009). Explosive blast neurotrauma. J. Neurotrauma 26, 815–825.
5. Elder, G.A., and Cristian, A. (2009). Blast-related mild traumatic brain injury: mechanisms of injury and impact on clinical care. Mt. Sinai J. Med. 76, 111–118.
6. Elsayed, N.M. (1997). Toxicology of blast overpressure. Toxicology 121, 1–15.
7. Taber, K.H., Warden, D.L., and Hurley, R.A. (2006). Blast-related traumatic brain injury: what is known? J. Neuropsychiatry Clin. Neurosci. 18, 141–145.
8. Przekwas, A., Somayaji, M.R., and Gupta, R.K. (2016). Synaptic mechanisms of blast-induced brain injury. Front. Neurol. 7, 2.
9. Savić, J. (1991). Primary blast injuries [in Serbian]. Vojnosanit Pregl 48, 489–498.
10. Stuhmiller, J.H. (1997). Biological response to blast overpressure: a summary of modeling. Toxicology 121, 91–103.
11. Garman, R.H., Jenkins, L.W., Switzer, R.C., Bauman, R.A., Tong, L.C., Swauger, P.V., Parks, S.A., Ritzel, D.V., Dixon, C.E., Clark, R.S., Bayir, H., Kagan, V., Jackson, E.K., and Kochanek, P.M. (2011). Blast exposure in rats with body shielding is characterized primarily by diffuse axonal injury. J. Neurotrauma 28, 947–959.
12. Cernak, I., Wang, Z., Jiang, J., Bian, X., and Savic, J. (2001). Ultrastructural and functional characteristics of blast injury-induced neurotrauma. J. Trauma 50, 695–706.
13. Cernak, I., Wang, Z., Jiang, J., Bian, X., and Savic, J. (2001). Cognitive deficits following blast injury-induced neurotrauma: possible involvement of nitric oxide. Brain Inj. 15, 593–612.
14. Proctor, J.L., Fourney, W.L., Leiste, U.H., and Fiskum, G. (2014). Rat model of brain injury caused by under-vehicle blast-induced hyperacceleration. J. Trauma Acute Care Surg. 77, S83–S87.
15. Mac Donald, C.L., Dikranian, K., Bayly, P., Holtzman, D., and Brody, D. (2007). Diffusion tensor imaging reliably detects experimental traumatic axonal injury and indicates approximate time of injury. J. Neurosci. 27, 11,869–11,876.
16. Mayer, A.R., Ling, J., Mannell, M.V., Gasparovic, C., Phillips, J.P., Doezema, D., Reichard, R., and Yeo, R.A. (2010). A prospective diffusion tensor imaging study in mild traumatic brain injury. Neurology 74, 643–650.
17. Croall, I., Cowie, C., He, J., Peel, A., Wood, J., Aribisala, B., Mitchell, P., Mendelow, Smith, F., Millar, D., Kelly, T., and Blamire, A. (2014). White matter correlates of cognitive dysfunction after mild traumatic brain injury. Neurology 83, 494–501.
18. Wilde, E.A., McCauley, S.R., Hunter, J.V., Bigler, E.D., Chu, Z., Wang, Z.J., Hanten, G.R., Troyanskaya, M., Yallampalli, R., Li, X., Chia, J., and Levin, H.S. (2008). Diffusion tensor imaging of acute mild traumatic brain injury in adolescents. Neurology 70, 948–955.
19. Bazarian, J.J., Zhong, J., Blyth, B., Zhu, T., Kavcic, V., and Peterson, D. (2007). Diffusion tensor imaging detects clinically important axonal damage after mild traumatic brain injury: a pilot study. J. Neurotrauma 24, 1447–1459.

20. Xu, S., Zhuo, J., Racz, J., Shi, D., Roys, S., Fiskum, G., and Gullapalli, R. (2011). Early microstructural and metabolic changes following controlled cortical impact injury in rat: a magnetic resonance imaging and spectroscopy study. J. Neurotrauma 28, 2091–2102.
21. Sajja, V., Galloway, M., Ghoddoussi, F., Thiruthalinathan, D., Kepsel, A., Hay, K., Bir, C., and VandeVord, P. (2012). Blast-induced neurotrauma leads to neurochemical changes and neuronal degeneration in the rat hippocampus. NMR Biomed. 25, 1331–1339.
22. Gass, A., Niendorf, T., and Hirsch, J.G. (2001). Acute and chronic changes of the apparent diffusion coefficient in neurological disorders—biophysical mechanisms and possible underlying histopathology. J. Neurol. Sci. 186, Suppl. 1, S15–S23.
23. Song, S.K, Sun, S.W., Ju, W.K., Lin, S.J., Cross, A.H., and Neufeld, A.H. (2003). Diffusion tensor imaging detects and differentiates axon and myelin degeneration in mouse optic nerve after retinal ischemia. Neuroimage 20, 1714–1722.
24. Alsop, D.C., Murai, H., Detre, J.A., McIntosh, T.K., and Smith, D.H. (1996). Detection of acute pathologic changes following experimental traumatic brain injury using diffusion-weighted magnetic resonance imaging. J. Neurotrauma 13, 515–521.
25. Huisman, T.A., Sorensen, A.G., Hergan, K., Gonzalez, R.G., and Schaefer, P.W. (2003). Diffusion-weighted imaging for the evaluation of diffuse axonal injury in closed head injury. J. Comput. Assist. Tomogr. 27, 5–11.
26. Liu, A.Y., Maldjian, J.A., Bagley, L.J., Sinson, G.P., and Grossman, R.I. (1999). Traumatic brain injury: diffusion-weighted MR imaging findings. AJNR Am. J. Neuroradiol. 20, 1636–1641.
27. Mamere, A.E., Saraiva, L.A., Matos, A.L., Carneiro, A.A., and Santos, A.C. (2009). Evaluation of delayed neuronal and axonal damage secondary to moderate and severe traumatic brain injury using quantitative MR imaging techniques. AJNR. Am. J. Neuroradiol. 30, 947–952.
28. Arfanakis, K., Haughton, V.M., Carew, J.D., Rogers, B.P., Dempsey, R.J., and Meyerand, M.E. (2002). Diffusion tensor MR imaging in diffuse axonal injury. AJNR. Am. J. Neuroradiol. 23, 794–802.
29. Huisman, T.A., Schwamm, L.H., Schaefer, P.W., Koroshetz, W.J., Shetty-Alva, N., Ozsunar, Y., Wu, O., and Sorensen, A.G. (2004). Diffusion tensor imaging as potential biomarker of white matter injury in diffuse axonal injury. AJNR. Am. J. Neuroradiol. 25, 370–376.
30. Mac Donald, C.L., Dikranian, K., Song, S.K., Bayly, P.V., Holtzman, D.M., and Brody, D.L. (2007). Detection of traumatic axonal injury with diffusion tensor imaging in a mouse model of traumatic brain injury. Exp. Neurol. 205, 116–131.
31. Mayer, A.R., Ling, J., Mannell, M.V., Gasparovic, C., Phillips, J.P., Doezema, D., Reichard, R., and Yeo, R.A. (2010). A prospective diffusion tensor imaging study in mild traumatic brain injury. Neurology 74, 643–650.
32. Wilde, E.A., Chu, Z., Bigler, E.D., Hunter, J.V., Fearing, M.A., Hanten, G., Newsome, M.R., Scheibel, R.S., Li, X., and Levin, H.S. (2006). Diffusion tensor imaging in the corpus callosum in children after moderate to severe traumatic brain injury. J. Neurotrauma 23, 1412–1426.
33. Wozniak, J.R., Krach, L., Ward, E., Mueller, B.A., Muetzel, R., Schnoebelen, S., Kiragu, A., and Lim, K.O. (2007). Neurocognitive and neuroimaging correlates of pediatric traumatic brain injury: a diffusion tensor imaging (DTI) study. Arch. Clin. Neuropsychol. 22, 555–568.
34. Salmond, C.H., Menon, D.K., Chatfield, D.A., Williams, G.B., Pena, A., Sahakian, B.J., and Pickard, J.D. (2006). Diffusion tensor imaging in chronic head injury survivors: correlations with learning and memory indices. Neuromage 29, 117–124.
35. Kraus, M.F., Susmaras, T., Caughlin, B.P., Walker, C.J., Sweeney, J.A., and Little, D.M. (2007). White matter integrity and cognition in chronic traumatic brain injury: a diffusion tensor imaging study. Brain 130, 2508–2519.
36. Zhuo, J., Keledjian, K., Xu, S., Pampori, A., Gerzanich, V., Simard, J.M., and Gullapalli, R.P. (2015). Changes in diffusion kurtosis imaging and magnetic resonance spectroscopy in a direct cranial blast traumatic brain injury (dc-bTBI) model. PloS One 10, e0136151.
37. Harris, J.L., Yeh, H.-W.W., Choi, I.-Y.Y., Lee, P., Berman, N.E., Swerdlow, R.H., Craciunas, S.C., and Brooks, W.M. (2012). Altered neurochemical profile after traumatic brain injury: (1)H-MRS biomarkers of pathological mechanisms. J. Cereb. Blood Flow Metab. 32, 2122–2134.
38. Haase, A., Frahm, J., Matthaei, D., Hänicke W., and Merboldt, K.D. (2011). FLASH imaging: rapid NMR imaging using low flip-angle pulses. 1986. J. Magn. Reson. 213, 533–541.
39. Frahm, J., Haase, A., and Matthaei, D. (1986). Rapid NMR imaging of dynamic processes using the FLASH technique. Magn. Reson. Med. 3, 321–327.
40. Gruetter, R. (1993). Automatic, localized in vivo adjustment of all first- and second-order shim coils. Magn. Reson. Med. 29, 804–811.
41. Hennig, J., Nauerth, A., and Friedburg, H. (1986). RARE imaging: a fast imaging method for clinical MR. Magn. Reson. Med. 3, 823–833.
42. Xu, S., Ji, Y., Chen, X., Yang, Y., Gullapalli, R., and Masri, R. (2013). In vivo high-resolution localized (1) H MR spectroscopy in the awake rat brain at 7 T. Magn. Reson. Med. 69, 937–943.
43. Provencher, S.W. (2001). Automatic quantitation of localized in vivo 1H spectra with LCModel. NMR Biomed. 14, 260–264.
44. Urenjak, J., Williams, S.R., Gadian, D.G., and Noble, M. (1993). Proton nuclear magnetic resonance spectroscopy unambiguously identifies different neural cell types. J. Neurosci. 13, 981–989.
45. Norenberg, M.D., and Martinez-Hernandez, A. (1979). Fine structural localization of glutamine synthetase in astrocytes of rat brain. Brain Res. 161, 303–310.
46. Dixon, C.E., Clifton, G.L., Lighthall, J.W., Yaghmai, A.A., and Hayes, R.L. (1991). A controlled cortical impact model of traumatic brain injury in the rat. J. Neurosci. Methods 39, 253–262.
47. McIntosh, T.K., Vink, R., Noble, L., Yamakami, I., Fernyak, S., Soares, H., and Faden, A.L. (1989). Traumatic brain injury in the rat: characterization of a lateral fluid-percussion model. Neuroscience 28, 233–244.
48. Kuehn, R., Simard, P., Driscoll, I., Keledjian, K., Ivanova, S., Tosun, C., Williams, A., Bochicchio, G., Gerzanich, V., and Simard, J.M. (2011). Rodent model of direct cranial blast injury. J. Neurotrauma 28, 2155–2169.
49. Shah, A.S., Stemper, B.D., and Pintar, F.A. (2012). Development and characterization of an open-ended shock tube for the study of blast mTBI. Biomed. Sci. Instrum. 48, 393–400.
50. Budde, M.D., Janes, L., Gold, E., Turtzo, L.C., and Frank, J.A. (2011). The contribution of gliosis to diffusion tensor anisotropy and tractography following traumatic brain injury: validation in the rat using Fourier analysis of stained tissue sections. Brain 134, 2248–2260.
51. Kabu, S., Jaffer, H., Petro, M., Dudzinski, D., Stewart, D., Courtney, A., Courtney, M., and Labhasetwar, V. (2015). Blast-associated shock waves result in increased brain vascular leakage and elevated ROS levels in a rat model of traumatic brain injury. PLoS One 10, e0127971.
52. Miller, A.P., Shah, A.S., Aperi, B.V., Budde, M.D., Pintar, F.A., Tarima, S., Kurpad, S.N., Stemper, B.D., and Glavaski-Joksimovic, A. (2015). Effects of blast overpressure on neurons and glial cells in rat organotypic hippocampal slice cultures. Front. Neurol. 6, 20.
53. Rodriguez, O., Schaefer, M.L., Wester, B., Lee, Y.-C.C., Boggs, N., Conner, H.A., Merkle, A.C., Fricke, S.T., Albanese, C., and Koliatsos, V.E. (2016). Manganese-enhanced magnetic resonance imaging as a diagnostic and dispositional tool after mild-moderate blast traumatic brain injury. J. Neurotrauma 33, 662–671.
54. Chabai, A.J. (1965). On scaling dimensions of craters produced by buried explosives. J. Geophys. Res.70, 5075–5098.
55. Frounfelker, P., Benesch, B., Holdren, T., and Tegtmeyer, M. (2015). *US Army Research, Development & Engineering Command Report: WIAMan Baseline Environment (WBE): Loading Environment (U), Meeting with the Imperial College of London, April 30, 2012.* U.S. Army Research Laboratory, London, England.
56. Chen, Y., and Huang, W. (2011). Non-impact, blast-induced mild TBI and PTSD: concepts and caveats. Brain Inj. 25, 641–50.
57. Williamson, J.B., Heilman, K.M., Porges, E.C., Lamb, D.G., and Porges, S.W. (2013). A possible mechanism for PTSD symptoms in patients with traumatic brain injury: central autonomic network disruption. Front. Neuroeng. 6, 13.
58. Kitayama, N., Vaccarino, V., Kutner, M., Weiss, P., and Bremner, J.D. (2005). Magnetic resonance imaging (MRI) measurement of hippocampal volume in posttraumatic stress disorder: a meta-analysis. J. Affect. Disord. 88, 79–86.
59. Wang, Z., Neylan, T.C., Mueller, S.G., Lenoci, M., Truran, D., Marmar, C.R., Weiner, M.W., and Schuff, N. (2010). Magnetic resonance imaging of hippocampal subfields in posttraumatic stress disorder. Arch. Gen. Psychiatry 67, 296–303.

60. Shin, L.M., Shin, P.S., Heckers, S., Krangel, T.S., Macklin, M.L., Orr, S.P., Lasko, N., Segal, E., Makris, N., Richert, K., Levering, J., Schacter, D.L., Alpert, N.M., Fischman, A.J., Pitman, R.K., and Rauch, S.L. (2004). Hippocampal function in posttraumatic stress disorder. Hippocampus 14, 292–300.
61. Bremner, J.D., and Vermetten, E. (2005). Neuroanatomical changes associated with pharmacotherapy in posttraumatic stress disorder. Ann. N. Y. Acad. Sci. 1032, 154–7.
62. Maller, J.J., Thomson, R.H., Lewis, P.M., Rose, S.E., Pannek, K., and Fitzgerald, P.B. (2010). Traumatic brain injury, major depression, and diffusion tensor imaging: making connections. Brain Res. Rev. 64, 213–40.
63. Vermetten, E., Vythilingam, M., Southwick, S.M., Charney, D.S., and Bremner, J.D. (2003). Long-term treatment with paroxetine increases verbal declarative memory and hippocampal volume in posttraumatic stress disorder. Biol. Psychiatry 54, 693–702.
64. Douglas Bremner, J., Mletzko, T., Welter, S., Siddiq, S., Reed, L., Williams, C., Heim, C.M., and Nemeroff, C.B. (2004). Treatment of posttraumatic stress disorder with phenytoin: an open-label pilot study. J. Clin. Psychiatry 65, 1559–64.
65. Farace, E., and Alves, W.M. (2000). Do women fare worse: a metaanalysis of gender differences in traumatic brain injury outcome. J. Neurosurg. 93, 539–45.
66. Berry, C., Ley, E.J., Tillou, A., Cryer, G., Margulies, D.R., and Salim, A. (2009). The effect of gender on patients with moderate to severe head injuries. J. Trauma 67, 950–953.
67. Mychasiuk, R., Hehar, H., Farran, A., and Esser, M.J. (2014). Mean girls: sex differences in the effects of mild traumatic brain injury on the social dynamics of juvenile rat play behaviour. Behav. Brain Res. 259, 284–291.
68. Mychasiuk, R., Hehar, H., and Esser, M.J. (2015). A mild traumatic brain injury (mTBI) induces secondary attention-deficit hyperactivity disorder-like symptomology in young rats. Behav. Brain Res. 286, 285–292.

Address correspondence to:
Rao P. Gullapalli, PhD
Department of Diagnostic Radiology & Nuclear Medicine
University of Maryland School of Medicine
22 S. Greene Street
Baltimore, MD 21201

E-mail: rgullapalli@umm.edu

APPENDIX 4

Tchantchou F, Fourney WL, Leiste UH, Vaughan J, Rangghran P, Puche A, Fiskum G. Neuropathology and neurobehavioral alterations in a rat model of traumatic brain injury to occupants of vehicles targeted by underbody blasts. Exp Neurol. 2017 Mar;289:9-20. PMID: 27923561.

Experimental Neurology 289 (2017) 9–20

Contents lists available at ScienceDirect

Experimental Neurology

journal homepage: www.elsevier.com/locate/yexnr

Research Paper

Neuropathology and neurobehavioral alterations in a rat model of traumatic brain injury to occupants of vehicles targeted by underbody blasts

Flaubert Tchantchou [a], William L. Fourney [b], Ulrich H. Leiste [b], Joshua Vaughan [a], Parisa Rangghran [a], Adam Puche [c], Gary Fiskum [a,*]

[a] University of Maryland School of Medicine, Department of Anesthesiology, Center for Shock, Trauma, and Anesthesiology Research (STAR), 685 W. Baltimore St., Baltimore, MD 21201, United States
[b] University of Maryland School of Engineering, Department of Aerospace Engineering, 1131 Glenn L. Martin Hall, College Park, MD 20742, United States
[c] University of Maryland School of Medicine, Department of Anatomy and Neurobiology, Health Science Facility-2, Room 255, Baltimore, MD 21201, United States

ARTICLE INFO

Article history:
Received 7 September 2016
Received in revised form 21 November 2016
Accepted 2 December 2016
Available online 5 December 2016

Keywords:
Acceleration
Apoptosis
Inflammation
Anxiety
Synapse

ABSTRACT

Many victims of blast-induced traumatic brain injury are occupants of military vehicles targeted by land mines. Recently improved vehicle designs protect these individuals against blast overpressure, leaving acceleration as the main force potentially responsible for brain injury. We recently developed a unique rat model of under-vehicle blast-induced hyperacceleration where exposure to acceleration as low as 50G force results in histopathological evidence of diffuse axonal injury and astrocyte activation, with no evidence of neuronal cell death. This study investigated the effects of much higher blast-induced accelerations (1200 to 2800G) on neuronal cell death, neuro-inflammation, behavioral deficits and mortality. Adult male rats were subjected to this range of accelerations, in the absence of exposure to blast overpressure, and evaluated over 28 days for working memory (Y maze) and anxiety (elevated plus maze). In addition, brains obtained from rats at one and seven days post-injury were used for neuropathology and neurochemical assays. Sixty seven percent of rats died soon after being subjected to blasts resulting in 2800G acceleration. All rats exposed to 2400G acceleration survived and exhibited transient deficits in working memory and long-term anxiety like behaviors, while those exposed to 1200 acceleration G force only demonstrated increased anxiety. Behavioral deficits were associated with acute microglia/macrophage activation, increased hippocampal neuronal death, and reduced levels of tight junction- and synapse- associated proteins. Taken together, these results suggest that exposure of rats to high underbody blast-induced G forces results in neurologic injury accompanied by neuronal apoptosis, neuroinflammation and evidence for neurosynaptic alterations.

1. Introduction

Brain injuries resulting from direct or indirect exposure to explosions represent up to 68% of more than 300,000 U.S. military neurotrauma victims who served in the recent wars in Iraq and Afghanistan (Abdul-Muneer et al. 2013; DePalma et al., 2005; Hoge et al., 2008; Okie, 2005; Owens et al., 2008; Rosenfeld et al., 2013). Blast-induced traumatic brain injuries (bTBI) are mainly classified into four sub-categories: 1. primary injury, which results from blast overpressure, 2. penetrating injuries caused by debris propelled by the explosion, 3. "coup-countercoup" head injury resulting from secondary head impact, and 4. exposure to intensive heat, toxic chemicals, and electromagnetic radiation (Cernak et al., 2011; Mellor, 1988). Missing from these classifications is TBI induced by sudden, intense acceleration force without significant exposure to blast overpressure. Such injuries occur to occupants of vehicles targeted by land mines, where the V-shaped armored hulls deflect the bulk of blast overpressure laterally, away from the occupants. Nevertheless, the occupants are subjected to uniquely rapid and intense acceleration.

Clinical research and epidemiological studies suggest that the majority of all bTBI victims suffer from mild TBI (Hoge et al., 2008; Lange et al., 2013). Although most victims of mild-bTBI pass the Acute Concussion Evaluation (Brenner et al., 2009; Elder et al., 2010), many return to the hospital later, exhibiting cognitive and memory impairments, increased anxiety, and depression (Elder et al., 2010; Jaffee and Meyer, 2009; Rosenfeld and Ford, 2010). Thus, a better knowledge of the

* Corresponding author.
E-mail addresses: ftchantchou@anes.umm.edu (F. Tchantchou), four@umd.edu (W.L. Fourney), uleiste@umd.edu (U.H. Leiste), vaughan1009@gmail.com (J. Vaughan), prangghran@anes.umm.edu (P. Rangghran), apuche@umaryland.edu (A. Puche), gfiskum@anes.umm.edu (G. Fiskum).

http://dx.doi.org/10.1016/j.expneurol.2016.12.001
0014-4886/

pathophysiology of different forms of bTBI is needed to improve both short and long-term outcomes for bTBI casualties.

A number of different animal models of bTBI have been developed (Goldstein et al., 2014; Kovacs et al., 2014), with the goal of improving treatment for bTBI (Chen et al., 2013; Schultz et al., 2011). Such models have focused primarily on brain injuries caused by exposure to blast overpressure and shock waves, such as those experienced by "unmounted" warfighters on foot patrol. These models typically utilize rodents restrained within or just outside the end of a shock tube that exposes the animals to these forces. The results of these experiments demonstrate that exposure of laboratory animals to a single blast can cause significant pathological changes in the brain including the disruption of the blood brain barrier integrity (Abdul-Muneer et al., 2013; Elder et al., 2015), increased accumulation of inflammatory microglia/macrophages, neuronal cell death, and neurobehavioral deficits (Abdul-Muneer et al., 2013; Kwon et al., 2011; Vandevord et al., 2012).

To better understand the pathology of blast-induced brain injury sustained by occupants of military and other vehicles, we recently developed a unique rat model of underbody blast-induced vertical hyperacceleration where relatively low blast intensity (50G acceleration force) revealed histopathological evidence of diffuse axonal injury and astrocyte activation in rats, with no neuronal cell loss or obvious behavioral deficits (Proctor et al., 2014). The current study investigates the impact of much higher underbody blast-induced acceleration force of 1200–2800G on neuronal cell death, inflammation, levels of tight junction and synaptic proteins, behavioral impairments, and mortality at periods ranging from hours to 30 days post-injury.

2. Materials and methods

2.1. Animals and their environment

All animal research protocols were approved by the University of Maryland, Baltimore Animal Use and Care Committee and the US Army Animal Care and Use Review Office. Male Sprague-Dawley rats (Harlan Laboratories, CA), 300–350 g were maintained under a controlled environment with an ambient temperature of 23 ± 2 °C, a 12 h light/dark cycle, and continuous access to food and water ad libitum. Experimental groups consisted of 10 to 14 rats for behavioral studies, 4 to 8 rats for immunohistochemistry or biochemical analyses, and 8–14 rats for mortality incidence.

2.2. Exposure of rats to underbody blast-induced hyperacceleration force

Exposure of rats to underbody blast-induced hyperacceleration force was performed following scaling analysis to develop parameters to guide the design by a procedure modified from what we described previously (Proctor et al., 2014; Zhao et al., 2013). In brief, two rats were anesthetized concurrently with 4% isoflurane in room air for 5 min, allowing for placement within restraints without stress. Anesthesia was discontinued and the rats were secured, while still unconscious, within two fiberglass restrainers (Stoeling Inc., IL), with a custom addition of metallic cone to restrain the head and minimize secondary acceleration and head impact. The restrainers were bolted onto a 38 cm square and 2.5 cm thick aluminum platform. This platform was located immediately above a second 38 cm square aluminum platform that was either 5.0 cm thick (for 1200G acceleration force) or 2.5 cm thick (for 2800G acceleration). A 0.6 cm thick, hard rubber pad was present between the two platforms to dampen oscillatory acceleration forces. Both platforms had 2.5 cm wide holes located inside each of the four corners. Aluminum rods, 2.0 cm wide and 90 cm high, were inserted through each of the holes and secured to a steel base on which the platforms rested, thus allowing for only direct movement of the platforms vertically following an underbody blast. The steel base was bolted to the edges of a steel tank filled with water to different stand-off distances from the bottom platform, resulting in relatively low acceleration force at large distances and relatively high acceleration force at short distances.

An explosive charge of pentaerytritol tetranitrate (PETN) was secured in the water at a fixed 5 cm depth of burial from the water line. The explosives weighing 0.75 g, for 1200G blasts, and 2.00 g, for 2400G and 2800G blasts, were detonated electromagnetically at exactly 5 min after anesthesia was discontinued. Parallel exposure of rats to 4% isoflurane for 5 min indicated that they were fully conscious 5 min after discontinuing the anesthesia. Explosion within the water ensured a non-compressible transfer of the explosive energy onto the bottom of the lower platform and subsequently to the upper platform where the rats were located. Accelerometers were placed on the top of the higher platform near the front of the rat restraints and the velocity, acceleration force, and JERK (first derivative of acceleration force) measured using UERD-Tools software (U.S. NAVY). The peak acceleration force reached in these blast experiments was in the range of 0.30 to 0.50 m sec. Pressure sensors were also placed near the head-end of the restraints during several experiments, verifying that the pressure changes experienced by the rats were less than 1 lb/in^2. Sham animals were also anesthetized with 4% isoflurane for 5 min, secured on the platform and removed 5 min later.

All blast and sham animals were returned to their cages immediately after the blast or sham procedure and examined for any physical injuries every 30 min for 3 h. Necropsies were performed on all four animals that died immediately following the 2800G blasts.

2.3. Behavior

2.3.1. Y maze test

The Y maze is a Y-shaped platform that consists of three arms 50 cm long and 10 cm wide, each surrounded on three sides by 40 cm high walls. The open ends of the three arms are connected centrally and positioned radially at 120° angles (Stoelting Co., IL). The test was performed at approximately 1 h, and 6, 13 and 27 days post-injury, as previously described (Tchantchou and Zhang, 2013). Each rat was placed at the center of the maze and allowed to explore for 5 min. Movement was recorded using an overhead camera and analyzed using the Any-maze software (SD instruments, CA). Arm visit sequences and number of entries to each arm were recorded. Working memory was defined by the frequency of alternately exploring different arms and was determined using the formula: total number of alternations / (total number of arm entries − 2) × 100.

2.3.2. Elevated plus maze

This plus sign-shaped device consists of four perpendicular arms measuring 90 cm long and 10 cm wide, connected by a 10 cm × 10 cm central platform. Two of the arms are bordered on three sides by 20 cm high black plastic walls, while the other two arms together with the center of the maze are open. The arms are located 50 cm above the floor (Budde et al., 2013). The test was performed on days 1, 8, 14 and 28 post-blast, as previously described, with a minor modification (Budde et al., 2013). In brief, rats were individually placed on the central area and allowed to explore the maze for 10 min. Movement was recorded by an overhead camera and the data were analyzed by Any-maze software (SD instruments, CA), to provide information including the time spent in each arm and the central area and the total distance traveled. Anxiety like behavior is inversely proportional to the time the rats spend in the open arms.

2.4. Tissue collection and processing

At different times following blasts or sham procedure (Fig. 1), rats were deeply anesthetized by intraperitoneal injection of a mixture of ketamine (160 mg/kg) and xylazine (120 mg/kg), and euthanized by exsanguination via transcardial perfusion. Anesthetized rats were initially perfused for 5 min with oxygenated artificial CSF containing

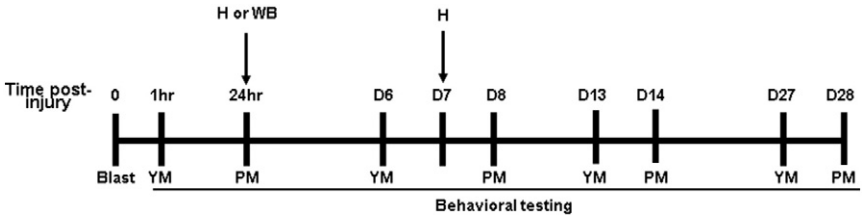

Fig. 1. Experimental design and timeline. Detailed timeline of behavioral tests and end points of experimental procedures starting on study day 0 (blast exposure). YM, Y-maze test; PM, plus-maze test; H, histology, WB, western blots.

148 mM NaCl, 5 mM glucose, 3.0 mM KCl, 1.85 mM $CaCl_2$, 1.7 mM $MgCl_2$, 1.5 mM Na_2HPO_4, and 0.14 mM NaH_2PO_4 (pH 7.4). Rats were then perfused with a 500 ml fixative consisting of 4% paraformaldehyde in 50 mM K_2HPO_4 and 50 mM KH_2PO_4 (pH 7.4). The brains were removed, maintained in fixative for 24 h, and transferred to 30% sucrose. After a few days when the brains sank to the bottom of their containers, each was sectioned in serial sections of 40 μm, preserved in cryoprotectant (66 mM NaH_2PO_4, 190 mM Na_2HPO_4, 0.87 M sucrose, 30% ethylene glycol, and 1.25 mM povidone), and stored at −20 °C for histology and immunohistochemistry.

For western blot analysis, ketamine-anesthetized rats were decapitated with a guillotine. Their brains were rapidly removed and dissected to yield the hippocampus, cortex and cerebellum, which were immediately frozen on dry ice and stored at −80 °C.

2.5. Immunostaining

Immunohistochemical analysis of fixed, frozen sections was performed to determine the expression of inflammation biomarkers, F4/80, inducible nitric oxide synthase (iNOS), and the apoptosis biomarker, cleaved caspase 3. Visualization utilized either fluorescence immunostaining or nickel diaminobenzadine (DAB) immunostaining. The number of dead or dying cells was quantified using terminal deoxynucleotidyl transferase dUTP nick end labeling (TUNEL).

2.5.1. Immunofluorescence staining

Brain sections were co-stained for the expression of cleaved caspase 3 and neuronal nuclear antigen (NeuN) or F4/80 and iNOS as previously described (Tchantchou et al., 2007). In brief, free floating sections were rinsed in phosphate buffered saline (PBS), then blocked in 1% horse serum in PBS containing 0.3% Triton X for 1 h. Sections were then transferred in a solution containing rabbit anti-cleaved caspase-3 polyclonal antibody (1:10,000; Millipore, Temecula, CA) and mouse anti-NeuN monoclonal antibody clone, A60 (1:2000; Millipore, Temecula, CA) or rat anti-F4/80 monoclonal antibody (1:500; eBioscience, San Diego, CA) and rabbit anti-iNOS polyclonal antibody (1:3000; Millpore, Temecula, CA) and incubated at 4 °C overnight. The sections were washed in PBS and incubated for 1 h at room temperature in a mixture of corresponding secondary antibodies Alexa Fluor 488 or Alexa Fluor 594 (1:1500; Invitrogen, NY). Sections were washed with PBS and counterstained with 4′,6-diamidino-2-phenylindole (DAPI).

2.5.2. Nickel DAB immunostaining

Brain sections were single-labeled for the expression of F4/80, using nickel DAB. Free floating sections were rinsed in PBS, blocked with 1% horse serum, and incubated with rat anti-F4/80 monoclonal antibody (1:15,000; eBioscience, CA) overnight at 4 °C. Sections were washed and incubated at room temperature in biotinylated goat anti-rat secondary antibody (1/2000; Vector Laboratories Inc., CA), for 1 h , followed by incubation in Vestastain solution and in nickel DAB and rinsed in PBS.

2.5.3. TUNEL assay

Floating sections were rinsed in PBS, transferred onto glass slides and allowed to air dry for 1 h. They were rehydrated in PBS and stained to detect apoptotic cells marked by DNA fragmentation using a kit (Millipore, NY) and following the manufacturer's instructions. DAPI was used as a counterstain. All stained sections were mounted and examined under a Zeiss Axio-Imager microscope and images captured with 20× or 63× magnification objectives.

2.6. Western blot analysis

Western blotting was performed to determine the expression of Zona occluden (ZO-1), occludin, von Willebrand Factor (VWF), Bcl-2, heat shock proteins 70 (Hsp70), synaptophysin, PSD-95, spinophilin and beta-actin (used as loading control). The hippocampus, cortex and cerebellum were manually homogenized in lysis buffer containing 50 mM HEPES (pH 7.5), 6 mM $MgCl_2$, 1 mM EDTA, 75 mM sucrose, 1 mM dithiothreitol, 1% Triton X-100 and 1% protease/phosphatase inhibitor cocktail (Cell Signaling Technology, MA) and centrifuged at 10,000*g* for 20 min. Proteins (20–30 μg) present in the supernatants were separated by electrophoresis on 4–12% SDS-polyacrylamide gels (Invitrogen, CA), then transferred to a nitrocellulose membrane. Membranes were blocked with 1% BSA and incubated overnight at 4 °C with rabbit polyclonal antibodies against VWF (1:400; Santa Cruz, CA), occludin (1:2000; Abcam, MA), spinophilin (1:500; Millipore, MA), synaptophysin (1:1000), PSD-95 (1:1000), and Bcl-2 (1:750) all from Cell Signaling Technology, MA; a rat anti-ZO-1 monoclonal antibody (1:400, Millipore, MA) or mouse monoclonal antibodies against Hsp70 (1:750; Cayman chemical, MI) or β-actin (1:4000; Sigma, MO). Blots were washed in Tris-buffered saline with 0.1% Tween 20 and incubated for 1 h at room temperature with corresponding HRP-conjugated secondary antibodies (1: 5000; Millipore, MA). Horseradish peroxidase labeled proteins were detected by enhanced chemiluminescence (ECL, Thermo Scientific, IL) and protein bands were visualized using a digital blot scanner (LI-COR, NE).

2.7. Quantification and statistical analysis

The optical fractionator method of stereology was employed to quantify cleaved caspase 3 or TUNEL positive cells in 40 μM thick immuno-stained sections, using the stereo-investigator software (MBF Bioscience, VT). A total of 6 sections selected to cover the entire hippocampus region, −1.60 mm to −6.3 mm from bregma, corresponding to every 12 serial sections were analyzed for each brain. For quantification, the dentate gyrus and the Cornu Ammonis 2/3 (Ca2/3) sub-regions in the hippocampus of each brain hemisphere were demarcated. Using a grid spacing of 75 μm × 75 μm in the *x* and *y*-axis and guard zones of 2 μm at the top and bottom of each section, immunopositive cell bodies were counted. The total number of cleaved caspase 3 or TUNEL positive cells in the hippocampal sub-region of interest was divided by the area to determine the cellular density per area unit, expressed as cells/mm^2.

Image J software (NIH) was used to measure immunoblot protein band signal intensity and the percent area of F4/80 immunostaining in

brain tissue. Sections stained for F4/80 were optically segmented by threshold with the threshold greyscale value selected at 0.3 μm. These thresholded images were automatically measured for the relative percent containing a positive F4/80 signal in ImageJ. This method is proportional to the percent area covered by F4/80 immuno-positive cells.

Statistical analyses were performed using GraphPad InStat 3 software (GraphPad Software, Inc., La Jolla, CA). Analysis of Variance together with Tukey-Kramer multiple comparisons post-test was used to compare differences among the multiple groups. Results are expressed as mean ± standard error of the mean (SEM). Statistical significance was defined as $p < 0.05$.

The individuals who performed the histologic, biochemical, and behavioral assays were blinded to animal group identifications, using codes that were revealed after data collection was completed.

3. Results

3.1. Blast-induced G force levels and mortality

Our previously reported underbody-blast experiments were conducted under conditions generating maximum acceleration forces in the range of 30–50G, with histologic evidence of TBI, but no obvious behavioral abnormalities, external injuries or mortality (Proctor et al., 2014). In this study, the blast-induced G force was escalated to determine the maximum survivable underbody blast induced acceleration force and to characterize the effects of these higher blast levels on histologic and behavioral measures of TBI. The acceleration force target for the first set of experiments was 1200G. Based on calibration curves generated with blasts using 0.75 g of PETN explosive present at different stand-off distances, we determined that a stand-off distance of 2.5 mm from the top of the water to the bottom of the lower platform would generate a peak acceleration force of approximately 1200G. The mean maximal force measured by accelerometers attached to the top plate near the head-end of the rat restraint was 1187 ± 115G (SEM) for $n = 10$ blasts. The change in acceleration force with time, referred to as JERK, was 0.48×10^7 m sec^3. All rats survived these blast-induced G and JERK levels with no apparent external injury.

The second acceleration force target was 2400G. In order to reach this level, we used the same stand-off distance of 2.5 mm that generated 1200G forces, but increased the amount of PETN to 2.0 g. The mean maximal force generated under these conditions was 2460 ± 76G for $n = 6$ blasts. For these blasts, JERK was 1.09×10^8 m sec^3. Although all animals survived these relatively high G forces, they exhibited lethargy and disorientation lasting several minutes immediately after the blast. These symptoms suggested that the 2400G force was close to the maximum survivable. We therefore set a third target of 2800G to test this hypothesis. In order to reach this level, we used the same 2.0 g of PETN and a stand-off distance of 2.5 mm but the mass of the two platforms was reduced by a net 33%, which increased the peak acceleration. The mean maximal force generated under these conditions was 2851 ± 359G for $n = 3$ blasts (6 rats). The JERK level was $1.77 \pm 0.33 \times 10^8$ m sec^3. Four of the six rats subjected to this blast force died either immediately or within a few minutes after the blast. Necropsies performed on these animals revealed severe pulmonary hemorrhaging and edema, without obvious damage to the heart, liver, or spleen. The two animals that survived this blast level were used for behavioral measurements through 28 days post injury.

3.2. Behavioral outcomes

Two different neurobehavioral tests were conducted to assess the effects of blast-induced acceleration on hippocampus-dependent memory and anxiety, respectively. The Y-maze test for memory was used on day zero, at 1 h post-blast, and again on days 6, 13, and 27 (Fig. 1). The plus maze test for anxiety was conducted on days 1, 8, 14, and 28. Each animal group consisted of $n = 10$–14 rats.

3.2.1. Hippocampus-dependent working memory

The Y maze tests the innate ability of a rodent to continuously alternate visits in the three arms during the maze exploration. Rats with a good "working" memory 'recognize' the most recently explored arm of the maze and will successfully alternate arm visits approximately 70% of the time (Maurice et al., 2009). The mean percent alternation for sham rats was only approximately 35% on day zero when tested 1 h after brief anesthesia but improved to a normal range of between 65 and 75% on days 6, 13, and 27 days later (Fig. 2A). Rats subjected to a 1200G blast force exhibited a similar alternation deficit on day zero and recovery on the subsequent test days to levels very similar to those of shams. In contrast, rats exposed to a 2400G blast force displayed only 5% successful alternation on day zero, 30% on day 6, and between 50 and 65% on days 13 and 27. Spontaneous alternation by rats exposed to 2400G acceleration was significantly lower than that of shams on day zero ($p < 0.05$) and day 6 ($p < 0.001$) and lower than 1200G rats on both days zero and 6 ($p < 0.05$) (Fig. 2A). The two rats that survived the blasts that generated a 2800G force exhibited spontaneous alternations of between 72% on day 13 and 80% on day 27.

3.2.2. Anxiety-like behavior

The elevated plus maze was used to test anxiety-like behaviors in rats subjected to blast-induced acceleration forces of 1200G and 2400G. Normal rats spend most of their time in the plus maze in the closed arms but display significant periods of inquisitive venture into the open arms. Rats that are interpreted as 'fearful and anxious' generally spend much less time in the open arms in comparison with normal rats. Sham rats spent more than twice as much time in the open arms on days 8, 14, and 28 compared to day 1 ($p < 0.05$) (Fig. 2B). Animals that experienced either 1200G or 2400G acceleration spent between 10 and 30% as much time as shams in the open arms on days 8, 14, and 28 ($p < 0.05$) and did not improve over this period. There were also no significant differences in time spent in open arms by rats in the 1200 and 2400G acceleration groups.

In this paradigm, the decision to explore either the open arms or to enter a closed arm can only be made in the central zone where the open and closed arms cross. Rats subjected to both blast levels spent the same relative time in the central area (Fig. 2C). Total distance traveled was identical for sham and 1200G blasts; however 2400G blast rats traveled significantly less than both shams and 1200G rats on day 1 ($p < 0.05$) (Fig. 2D). The finding that the distance traveled by rats in the 2400G group was not significantly different than that of shams and rats in the 1200G group on days 8, 14, and 28 indicates that the deficit in time spent by the 1200 and 2400G groups in the open arms was not due to impaired motor performance. One of the two rats that survived the 2800G blasts spent essentially no time in the open arms on any of the test days but also exhibited total distance traveled that was less than any of the rats in the other groups. The other rat that survived the 2800G blast spent times in the open arms ranging from 26 to 38 sec during each of the four days of testing, which is similar to what was spent by rats in the 2400G group.

3.3. Accumulation of inflammatory cells

Activated microglia, macrophages, and astrocytes are commonly observed in other animal models of TBI (Ramlackhansingh et al., 2011). To test whether our blast-induced hyperacceleration force TBI model results in neuroinflammation, we immunostained for activated microglia/macrophages present at one and seven days post-blast, using antibodies to the F4/80 marker protein. F4/80 immunostaining was observed primarily in perivascular and periventricular regions throughout the cortex (Fig. 3A) and hippocampus (not shown). Staining was quantified by expressing the total stained area as a percentage of the total area present in each coronal section. The number of animals per group ranged from $n = 4$–8. Compared to shams that exhibited F4/80 immunostaining equivalent to 1.65 ± 0.47% of total brain area, rats subjected

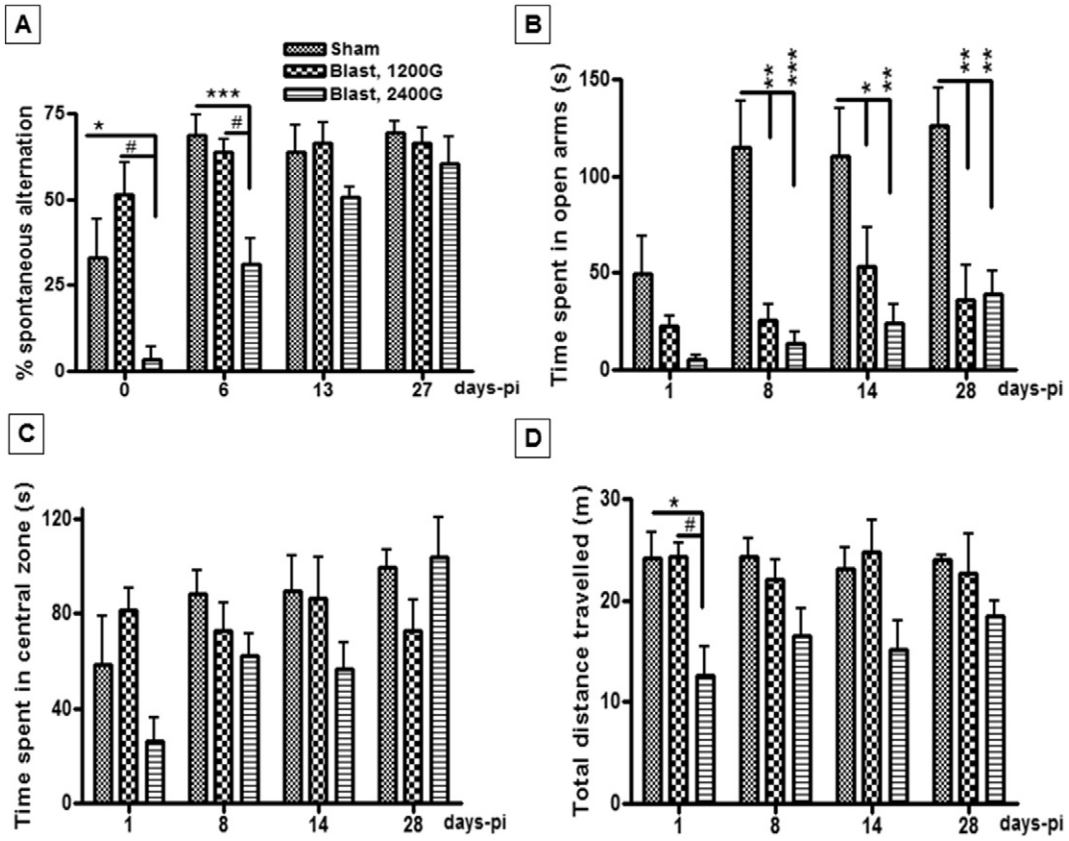

Fig. 2. Behavioral outcomes after underbody blast. (A) Y-maze test results demonstrating significantly lower spontaneous alternation among maze arms by 2400G blast rats than shams or rats exposed to 1200G acceleration force ($^{*,\#}p < 0.05$ for day 0-pi and $^{\#}p < 0.05$, $^{**}p < 0.01$ for day 6 post-injury (pi) respectively). (B) Plus maze test demonstrating that rats exposed to either 1200 or 2400G blasts spent significantly less time in the open arms on days 8, 14 and 28-pi compared to shams ($^{*}p < 0.05$, $^{**}p < 0.01$ and $^{***}p < 0.001$). There were no significant differences in the time spent in the central area (C) and in the total distance traveled (D) among blast and sham rats ($p > 0.05$), except on day 1 post-injury when 2400G blast rats traveled significantly less distance than sham and 1200G blast animals ($^{*,\#}p < 0.05$). For both the Y maze and the Plus maze tests, the number of rats used in each experimental group was Shams, $n = 10$, Blast 1200 G, $n = 14$ and Blast 2400 G $n = 14$.

to underbody blasts that generated 1200G acceleration exhibited almost five-times greater F4/80 immunostaining at 24 h post-blast ($7.62 \pm 1.35\%$; $p < 0.05$) (Fig. 3B). Rats subjected to 2400G blasts exhibited 9 times as much staining for activated microglia/macrophages as shams ($15.07 \pm 1.28\%$; $p < 0.01$). These results indicate a rapid extensive microglial/macrophage inflammatory response. However, by seven days post-injury, neuroinflammation measured by F4/80 subsided in both the 1200G and 2400G blast groups ($3.58 \pm 0.88\%$ and $2.83 \pm 1.52\%$). Double labeling with antibodies to both F4/80 and inducible nitric oxide synthase (iNOS) confirms the pro-inflammatory identify of these cells (Fig. 3C) as iNOS is highly specific for pro-inflammatory cells, e.g., activated microglia and macrophages (Loane et al., 2014; Tchantchou et al., 2014). Secondary antibody specificity control measurements were performed by incubating brain sections from all experimental groups with the secondary antibody used in the nickel DAB or fluorescence staining, respectively. No significant immunoreactivity was observed in the presence of secondary antibody alone.

3.4. Tight junction proteins and vascular endothelial cell damage

Brain injuries, including those caused by models of open field explosions, have been associated with the alteration of vascular proteins, which play important roles in the maintenance of the blood brain barrier integrity (Abdul-Muneer et al., 2013; Walls et al., 2015). To determine if vascular protein levels are altered in response to underbody blasts, we performed western blot analyses of the tight junction proteins occludin and ZO-1 and the vascular endothelial damage marker von Willebrand Factor (VWF) in different regions of the brains of rats at 24 h following blast or sham procedures. This time was chosen to coincide with the peak of neuroinflammatory cellular responses occurring primarily at perivascular and periventricular regions, as seen with F4/80 immunohistochemistry. Representative immunoblots for proteins present in the hippocampus, cortex, and cerebellum are shown in Fig. 4A, B, and C, respectively. The number of animals used for these assays ranged from $n = 4$–8. Compared to sham animals, the expression of occludin was reduced by ~40% in the hippocampus ($p < 0.01$) and cortex ($p < 0.001$) of rats subjected to 2400G acceleration force intensity (Fig. 4D), with no significant change in the cerebellum (Fig. 4D). Blasts that generated 1200G force levels did not result in significant alterations of occludin expression. Furthermore, the expression of ZO-1 was decreased in the cortex ($p < 0.01$) and hippocampus ($p < 0.05$) of 2400G blast rats compared to sham rats (Fig. 4E). Similar to occludin, ZO-1 expression levels were not affected in the cerebellum or after 1200G blasts (Fig. 4E). von Willebrand Factor is a protein produced and released from vascular endothelial cells in response to stress. VWF expression was significantly increased in the hippocampus following a 2400G blast ($p < 0.05$) and in the cerebellum following 2400 and 1200G blasts (Fig. 4F; $p < 0.05$).

3.5. Expression of the anti-apoptotic protein Bcl-2 and heat shock protein 70

In many models of TBI, neuroinflammation is accompanied by oxidative stress, which contributes to cell death cascades. We therefore examined the expression levels of the oxidative stress response protein Hsp70 and the anti-apoptotic protein Bcl-2 in different brain regions 24 h following blast exposure. Representative immunoblots for these proteins present at 24 h post-blast in the hippocampus, cortex, and

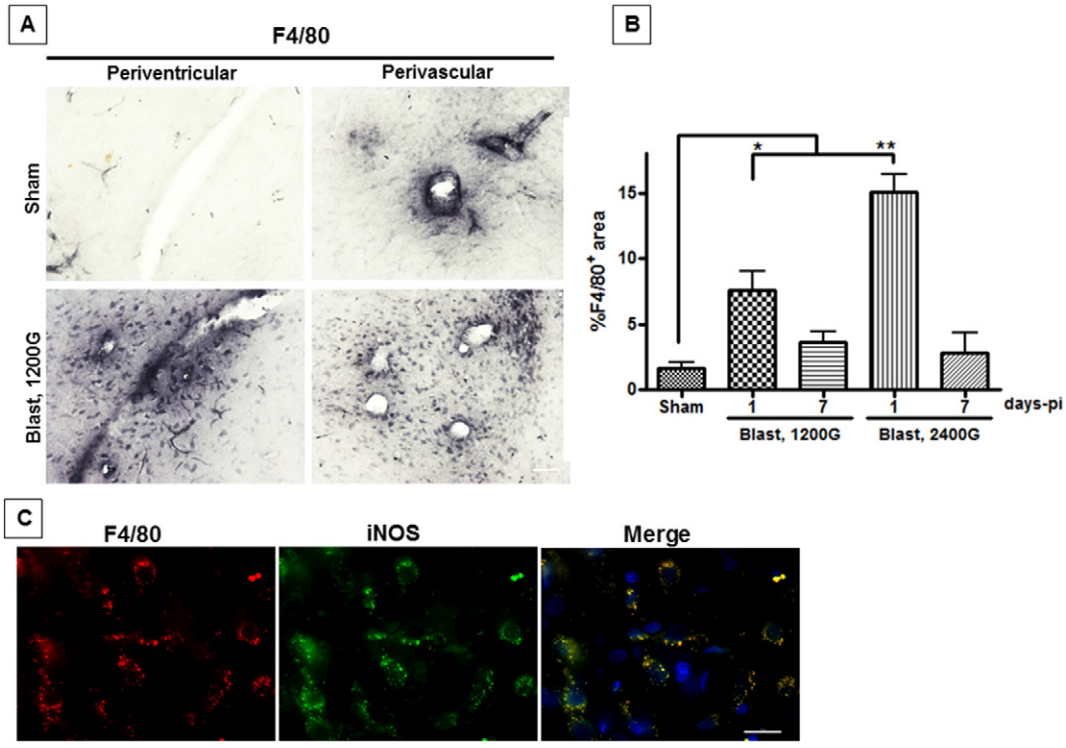

Fig. 3. Accumulation of inflammatory cells in the brain. (A) Representative microphotograph exhibiting F4/80 immuno-positive cells in the perivascular and periventricular regions of blast rats. (B) Quantification of the percent of F4/80 immuno-reactive area indicating a significant increase in microglia/macrophage accumulation in the brain of 1200G and 2400G blast rats compared to shams 24 h post-trauma ($^{*}p < 0.05$ and $^{**}p < 0.01$ respectively). (C) F4/80 immunopositive cells (red) co-expressed the pro-inflammatory enzyme iNOS (green); DAPI was used as counterstain. Experimental groups consisted of Sham ($n = 4$), Blast 1200 G ($n = 8$), Blast 2400 G ($n = 8$) for each time point.

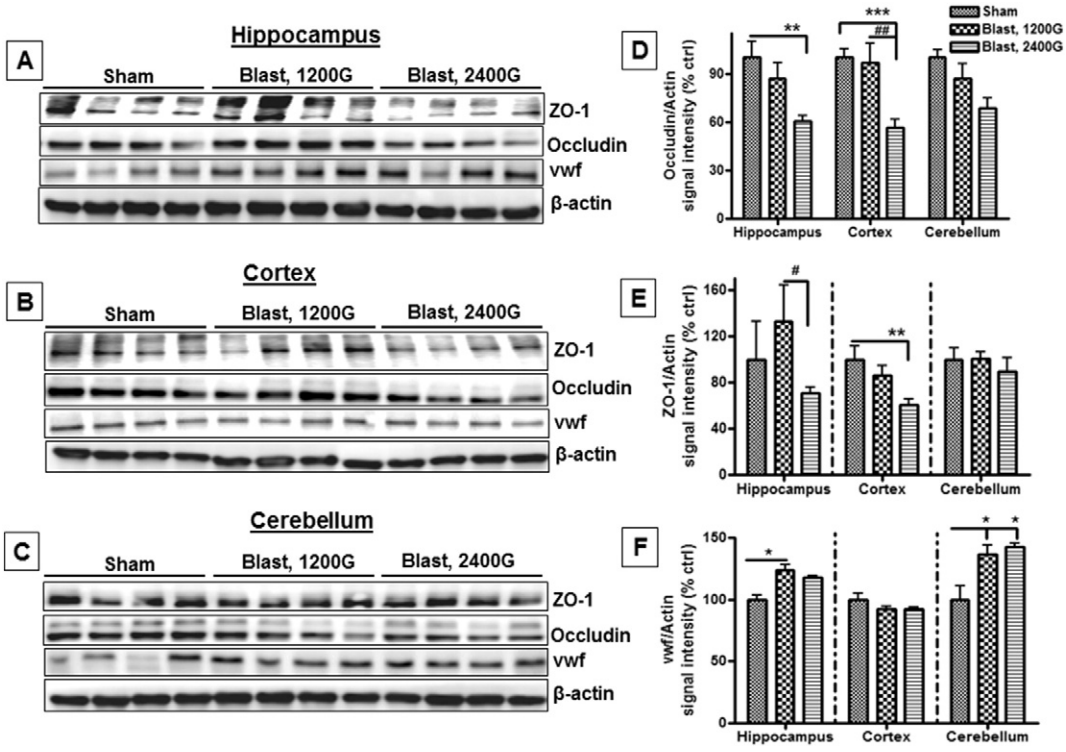

Fig. 4. Vascular injury biomarkers. (A–C) Representative immunoblots illustrating the expression of Occludin, ZO-1, VWF and beta actin in the hippocampus, cortex and cerebellum 24 h post-injury. Quantification of protein bands indicating that (D) Occludin expression was significantly reduced in the hippocampus and cortex of 2400G blast rats compared to shams ($^{**}p < 0.01$ and $^{***}p < 0.001$ respectively). (E) ZO-1 expression was significantly decreased in the cortex of 2400G blast rats compared to shams ($^{**}p < 0.01$). In contrast, ZO-1 levels were significantly lower in the hippocampus of 2400G blast rats compared to 1200G blast rats ($^{\#}p < 0.05$). (F) Expression levels of VWF in the hippocampus were significantly higher in 2400G blast rats versus shams ($^{*}p < 0.05$). In addition, VWF levels were also significantly higher in the cerebellum of 1200G and 2400G blast rats compared to shams ($^{*}p < 0.05$). Experimental groups included Shams ($n = 6$), Blast 1200 G ($n = 6$) and Blast 2400 G ($n = 6$).

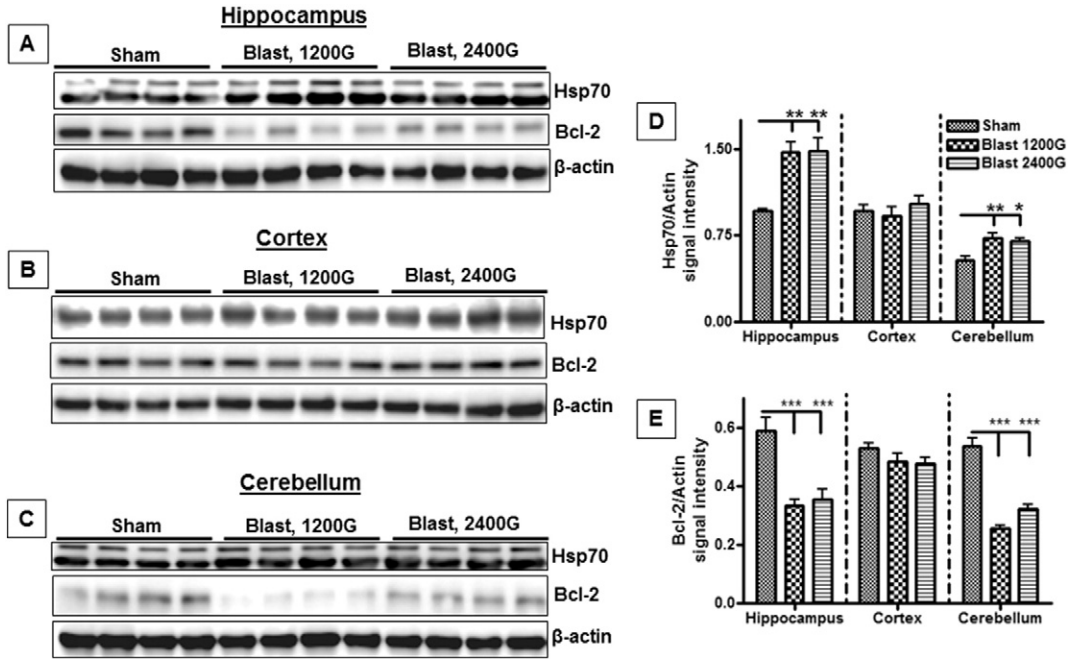

Fig. 5. Reciprocal changes in the levels of Hsp70 stress response protein and Bcl-2 anti-apoptotic protein in different brain regions following blast exposure. (A–C) Representative immunoblots describing the expression of Hsp70, Bcl-2 and beta actin in the hippocampus, cortex and cerebellum. Quantification of protein bands' signal intensity indicated that (D) Bcl-2 expression was significantly reduced in the hippocampus and cerebellum of rats exposed to 1200G blasts (***$p < 0.001$) as well as 2400G blasts (***$p < 0.001$), respectively, versus shams. (E) Conversely, the expression of Hsp70 was significantly increased in the hippocampus and cerebellum of 1200G blast rats (**$p < 0.01$) and 2400G blast rats (**$p < 0.01$ and *$p < 0.05$), respectively, compared to shams. Number of rats in each experimental group was Shams ($n = 6$), Blast 1200 G ($n = 6$) and Blast 2400 G ($n = 6$).

cerebellum are shown in Fig. 5A, B, and C, respectively. The number of animals used for these assays ranged from $n = 4$–8. Following both 1200G and 2400G blasts, there was a 50% increase in Hsp70 expression in the hippocampus ($p < 0.01$) and 30% increase in the cerebellum ($p < 0.05$), compared to sham animals (Fig. 5E). In contrast, exposure to blast-induced acceleration forces of 1200 and 2400G dramatically reduced Bcl-2 immunoreactive protein levels in both the hippocampus, by 40% ($p < 0.001$), and the cerebellum, by 50% ($p < 0.001$) (Fig. 5D). Hsp70 and Bcl-2 levels in the cortex were unaffected by underbody blasts. Since a reduction in Bcl-2 can increase susceptibility to cell death, we quantified cell death in the hippocampus, using TUNEL staining, and immunohistostaining for active (cleaved) caspase 3.

3.6. Hippocampal cell death

Blast exposure at 1200G and 2400G acceleration forces increased the appearance of cleaved caspase 3 (C-casp-3) immunoreactive cells in the dentate gyrus (Fig. 6A) and the Ca2/Ca3 areas (not shown) of the hippocampus; however, very sparse staining for either biomarker was observed in the Ca1 area (not shown). The number of animals used for these assays ranged from $n = 4$–8. The number of cleaved caspase 3 positive cells present in the dentate gyrus was 11 ± 2 per mm^2 for rats exposed to 1200G acceleration force and 13 ± 3 per mm^2 for 2400G blast rats, in comparison to 2 ± 1 per mm^2 for sham animals ($p < 0.01$) (Fig. 6B). In the Ca2/Ca3 area of the hippocampus, the cell count was 7 ± 1 per mm^2 for 1200G blast rats ($p < 0.05$) and 11 ± 2 per mm^2 for 2400G blast rats ($p < 0.01$), as opposed to 1 ± 1 per mm^2 for sham rats (Fig. 6B). After counting 350 cleaved caspase 3 immunoreactive cells in the DG using a 63× magnification objective, we found that 92% of these cells co-labeled with the neuronal marker NeuN (Fig. 6A).

Cleaved caspase 3 immunoreactivity reflects the presence of a caspase 3 dependent apoptotic pathway but is not a direct indicator of cell death. Additional evidence that exposure of rats to blast-induced acceleration forces of 1200–2400G causes cell death came from quantification of TUNEL positive cells (Fig. 7A), which is a marker of DNA fragmentation and late stage cell death. The number of TUNEL-positive cells present in the DG at 24 h post-injury was 8 ± 1 per mm^2 for rats exposed to 1200G blast intensity ($p < 0.001$) and 11 ± 2 per mm^2 for 2400G blast rats ($p < 0.001$) in comparison to 2 ± 1 per mm^2 for sham animals (Fig. 7B). Similar results were observed on the Ca2/Ca3 area where the count was 4 ± 1 per mm^2 for 1200G blast rats ($p < 0.05$) and 8 ± 1 per mm^2 for 2400G blast rats ($p < 0.001$), compared to 2 ± 1 per mm^2 for shams (Fig. 6B).

3.7. Expression of synaptic proteins

In addition to cerebrovascular damage, inflammation, and neuronal death, significant disruption to synaptic connectivity is a hallmark of even mild forms of TBI (Gao et al., 2011; Przekwas et al., 2016). Evidence suggestive of synaptic disruptions following exposure of rats to underbody blasts came from immunoblot measurements of the synaptic proteins PSD95, synaptophysin, and spinophilin, as shown in Fig. 8A. The number of animals used for these assays ranged from $n = 4$–8. These analyses revealed significant, 25–50% reductions in the expression levels of synaptic markers PSD95, synaptophysin and of the dendritic spine marker spinophilin in different brain regions 24 h following exposure to underbody blasts that produced either 1200 or 2400G acceleration forces (Fig. 8D–F). PSD95 levels were reduced in the hippocampus, cortex, and cerebellum ($p < 0.01$). Synaptophysin was reduced in the hippocampus ($p < 0.01$) and cerebellum ($p < 0.001$) but not the cortex. Spinophilin immunoreactivity was reduced in the hippocampus ($p < 0.05$) but not the cortex and was not detected in the cerebellum.

Table 1 provides a summary of the changes in levels of important proteins related to synaptic neurotransmission, cerebrovascular damage, and cell death that occur in different brain regions following exposure of rats to blast-induced accelerations of either 1200 or 2400G.

4. Discussion

Several conclusions can be drawn from our observations. First, high blast-induced acceleration loads result in a transient deficit in working memory and a chronic increase in anxiety, as measured using the Y

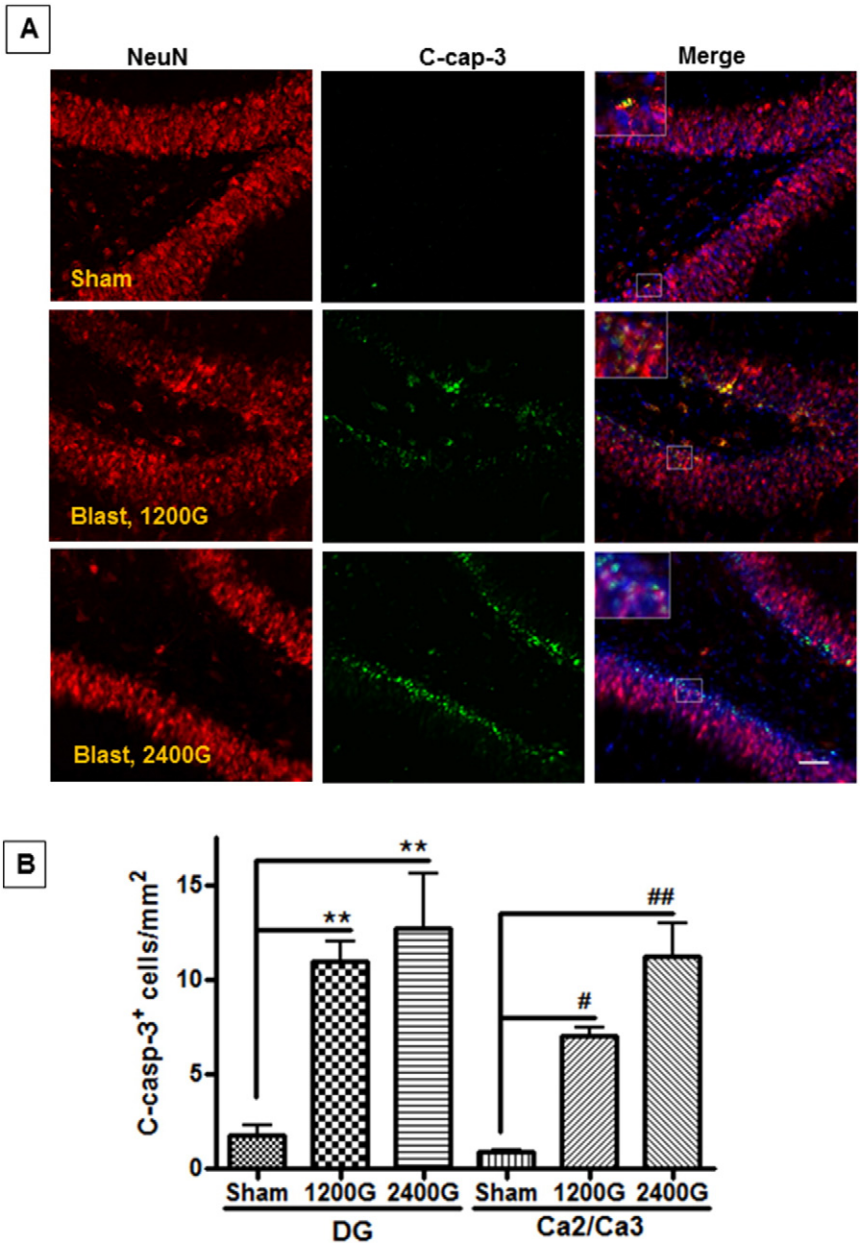

Fig. 6. Cleaved caspase-3 immunoreactive cells present in rat hippocampus. (A) Representative fluorescent image showing the expression of cleaved caspase-3 (green) in DG cells that overlap with NeuN positive cells (red) and DAPI. (B) Quantification of cleaved-caspase-3 immunopositive cells 24 h post-insult indicated a significant increase in positive cells in the DG and Ca2/Ca3 area of both 1200G ($^{**}p < 0.01$ and $^{\#}p < 0.05$) and 2400G ($^{**}p < 0.01$ and $^{\#\#}p < 0.01$) blast rats, respectively, compared to shams. Experimental groups included Shams ($n = 4$), Blast 1200 G ($n = 8$) and Blast 2400 G ($n = 8$).

maze and elevated plus maze, respectively. Second, a decrease in the levels of tight junction proteins taken together with an increase in VWF immunoreactivity suggest that high underbody blast loads result in cerebrovascular damage. Third, these blasts result in neuroinflammation, as reflected by increased perivascular and periventricular F4/80 immunopositive cells during the first week following injury. Fourth, underbody blasts cause significant neuronal death primarily within the hippocampus. Fifth, the significant reduction in both presynaptic and postsynaptic proteins that occurs within 24 h following high blast loads presents the possibility that functional neuronal synapses are compromised. We previously reported significant axonal injury at lower underbody blast acceleration force (Proctor et al., 2014).

Linear acceleration and rotational acceleration were two of the first forces postulated to be primarily responsible for TBI caused by head impacts. While linear acceleration was found to produce mostly focal brain injuries caused by pressure gradient resulting in well-circumscribed intracerebral hematomas (Ommaya et al., 1966; Zhang et al., 2001), rotational acceleration produced both focal and diffuse brain injuries caused by shear strain (Gennarelli et al., 1982; Zhang et al., 2001). In contrast, our underbody blast-induced vertical acceleration model does not produce any detectable focal lesions but rather diffuse damage to blood vessels, synapses, and hippocampal neurons. Previous work also provided qualitative evidence for diffuse axonal injury (Proctor et al., 2014).

Impairments in Y and elevated plus maze tests could be impacted by motor deficits as well as by cognitive deficits. However, with the exception of the rats analyzed one day following 2400G blasts, there was no difference in the total distance traveled between sham and blast rats at 1–28 days post-blast in any of the behavioral metrics. Thus, motor impairments are unlikely to be complicating interpretation of behavioral alterations observed at 6–28 days after the blasts. The results obtained on day zero or one are possibly less reliable than those obtained at

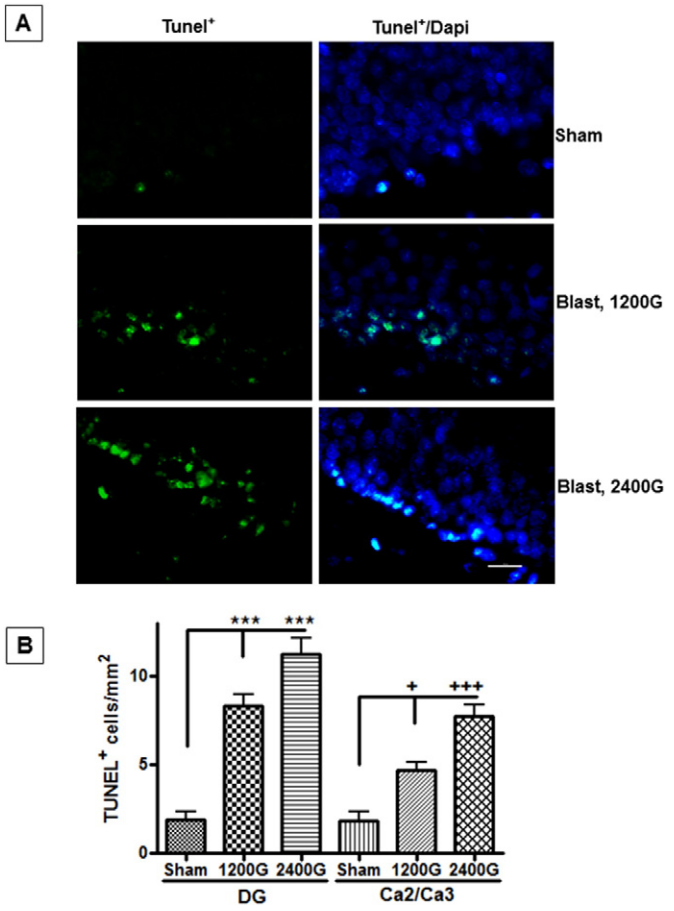

Fig. 7. TUNEL positive cells in rat hippocampus. (A) Representative fluorescent image demonstrating the presence of TUNEL positive cells (green) and DAPI-stained nuclei in the DG. (B) In comparison with shams, there was a significant increase in TUNEL positive cells 24 h post-insult in the DG and Ca2/Ca3 areas of 1200G (***$p < 0.001$ and $^{+}p < 0.05$) and 2400G blast animals (***$p < 0.001$ and $^{+++}p < 0.001$) respectively. Experimental groups were Shams ($n = 4$), Blast 1200 G ($n = 8$) and Blast 2400 G ($n = 8$).

later times since the values in the shams for both tests were lower than the values obtained a later times. Most likely, relatively poor performance by shams on days zero or one is due to behavioral disruption from anesthesia or other stress factors during the first 24 h.

The behavioral alterations apparent in our underbody blast model exhibit some of the characteristics observed in blast overpressure rodent models of TBI. For example, a single exposure of mice to open field overpressure blast causes significant deficits in cognition and spatial memory, both occurring seven days post-insult (Rubovitch et al., 2011). In other studies, rodents subjected to overpressure as well as blast shock waves showed significant deficits in learning, spatial memory and increased anxiety at up to at least one month following blast exposure (Cernak et al., 2011; Kamnaksh et al., 2012; Vandevord et al., 2012). Thus, either open field blast overpressure or under-vehicle blast-induced acceleration is sufficient to cause mild to moderate, long-term behavioral alterations. Thus, it may not be sufficient to protect from overpressure in vehicle design without considering the acceleration injury caused by transfer of kinetic energy to the vehicle.

Neurobehavioral impairments observed following TBI are often associated with markers of neuroinflammation. Neuroinflammatory mechanisms are emerging as a potential common effector of TBI damage to the brain, as well as markers of injury. In our model, we observed a blast dose-dependent increase in F4/80-positive, activated microglia and/or macrophages in perivascular and periventricular regions of the brain. F4/80 positive cells co-labeled with antibodies to inducible nitric oxide synthase (iNOS), which contributes nitrous oxide dependent exacerbation of brain damage caused by inflammation (Foley et al., 2008). F4/80 immunostaining returned to nearly normal levels by 7 days post-blast suggesting that the microglial phase of acceleration induced injury peaks rapidly following the blast.

A range of evidence supports the role of inflammation in the pathogenesis of open field blast-induced TBI. Observations include the increased expression of inflammatory mediators including macrophage inflammatory proteins, monocytes chemotactic proteins, IL-1β, IL-6 TNF-α and INF-γ (Dalle Lucca et al., 2012; Kamnaksh et al., 2012; Kovesdi et al., 2011; Tompkins et al., 2013). cDNA microarray measurements indicate an increase in the mRNA levels of many pro-inflammatory genes including interleukins and TNF-α (Valiyaveettil et al., 2013). At the cellular level, microglia activation and increase macrophage levels have been reported in the rodent brains following blast exposure (Cho et al., 2013; Dalle Lucca et al., 2012; Sosa et al., 2013; Tompkins et al., 2013). In most of these studies, including ours, markers of inflammation responses from microglia occur acutely at 3–48 h post-blast.

An elevation in the presence of inflammatory cells in the brain after TBI can be caused by endogenous microglial activation, migration, and proliferation. Systemically circulating macrophages can also invade the brain parenchyma, particularly if there is disruption in the blood brain barrier (BBB) and/or vascular endothelial cells. Two major components of tight junctions (Occludin and ZO-1), crucial in maintaining BBB integrity (Abdul-Muneer et al., 2013; Armulik et al., 2010), showed significant reductions in cortex and hippocampus. The mechanisms resulting in the reduction are unclear, but could be reduced synthesis rate or alterations in the proteolytic activity of enzymes such as the metalloproteinase-9, which is associated with effectors of BBB dysfunction following TBI (Higashida et al., 2011). In contrast, an increase in VWF was observed primarily in the cerebellum after either 1200 or 2400G blasts. VWF activation may represent a compensatory mechanism to promote blood coagulation after vascular injury that occurs after TBI (De Oliveira et al., 2007; Yokota et al., 2002). The reduction in occludin and ZO-1 protein levels seen after underbody blasts is consistent with a recent report by Abdul-Muneer and colleagues indicating that exposure of rats to a single blast-relevant shock wave caused a downregulation of tight junction protein expression, associated with increased levels of the oxidative stress markers 3-nitrotyrosine (3-NT) and 4-hydroxynonenal (4-HNE) (Abdul-Muneer et al., 2013). In contrast to downregulation of occludin and ZO-1 proteins, an increase in the platelet adhesion regulating molecule VWF was only observed in the cerebellum. VWF activation may represent a compensatory mechanism to promote blood coagulation after vascular injury (De Oliveira et al., 2007; Yokota et al., 2002) and be protective of this brain region. Additional studies are needed, however, to test whether these molecular changes are actually accompanied by BBB disruption.

We previously reported the absence of significant cell death in the brains of rats following underbody blasts at low G forces (50G). However at the higher accelerations used in the present study (1200–2400G) there was significant cell death. Some studies have concluded apoptosis in different brain regions following exposure to blast that correlated with cognitive impairments associated with a function of those regions (Kobeissy et al., 2013; Kwon et al., 2011; Vandevord et al., 2012). We detected the presence of apoptotic cells in the hippocampus, which was associated with a decrease in Bcl-2 expression and an upregulation of the stress response protein Hsp70. Although the increased expression of Hsp70 may represent an attempt to protect against the deleterious effects of oxidative and other forms of stress (Adachi et al., 2009; Kim et al., 2015), the downregulation of the anti-apoptotic protein Bcl-2 is very likely to promote apoptotic and other forms of cell death. While loss of viable neurons in the hippocampus may contribute to deficits in working memory and anxiety like behavior, the effects of under-vehicle blasts on other factors, including axonal and synaptic neuroanatomy and neurophysiology may also contribute to behavioral alterations.

Adequate synaptic transmission is clearly required for the maintenance of neurobehavioral functions (Shankar and Walsh, 2009; Stancu

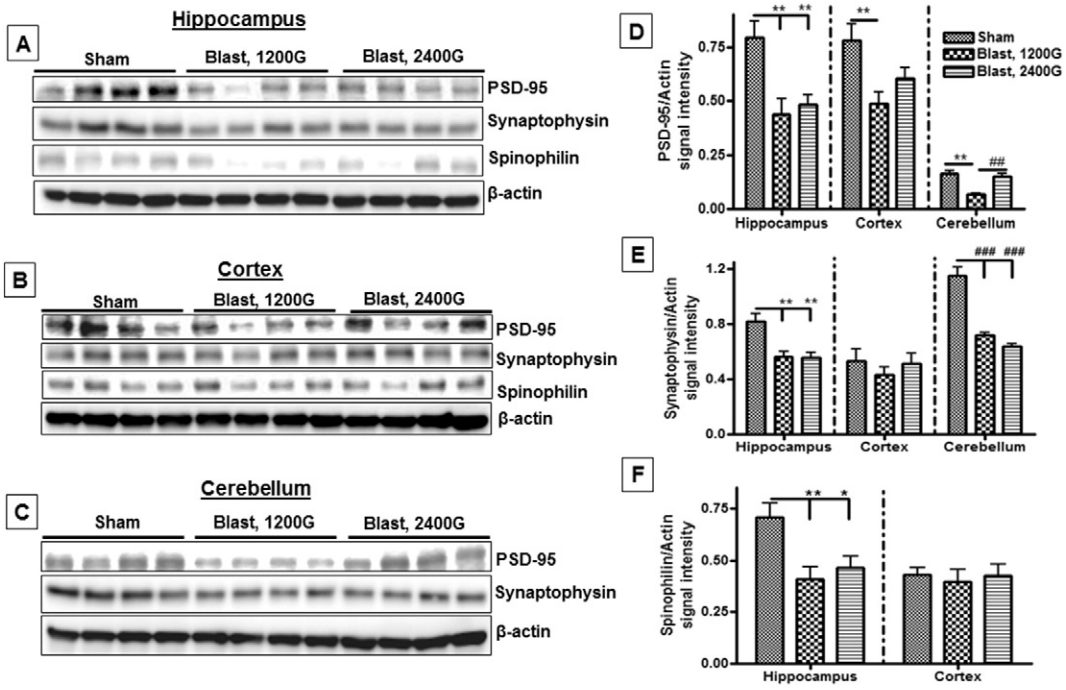

Fig. 8. Brain region selective reduction in the expression of synaptic proteins following exposure to blasts. (A–C) Representative immunoblots illustrating the expression of PSD-95, synaptophysin, and spinophilin in the hippocampus, cortex, and cerebellum (spinophilin was not detectable in the cerebellum). Quantification of protein bands indicate that (D) PSD-95 expression was significantly reduced in the hippocampus, cortex and cerebellum of both 1200G and 2400G blast animals ($^{**}p < 0.01$). Conversely, PSD-95 expression was only significantly affected in the hippocampus of rats exposed to a 2400G blast ($^{**}p < 0.01$). (E) Synaptophysin expression was dramatically reduced in the hippocampus and cerebellum of 1200G ($^{**}p < 0.01$ and $^{\#\#\#}p < 0.001$) and 2400G blast rats ($^{**}p < 0.01$ and $^{\#\#\#}p < 0.001$), respectively, in comparison with shams. (F) Spinophilin expression was only significantly affected in the hippocampus of 1200G and 2400G blast rats ($^{**}p < 0.01$ and $^{*}p < 0.05$ respectively). Number of animals in each experimental group was Shams ($n = 6$), Blast 1200 G ($n = 6$) and Blast 2400 G ($n = 6$).

et al., 2014). Loss of synapses and dendritic spine has been reported in models of focal brain injury shortly after trauma and affect learning and memory performance (Gao et al., 2011; Scheff et al., 2005). Interestingly, in our blast model, we observed decreased expression of synaptic markers synaptophysin and PSD-95 and that of the dendritic spine marker spinophilin, which all suggest a deficit in synaptic transmission. However, similar to changes seen with the expression of tight junction proteins between shams and blast rats, their expression was heterogeneous in different regions of the brain with a decrease observed in the hippocampus and little or no change in the cortex. This heterogeneous expression pattern could be due to anatomical differences in various brain regions and differences in sensitivity to excitotoxic insult (Geddes et al., 2003). Prior studies in models of experimental brain trauma demonstrated increased vulnerability of hippocampal neurons and cerebellar purkinje cells to trauma (Anderson et al., 2005; Igarashi et al., 2007; Nawashiro et al., 1995).

The degree to which our model applies to the brain injury suffered by humans present within vehicles targeted by underbody blasts is difficult to define, based on the complex array of forces that participate in these brain injuries and the tremendous difference in the mass of rats and humans. Based simply on the equation that force equals mass times acceleration, the 2400G experienced by our 350 g rats would be equivalent to 11G for a 75 kg human. Since the brain is the organ of interest in our study, the same scaling projects that the load of 2400G on a 2 g rat brain is equivalent to 4G on a 1300 g human brain. While most studies indicate that exposure to linear acceleration of less than or equal to 10G for a short period is unlikely to produce chronic or possibly even acute neuropsychologic symptoms, the conditions used to model linear acceleration are very different than those produced by an explosion under the belly of a vehicle. For example, the peak acceleration of 2400G induced by the underbody explosion in our model was reached within 0.3 msec, which is at least two orders of magnitude shorter than the duration when the maximum G force is reached during motor vehicle collisions. Thus, the rate at which the acceleration changes, known as JERK, may be an even more important factor than simply maximum G force. This hypothesis is supported by the fact that when we increased the

Table 1
Summary of changes in levels of proteins present in the hippocampus, cortex, and cerebellum 24 h following exposure to underbody blast-induced accelerations of either 1200G or 2400G. (▼: significantly decreased; ▲: significantly increased; ▬: no significant change; ND: not detected).

Proteins	Acceleration G force					
	1200G			2400G		
	Hippocampus	Cortex	Cerebellum	Hippocampus	Cortex	Cerebellum
ZO-1	▬	▬	▬	▬	▼	▬
Occludin	▬	▬	▬	▼	▼	▬
VWF	▲	▬	▲	▬	▬	▲
Hsp70	▲	▬	▲	▲	▬	▲
Bcl-2	▼	▬	▼	▼	▬	▼
PSD-95	▼	▼	▼	▼	▬	▬
Synaptophysin	▼	▬	▼	▼	▬	▼
Spinophilin	▼	▬	ND	▼	▬	ND

peak G force by only 17% from 2400 to 2800G by reducing the weight of our "vehicle" the JERK rose by 62% and was followed immediately by death to four out of 6 rats and severe, chronic anxiety to one of the two surviving rats. Despite these scaling issues, we believe that insight into the pathophysiology of brain injury caused by underbody blast-induced acceleration is a very important addition to the knowledge gained from animal models of TBI caused by shock waves, which is more relevant to blast induced injury to the brains of unmounted warfighters.

5. Conclusions

In summary, our results demonstrate that high acceleration force induced brain injury altered the expression of proteins which have a crucial function maintaining blood brain integrity, potentially leading to increased accumulation of inflammatory cells in the brain. Blast-induced brain trauma also caused neuronal cell loss in the hippocampus associated with reduced expression of proteins which modulate synaptic transmission. The neurologic consequences of these neuropathological alterations are a transient deficit in working memory and a chronic change in behavior interpreted as anxiety or depression. Overall, findings from our unique model of underbody blasts indicate that exposure to acceleration force alone is sufficient to cause at least mild TBI relevant to what survivors of under-vehicle explosions often experience. Work is in progress to develop new vehicle hull designs that dramatically reduce the force that these blasts transfer to the occupants, thus reducing both mortality and injury to the brain and other vital organs.

Acknowledgments

This research was supported by grants from the U.S. Department of Defense (W81-xWH-13-1-0016) and from the U.S. Air Force Medical Service (FA8650-11-2-6D04).

References

Abdul-Muneer, P.M., Schuetz, H., Wang, F., Skotak, M., Jones, J., Gorantla, S., Zimmerman, M.C., Chandra, N., Haorah, J., 2013. Induction of oxidative and nitrosative damage leads to cerebrovascular inflammation in an animal model of mild traumatic brain injury induced by primary blast. Free Radic. Biol. Med. 60, 282–291.

Adachi, M., Liu, Y., Fujii, K., Calderwood, S.K., Nakai, A., Imai, K., Shinomura, Y., 2009. Oxidative stress impairs the heat stress response and delays unfolded protein recovery. PLoS One 4, e7719.

Anderson, K.J., Miller, K.M., Fugaccia, I., Scheff, S.W., 2005. Regional distribution of fluorojade B staining in the hippocampus following traumatic brain injury. Exp. Neurol. 193, 125–130.

Armulik, A., Genove, G., Mae, M., Nisancioglu, M.H., Wallgard, E., Niaudet, C., He, L., Norlin, J., Lindblom, P., Strittmatter, K., Johansson, B.R., Betsholtz, C., 2010. Pericytes regulate the blood-brain barrier. Nature 468, 557–561.

Brenner, L.A., Vanderploeg, R.D., Terrio, H., 2009. Assessment and diagnosis of mild traumatic brain injury, posttraumatic stress disorder, and other polytrauma conditions: burden of adversity hypothesis. Rehabil. Psychol. 54, 239–246.

Budde, M.D., Shah, A., McCrea, M., Cullinan, W.E., Pintar, F.A., Stemper, B.D., 2013. Primary blast traumatic brain injury in the rat: relating diffusion tensor imaging and behavior. Front. Neurol. 4, 154.

Cernak, I., Merkle, A.C., Koliatsos, V.E., Bilik, J.M., Luong, Q.T., Mahota, T.M., Xu, L., Slack, N., Windle, D., Ahmed, F.A., 2011. The pathobiology of blast injuries and blast-induced neurotrauma as identified using a new experimental model of injury in mice. Neurobiol. Dis. 41, 538–551.

Chen, Y., Huang, W., Constantini, S., 2013. Concepts and strategies for clinical management of blast-induced traumatic brain injury and posttraumatic stress disorder. J. Neuropsychiatry Clin. Neurosci. 25, 103–110.

Cho, H.J., Sajja, V.S., Vandevord, P.J., Lee, Y.W., 2013. Blast induces oxidative stress, inflammation, neuronal loss and subsequent short-term memory impairment in rats. Neuroscience 253, 9–20.

Dalle Lucca, J.J., Chavko, M., Dubick, M.A., Adeeb, S., Falabella, M.J., Slack, J.L., McCarron, R., Li, Y., 2012. Blast-induced moderate neurotrauma (BINT) elicits early complement activation and tumor necrosis factor alpha (TNFalpha) release in a rat brain. J. Neurol. Sci. 318, 146–154.

De Oliveira, C.O., Reimer, A.G., Da Rocha, A.B., Grivicich, I., Schneider, R.F., Roisenberg, I., Regner, A., Simon, D., 2007. Plasma von Willebrand factor levels correlate with clinical outcome of severe traumatic brain injury. J. Neurotrauma 24, 1331–1338.

DePalma, R.G., Burris, D.G., Champion, H.R., Hodgson, M.J., 2005. Blast injuries. N. Engl. J. Med. 352, 1335–1342.

Elder, G.A., Mitsis, E.M., Ahlers, S.T., Cristian, A., 2010. Blast-induced mild traumatic brain injury. Psychiatry Clin. North Am. 33, 757–781.

Elder, G.A., Gama Sosa, M.A., De Gasperi, R., Stone, J.R., Dickstein, D.L., Haghighi, F., Hof, P.R., Ahlers, S.T., 2015. Vascular and inflammatory factors in the pathophysiology of blast-induced brain injury. Front. Neurol. 6, 48.

Foley, L.M., Hitchens, T.K., Melick, J.A., Bayir, H., Ho, C., Kochanek, P.M., 2008. Effect of inducible nitric oxide synthase on cerebral blood flow after experimental traumatic brain injury in mice. J. Neurotrauma 25, 299–310.

Gao, X., Deng, P., Xu, Z.C., Chen, J., 2011. Moderate traumatic brain injury causes acute dendritic and synaptic degeneration in the hippocampal dentate gyrus. PLoS One 6, e24566.

Geddes, D.M., LaPlaca, M.C., Cargill 2nd, R.S., 2003. Susceptibility of hippocampal neurons to mechanically induced injury. Exp. Neurol. 184, 420–427.

Gennarelli, T.A., Thibault, L.E., Adams, J.H., Graham, D.I., Thompson, C.J., Marcincin, R.P., 1982. Diffuse axonal injury and traumatic coma in the primate. Ann. Neurol. 12, 564–574.

Goldstein, L.E., McKee, A.C., Stanton, P.K., 2014. Considerations for animal models of blast-related traumatic brain injury and chronic traumatic encephalopathy. Alzheimers Res. Ther. 6, 64.

Higashida, T., Kreipke, C.W., Rafols, J.A., Peng, C., Schafer, S., Schafer, P., Ding, J.Y., Dornbos 3rd, D., Li, X., Guthikonda, M., Rossi, N.F., Ding, Y., 2011. The role of hypoxia-inducible factor-1alpha, aquaporin-4, and matrix metalloproteinase-9 in blood-brain barrier disruption and brain edema after traumatic brain injury. J. Neurosurg. 114, 92–101.

Hoge, C.W., McGurk, D., Thomas, J.L., Cox, A.L., Engel, C.C., Castro, C.A., 2008. Mild traumatic brain injury in U.S. soldiers returning from Iraq. N. Engl. J. Med. 358, 453–463.

Igarashi, T., Potts, M.B., Noble-Haeusslein, L.J., 2007. Injury severity determines Purkinje cell loss and microglial activation in the cerebellum after cortical contusion injury. Exp. Neurol. 203, 258–268.

Jaffee, M.S., Meyer, K.S., 2009. A brief overview of traumatic brain injury (TBI) and posttraumatic stress disorder (PTSD) within the Department of Defense. Clin. Neuropsychol. 23, 1291–1298.

Kamnaksh, A., Kwon, S.K., Kovesdi, E., Ahmed, F., Barry, E.S., Grunberg, N.E., Long, J., Agoston, D., 2012. Neurobehavioral, cellular, and molecular consequences of single and multiple mild blast exposure. Electrophoresis 33, 3680–3692.

Kim, N., Kim, J.Y., Yenari, M.A., 2015. Pharmacological induction of the 70-kDa heat shock protein protects against brain injury. Neuroscience 284, 912–919.

Kobeissy, F., Mondello, S., Tumer, N., Toklu, H.Z., Whidden, M.A., Kirichenko, N., Zhang, Z., Prima, V., Yassin, W., Anagli, J., Chandra, N., Svetlov, S., Wang, K.K., 2013. Assessing neuro-systemic & behavioral components in the pathophysiology of blast-related brain injury. Front. Neurol. 4, 186.

Kovacs, S.K., Leonessa, F., Ling, G.S., 2014. Blast TBI models, neuropathology, and implications for seizure risk. Front. Neurol. 5, 47.

Kovesdi, E., Gyorgy, A.B., Kwon, S.K., Wingo, D.L., Kamnaksh, A., Long, J.B., Kasper, C.E., Agoston, D.V., 2011. The effect of enriched environment on the outcome of traumatic brain injury; a behavioral, proteomics, and histological study. Front. Neurosci. 5, 42.

Kwon, S.K., Kovesdi, E., Gyorgy, A.B., Wingo, D., Kamnaksh, A., Walker, J., Long, J.B., Agoston, D.V., 2011. Stress and traumatic brain injury: a behavioral, proteomics, and histological study. Front. Neurol. 2, 12.

Lange, R.T., Brickell, T.A., Ivins, B., Vanderploeg, R.D., French, L.M., 2013. Variable, not always persistent, postconcussion symptoms after mild TBI in U.S. military service members: a five-year cross-sectional outcome study. J. Neurotrauma 30, 958–969.

Loane, D.J., Stoica, B.A., Tchantchou, F., Kumar, A., Barrett, J.P., Akintola, T., Xue, F., Conn, P.J., Faden, A.I., 2014. Novel mGluR5 positive allosteric modulator improves functional recovery, attenuates neurodegeneration, and alters microglial polarization after experimental traumatic brain injury. Neurotherapeutics 11, 857–869.

Maurice, T., Hippert, C., Serratrice, N., Dubois, G., Jacquet, C., Antignac, C., Kremer, E.J., Kalatzis, V., 2009. Cystine accumulation in the CNS results in severe age-related memory deficits. Neurobiol. Aging 30, 987–1000.

Mellor, S.G., 1988. The pathogenesis of blast injury and its management. Br. J. Hosp. Med. 39, 536–539.

Nawashiro, H., Shima, K., Chigasaki, H., 1995. Selective vulnerability of hippocampal Ca3 neurons to hypoxia after mild concussion in the rat. Neurol. Res. 17, 455–460.

Okie, S., 2005. Traumatic brain injury in the war zone. N. Engl. J. Med. 352, 2043–2047.

Ommaya, A.K., Hirsch, A.E., Flamm, E.S., Mahone, R.H., 1966. Cerebral concussion in the monkey: an experimental model. Science 153, 211–212.

Owens, B.D., Kragh Jr., J.F., Wenke, J.C., Macaitis, J., Wade, C.E., Holcomb, J.B., 2008. Combat wounds in operation Iraqi Freedom and operation Enduring Freedom. J. Trauma 64, 295–299.

Proctor, J.L., Fourney, W.L., Leiste, U.H., Fiskum, G., 2014. Rat model of brain injury caused by under-vehicle blast-induced hyperacceleration. J. Trauma Acute Care Surg. 77, S83–S87.

Przekwas, A., Somayaji, M.R., Gupta, R.K., 2016. Synaptic mechanisms of blast-induced brain injury. Front. Neurol. 7, 2.

Ramlackhansingh, A.F., Brooks, D.J., Greenwood, R.J., Bose, S.K., Turkheimer, F.E., Kinnunen, K.M., Gentleman, S., Heckemann, R.A., Gunanayagam, K., Gelosa, G., Sharp, D.J., 2011. Inflammation after trauma: microglial activation and traumatic brain injury. Ann. Neurol. 70, 374–383.

Rosenfeld, J.V., Ford, N.L., 2010. Bomb blast, mild traumatic brain injury and psychiatric morbidity: a review. Injury 41, 437–443.

Rosenfeld, J.V., McFarlane, A.C., Bragge, P., Armonda, R.A., Grimes, J.B., Ling, G.S., 2013. Blast-related traumatic brain injury. Lancet Neurol. 12, 882–893.

Rubovitch, V., Ten-Bosch, M., Zohar, O., Harrison, C.R., Tempel-Brami, C., Stein, E., Hoffer, B.J., Balaban, C.D., Schreiber, S., Chiu, W.T., Pick, C.G., 2011. A mouse model of blast-induced mild traumatic brain injury. Exp. Neurol. 232, 280–289.

Scheff, S.W., Price, D.A., Hicks, R.R., Baldwin, S.A., Robinson, S., Brackney, C., 2005. Synaptogenesis in the hippocampal Ca1 field following traumatic brain injury. J. Neurotrauma 22, 719–732.

Schultz, B.A., Cifu, D.X., McNamee, S., Nichols, M., Carne, W., 2011. Assessment and treatment of common persistent sequelae following blast induced mild traumatic brain injury. NeuroRehabilitation 28, 309–320.

Shankar, G.M., Walsh, D.M., 2009. Alzheimer's disease: synaptic dysfunction and Abeta. Mol. Neurodegener. 4, 48.

Sosa, M.A., De Gasperi, R., Paulino, A.J., Pricop, P.E., Shaughness, M.C., Maudlin-Jeronimo, E., Hall, A.A., Janssen, W.G., Yuk, F.J., Dorr, N.P., Dickstein, D.L., McCarron, R.M., Chavko, M., Hof, P.R., Ahlers, S.T., Elder, G.A., 2013. Blast overpressure induces shear-related injuries in the brain of rats exposed to a mild traumatic brain injury. Acta Neuropathol. Commun. 1, 51.

Stancu, I.C., Ris, L., Vasconcelos, B., Marinangeli, C., Goeminne, L., Laporte, V., Haylani, L.E., Couturier, J., Schakman, O., Gailly, P., Pierrot, N., Kienlen-Campard, P., Octave, J.N., Dewachter, I., 2014. Tauopathy contributes to synaptic and cognitive deficits in a murine model for Alzheimer's disease. FASEB J. 28, 2620–2631.

Tchantchou, F., Zhang, Y., 2013. Selective inhibition of alpha/beta-hydrolase domain 6 attenuates neurodegeneration, alleviates blood brain barrier breakdown, and improves functional recovery in a mouse model of traumatic brain injury. J. Neurotrauma.

Tchantchou, F., Xu, Y., Wu, Y., Christen, Y., Luo, Y., 2007. EGb 761 enhances adult hippocampal neurogenesis and phosphorylation of CREB in transgenic mouse model of Alzheimer's disease. FASEB J. 21, 2400–2408.

Tchantchou, F., Tucker, L.B., Fu, A.H., Bluett, R.J., McCabe, J.T., Patel, S., Zhang, Y., 2014. The fatty acid amide hydrolase inhibitor PF-3845 promotes neuronal survival, attenuates inflammation and improves functional recovery in mice with traumatic brain injury. Neuropharmacology 85, 427–439.

Tompkins, P., Tesiram, Y., Lerner, M., Gonzalez, L.P., Lightfoot, S., Rabb, C.H., Brackett, D.J., 2013. Brain injury: neuro-inflammation, cognitive deficit, and magnetic resonance imaging in a model of blast induced traumatic brain injury. J. Neurotrauma 30, 1888–1897.

Valiyaveettil, M., Alamneh, Y., Wang, Y., Arun, P., Oguntayo, S., Wei, Y., Long, J.B., Nambiar, M.P., 2013. Contribution of systemic factors in the pathophysiology of repeated blast-induced neurotrauma. Neurosci. Lett. 539, 1–6.

Vandevord, P.J., Bolander, R., Sajja, V.S., Hay, K., Bir, C.A., 2012. Mild neurotrauma indicates a range-specific pressure response to low level shock wave exposure. Ann. Biomed. Eng. 40, 227–236.

Walls, M.K., Race, N., Zheng, L., Vega-Alvarez, S.M., Acosta, G., Park, J., Shi, R., 2015. Structural and biochemical abnormalities in the absence of acute deficits in mild primary blast-induced head trauma. J. Neurosurg. 1–12.

Yokota, H., Naoe, Y., Nakabayashi, M., Unemoto, K., Kushimoto, S., Kurokawa, A., Node, Y., Yamamoto, Y., 2002. Cerebral endothelial injury in severe head injury: the significance of measurements of serum thrombomodulin and the von Willebrand factor. J. Neurotrauma 19, 1007–1015.

Zhang, L., Yang, K.H., King, A.I., 2001. Biomechanics of neurotrauma. Neurol. Res. 23, 144–156.

Zhao, X., Tiwari, V., Sutton, M.A., Deng, X., Fourney, W.L., Leiste, U., 2013. Scaling of the deformation histories for clamped circular plates subjected to blast loading by buried charges. Int. J. Impact Eng. 54, 31–50.

APPENDIX 5

Tchantchou F, Puche AC, Leiste U, Fourney W, Blanpied TA, Fiskum G. Rat Model of Brain Injury to Occupants of Vehicles Targeted by Land Mines: Mitigation by Elastomeric Frame Designs. J Neurotrauma. 2017 Epub Nov 29. PMID: 29187028.

Journal of Neurotrauma

DOI: 10.1089/neu.2017.5401

TITLE

Rat Model of Brain Injury to Occupants of Vehicles Targeted by Land Mines: Mitigation by Elastomeric Frame Designs

AUTHORS

Flaubert Tchantchou, PhD, Research Associate[1], Adam A. Puche, PhD, Professor[2], Ulrich Leiste, PhD, Assistant Research Engineer[3], William Fourney, PhD, Professor[3], Thomas A. Blanpied, PhD, Associate Professor[4], and Gary Fiskum, PhD, Professor[1]

AFFILIATIONS

[1]Department of Anesthesiology and the Center for Shock, Trauma, and Anesthesiology Research (STAR), University of Maryland School of Medicine

[2]Department of Anatomy and Neurobiology, University of Maryland School of Medicine

[3]Department of Aerospace Engineering, University of Maryland School of Engineering

[4]Department of Physiology, University of Maryland School of Medicine

CORRESPONDENCE

Dr. Gary Fiskum

685 W. Baltimore St., MSTF 5.34

Baltimore MD, 21201

Phone: 410-706-4711

Email: gfiskum@som.umaryland.edu

AUTHOR CONTACT INFORMATION

Flaubert Tchantchou, Ph.D, Department of Anesthesiology, University of Maryland School of Medicine, MSTF 5.34, 685 W. Baltimore, MD 21201; Phone 410-706-3418; ftchantchou@som.umaryland.edu

Adam Puche, PhD, Department of Anatomy and Neurobiology, Health Sciences Facility, Room 280 M, Baltimore, MD 21201; 410-706-3530; Email: apuche@som.umaryland.edu

Ulrich Leiste, PhD, Department of Aerospace Engineering, 1131 Glenn L. Martin Hall, University of Maryland, College Park, MD; Phone: 301-405-5339; Email: uleiste@umd.edu

William L Fourney, Ph.D, Department of Aerospace Engineering, 1131 Glenn L. Martin Hall, University of Maryland, College Park, MD; Phone: 301-405-5339; Email: four@umd.edu

Thomas A. Blanpied, PhD, Department of Physiology, 505 Howard Hall, 660 W Redwood St. Baltimore, MD 21201; Phone: 410-706-4769; Email: tblanpied@som.umaryland.edu

Gary Fiskum, Ph.D, Department of Anesthesiology, University of Maryland School of Medicine, MSTF 5.34, 685 W. Baltimore, MD 21201; Phone: 410-706-4711; Email: gfiskum@som.umaryland.edu

Funding sources: US Army W81XWH-13-1-0016 and US Air Force FA8650-11-2-6D04

RUNNING TITLE

Mitigation of Under-Vehicle Blast-Induced Brain Injury

TABLE OF CONTENTS TITLE

Mitigation of Under-Vehicle Blast-Induced Brain Injury

ABSTRACT

Many victims of blast traumatic brain injury (TBI) are occupants of vehicles targeted by land mines. A rat model of under-vehicle blast TBI was used to test the hypothesis that the ensuing neuropathology and altered behavior are mitigated by vehicle frame designs that dramatically reduce blast-induced acceleration (G force). Male rats were restrained on an aluminum platform that was accelerated vertically at up to 2850G, in response to detonation of an explosive positioned under a second platform in contact with the top via different structures. The presence of elastomeric, polyurea-coated aluminum cylinders between the platforms reduced acceleration by 80% to 550G compared to 2350G with uncoated cylinders. Moreover, 67% of rats exposed to 2850G, and 20% of those exposed to 2350G died immediately after blast, whereas all rats subjected to 550G-blast survived. Assays for working memory (Y maze) and anxiety (Plus maze) were conducted for up to 28 days. Rats were euthanized at 24 h or 29 days and their brains used for histopathology and neurochemical measurements. Rats exposed to 2350G-blasts exhibited increased cleaved caspase-3 immunoreactive neurons in the hippocampus. There was also increased vascular IgG effusion and F4/80 immunopositive macrophages/microglia. Blast exposure reduced hippocampal levels of synaptic proteins bassoon and homer-1, which were associated with impaired performance in the Y maze and the Plus maze tests. These changes observed after 2350G-blasts were reduced or eliminated with the use of polyurea coated cylinders. Such advances in vehicle designs should aid in the development of the next generation of blast-resistant vehicles.

Key Words: Acceleration, synapses, inflammation, blast, blood brain barrier

INTRODUCTION

Exposure to blasts has resulted in traumatic brain injury (TBI) to over 250,000 US military personnel during the last 10 years. Many of these victims were occupants within vehicles targeted by land mines and improvised explosive devices (IEDs). While there are many animal models of blast TBI, most are designed to replicate primarily the effects of blast-induced barometric pressure changes, also known as overpressure, on the brain and other organs. Individuals present within vehicles targeted by under-body explosions experience far-less change in barometric pressure due to transmission of most force to the bottom of the vehicle. This energy transduction results in extreme acceleration of the vehicle and its occupants, reaching G forces in the range of 300 to 3000G [1].

We developed a small-scale model of under-vehicle explosions and used this model to describe how different frame designs, including the double V-shaped hull, affect the loads imparted from an explosive on to the vehicle. The double V-shaped hull was subsequently incorporated into the mine-resistant, armor protected (MRAP) US military vehicles in 2007 [2]. During the year prior to this transformation, the fatality rate for exposure to under-vehicle blasts was 60%. As the number of MRAPs deployed to combat zones rose steadily to over 10,000 by the end of December 2008, the fatality rate dropped to less than 10% [3]. Most of this improvement in survival was due to a dramatic reduction in penetrance of the explosions through vehicle hulls into the cabins. While this was a tremendous achievement, many of those present in the targeted vehicles suffered severe, albeit survivable injuries, including TBI.

Considering the lack of animal models for TBI experienced by victims present within blast-targeted vehicles, we initially developed a model that used anesthetized rats exposed to under-vehicle blasts that generated acceleration G forces in the range of 30 – 50G [4]. This force range resulted in histologic evidence of axonal damage but no evidence for change in neurobehavioral measurements. When the force was elevated to 100G, we obtained strong quantitative verification of axonal injury and indications of vestibulomotor alterations [5]. These experiments were followed by a G-force dose escalation study performed with awake rats present within restraints secured to the top of an aluminum

platform that was accelerated vertically at up to 2850G, in response to the detonation of a small explosive positioned under a second, bottom platform. Seventy percent of rats exposed to 2850G died soon thereafter, while all rats exposed to 2400G survived but demonstrated evidence for a transient deficit in working memory, chronic anxiety, and neuropathology [6]. In these experiments, only a thin, 0.6 cm rubber pad was located between the top and bottom platforms, which dampened oscillations but had no significant effect on the maximum transmission of force between the two plates.

The current study used this same model of under-vehicle blast TBI to test the hypothesis that the neuropathology and altered behavior that ensue can be mitigated by vehicle frame designs that dramatically reduce the acceleration experienced by the rats. Specifically, we tested the effectiveness of the presence of uncoated and polyurea-coated crushable aluminum cylinders within the chassis at reducing maximum G-force, mortality, neuropathology, and neurologic injury following exposure to under-vehicle blasts.

Materials and Methods

Animals and housing

All animal protocols were approved by the University of Maryland, Baltimore Animal Use and Care Committee (IACUC) and the US Army Animal Care and Use Review Office (ACURO). Male Sprague-Dawley rats (300-350 gm; Envigo, CA), were maintained under a controlled environment with an ambient temperature of 23 ± 2 °C, a 12 h light/dark cycle, and continuous access to food and water *ad libitum*. Experimental groups consisted of 10 to 15 rats/group for behavioral studies and 5-6 rats/group for immunohistochemistry or biochemical analyses.

Underbody blast and blast mitigation design

Following scaling analysis and procedures previously described [4,7], rats were exposed to underbody blast paradigms generating a mean maximal G-force of approximately 2850G, as recently reported [6]. In brief, two isoflurane anesthetized rats were secured, while unconscious, within fiberglass restrainers (Stoeling Inc., IL) bolted to

the top aluminum platform, which was 38 cm square and 2.5 cm thick. The restraints included a custom-fit metallic cone to minimize head movement, secondary, acceleration, and head impact. The top platform was located directly above another 38 cm square aluminum platform, which was 5.0 cm thick. Both platforms were separated by a 0.6 cm thick, hard-rubber pad to dampen oscillatory acceleration forces. Each platform had a 3.5 cm hole located at each corner though which 2.0 cm thick guide-poles were located, allowing for purely vertical movement. This device was located in a steel water tank at a water level of either 0.2 cm below the bottom platform. An explosive charge of 2.0 gm pentaerythritol tetranitrate (PETN) was secured at a fixed 5 cm depth (stand-off distance) in the water beneath the center of the lower platform. This charge was detonated electrically exactly 5 min after anesthesia was discontinued, when the rats were fully conscious.

Experiments were performed to test the ability of unique, acceleration absorbing frame designs to reduce the G-force transmitted to the rats. Five uncoated or polyurea-coated, crushable aluminum cylinders were placed between the top and bottom platforms in an effort to mitigate the force transduction between the bottom and top platforms. The dimensions of each cylinder were 66 mm wide and 38 mm high, with an aluminum wall thickness of 0.1 mm. When present, the polyurea coating thickness was 1.6 mm thick. The weight of each uncoated cylinder was 2.1 gm and 14.6 gm for the polyurea-coated cylinder. For all blast paradigms, with or without mitigation, two accelerometers were placed on the top of the higher platform near the head end of the restraints and used to determine the acceleration and JERK (first derivative of acceleration), measured by UERD-Tools software (U.S. NAVY). Pressure sensors were also placed near the head-end of the restraints during several experiments, verifying that the pressure changes experienced by the rats were less than 1 lb/in^2. Sham animals were also anesthetized with 4% isoflurane for 5 min, secured on the platform and removed 5 min later without blast exposure.

All blast and sham animals were returned to their respective cage immediately after blast or sham procedures and examined for any physical injuries every 30 min for 3 h. Necropsies were performed immediately on all animals that died following blast exposure.

Behavioral analysis

The Y maze test was performed to assess hippocampus-dependent working memory on day zero, at approximately 1 h, and at days 6, 13 and 27 post-injury, as previously described [6,8]. In brief, each rat was placed at the center of the maze and allowed to explore for 5 min. Movement was recorded using an overhead camera and analysis performed with the Any-Maze software (SD instruments, CA). Arm visit sequences and number of entries to each arm were recorded. Working memory was defined by the frequency of alternately exploring different arms and was determined using the formula: total number of alternations / (total number of arm entries − 2) × 100. The elevated plus maze test was performed to evaluate anxiety-like behaviors by rats on days 1, 8, 14 and 28 post-blast, as previously described [6,9]. In brief, rats were individually placed on the central area of the Plus maze and allowed to explore for 10 min. Movement was recorded by an overhead camera and data were analyzed by Any-maze software, to provide information including the time spent in each arm and the central area and the total distance traveled. Anxiety like behavior is inversely proportional to the time the rats spend in the open arms.

Experimental time points, tissue collection and processing

Rats were deeply anesthetized with an intraperitoneal (i.p) injection of a mixture of ketamine (160 mg/kg) and xylazine (120 mg/kg) at different times following blast or sham blast procedures (Fig. 1). They were then euthanized by exsanguination via transcardial perfusion for 5 min with oxygenated artificial cerebrospinal fluid containing 148 mM NaCl, 5 mM glucose, 3.0 mM KCl, 1.85 mM $CaCl_2$, 1.7 mM $MgCl_2$, 1.5 mM Na_2HPO_4, and 0.14 mM NaH_2PO_4 (pH 7.4). The rats were then perfused for 15 min with a fixative containing 4% paraformaldehyde in 50 mM K_2HPO_4 and 50 mM KH_2PO_4 (pH 7.4). Their brains were removed, maintained in fixative for 24 h, and transferred to 30% sucrose. After brains sank to the bottom of the 30% sucrose solution within a few days, they were individually sliced in 40 µm thick sections, preserved in cryoprotectant (66 mM NaH_2PO_4, 190 mM Na_2HPO_4, 0.87 M sucrose, 30% ethylene glycol, and 1.25 mM povidone), and stored for histology and

immunohistochemistry at −20 °C. For western blot analysis, rats were decapitated with a guillotine. Their brains were rapidly removed and dissected to collect different regions, including the hippocampus and the cortex, which were immediately frozen on dry ice and stored at −80 °C.

Immunostaining

Histological staining of frozen coronal brain sections was performed to assess the level of perivascular immunoglobulin G (IgG) effusion as a measure of blood-brain-barrier disruption. These sections were also used for immunostaining of the vascular endothelial marker glucose transporter 1 (GluT-1) and the intercellular adhesion molecule 1 (ICAM-1). We also assessed the presence of inflammatory cells by co-immunostaining for F4/80 (marker of activated microglia/macrophages) and inducible nitric oxide synthase (iNOS). Furthermore, we stained for the expression of apoptosis biomarker, cleaved caspase 3, and the density of pre- and post-synaptic markers bassoon and homer-1, respectively. Staining methods used were either fluorescence immunostaining or nickel diaminobenzadine (DAB) immunostaining. Brain sections were co-stained for the expression of ICAM-1 and GluT-1, F4/80 and iNOS, bassoon and homer-1 or cleaved caspase 3 and neuronal nuclear antigen as previously described [10]. In brief, free floating sections were rinsed in phosphate buffered saline (PBS) and then blocked in 1% horse serum in PBS containing 0.3% Triton X for 1 h. Sections were transferred in a solution containing goat anti-ICAM-1 antibody (1:2000; Santa Cruz, CA) and mouse anti-glucose transporter monoclonal antibody (1:1500; Abcam, MA), rabbit anti-cleaved caspase-3 polyclonal antibody (1:10,000; Millipore, CA) and mouse anti-NeuN monoclonal antibody clone, A60 (1:2000; Millipore, CA), rat anti-F4/80 monoclonal antibody (1:500; eBioscience, San Diego, CA) and rabbit anti-iNOS polyclonal antibody (1:3000; Millpore, CA) or mouse anti-bassoon (1:2000; Enzo life sciences, NY) and rabbit anti-homer-1 antibody (1:1000; Invitrogen/ ThermoFisher Scientific, NY) and incubated overnight at 4°C. They were washed in PBS and incubated for 1 h at room temperature in a mixture of corresponding secondary antibodies Alexa Fluor 488 or Alexa Fluor 594 (1:1500; Invitrogen, NY). Sections were washed with PBS followed by 4’,6-diamidino-2-phenylindole (DAPI) used for nuclei counterstaining.

Brain sections were single-labeled for the presence of IgG, using nickel diaminobenzidine (DAB). Free-floating sections were rinsed in PBS, blocked with 1% horse serum, and incubated with rabbit IgG antibody (1:2500; eBioscience, CA) overnight at 4°C. Sections were washed and incubated at room temperature in biotinylated goat anti-rabbit secondary antibody (1:2000; Vector Laboratories Inc., CA), for 1 h, followed by incubation in Vestastain solution and in nickel DAB and rinsed in PBS.

Western blot analysis

Western blotting analysis was used to evaluate the expression levels of the extracellular signal-regulated kinase 1/2 (ERK-1/2), phosphorylated ERK, Bcl-2, alpha ii spectrin and beta-actin proteins in the hippocampus of blast and sham rats. Hippocampal tissues were manually homogenized in lysis buffer composed of 50 mM HEPES (pH 7.5), 6 mM $MgCl_2$, 1 mM EDTA, 75 mM sucrose, 1 mM dithiothreitol, 1% Triton X-100 (Sigma, MO) and 1% protease/phosphatase inhibitor cocktail (Cell Signaling Technology, MA). Homogenates were centrifuged at 10,000G for 20 min. Proteins (20–40 µg) present in the supernatants were separated by electrophoresis on 4–12% SDS-polyacrylamide gels (Bio-rad, CA), and then transferred to a nitrocellulose membrane. Membranes were blocked with 1% BSA and incubated overnight at 4°C with rabbit polyclonal antibodies against ERK1/2, phosphor-ERK1/2 (1:1000; Cell Signaling Technology, MA), alpha ii spectrin (1:3000, Invitrogen/ThermoFisher scientific, NY), Bcl-2 (1:2000, ProteinTech, IL) and mouse monoclonal antibody against β-actin (1:4000; Sigma, MO). Blots were washed in Tris-buffered saline with 0.1% Tween 20 and incubated for 1 h at room temperature with corresponding HRP-conjugated secondary antibodies (1: 5000; Millipore, MA). Horseradish peroxidase labeled proteins were detected by enhanced chemiluminescence (ECL, Thermo Scientific, IL) and protein bands were visualized using a digital blot scanner (LI-COR, NE).

Data analysis

The number of cleaved caspase 3 immunopositive cells were quantified using 40 µm thick sections of the hippocampus dendate gyrus and ca2/3 regions by the optical fractionator method of stereology using the Stereo Investigator software (MBF Bioscience,

VT). For each brain, six sections corresponding to every 12 serial sections expanding from bregma region -1.60 to -6.3 to cover the whole hippocampus area were analyzed. For quantification, the dentate gyrus and the Cornu Ammonis 2/3 (Ca2/3) sub-regions in the hippocampus of each brain hemisphere were demarcated. Grid spacing of 75 µm × 75 µm in the *x* and *y*-axis and guard zones of 2 µm at the top and bottom of each section were used to count immunopositive cell bodies. The total number of cleaved caspase 3 positive cells in the hippocampal sub-region of interest was divided by the covered area to determine the cellular density per area, expressed as cells/mm^2.

Image J software (NIH) was used to measure immunoblot protein band signal intensity and the percent area of IgG, ICAM-1 or F4/80 immunostaining in brain tissue. The signal intensities for Bcl-2 and alpha ii spectrin were expressed as a ratio of beta actin signal intensity (used as loading control) and that of phospho-ERK1/2 as a ratio of total ERK1/2. Sections stained for IgG, ICAM-1 or F4/80 were optically segmented by threshold. These thresholded images were automatically measured for the relative percent containing positive IgG, ICAM-1 or F4/80 signal in Image J. This method is proportional to the percent area covered by IgG, ICAM-1 or F4/80 immuno-positive signal.

The puncta analyzer software was generously provided by Dr. Cagla Eroglu (Duke University Medical Center, Durham, NC) and incorporated in ImageJ to determine the bassoon, homer-1 and bassoon/homer-1 co-localized puncta as previously described [11,12]. In brief, sections co-immunostained against bassoon and homer-1 were highlighted and quantification performed with rolling ball radium set at 50 with “white background” unchecked and the puncta size for bassoon and homer-1 set at 4 pixels. At the end of the quantification, the puncta density for bassoon and homer-1 and the co-localized bassoon/homer-1 puncta were generated.

Statistical analyses were performed using GraphPad InStat 3 software (GraphPad Software, Inc., La Jolla, CA). Analysis of Variance together with Tukey-Kramer multiple comparisons post-hoc test were used to compare differences among the multiple groups. Results are expressed as mean ± standard error of the mean (SEM). Statistical significance was defined as $p < 0.05$.

The individuals who performed the histologic, biochemical, and behavioral assays were blinded to animal group identifications, using codes that were revealed after data collection was completed.

Results

Mitigation of under-vehicle, blast-induced mortality

We previously reported that exposure of rats to 2400G acceleration during an under-vehicle blast scenario causes significant neuropathology and neurobehavioral deficits; whereas, exposure to 2850G results in 67% acute mortality [6]. Moreover, when the peak acceleration was reduced to 1200G by reducing the size of the explosive, there were less neuropathology and neurobehavioral deficits. In this study, we used the same basic model to determine if different vehicle frame designs could be used to mitigate the acceleration experienced by the rats, and therefore reduce traumatic brain injury.

Table 1 provides a comparison of the maximal acceleration G-force, the rate of change in acceleration (JERK) and the incidence of mortality for rats subjected to under-vehicle blasts using three different vehicle designs. The previously reported experiments that generated 2850G were performed using a thin rubber pad (0.6 cm) placed between the bottom aluminum plate located above the explosive and the top plate on which the rats were restrained. In an attempt to reduce the G force transmitted to the rats, we placed five crushable aluminum cylinders between the two plates, with one located at each of the four corners and one located in the center. Under these conditions and using the same blast parameters that generated 2850G in the absence of cylinders, all five cylinders were completely crushed or compressed to approximately 10% of their original height. There was a small but statistically insignificant 18% reduction in maximal G and a 15% reduction in JERK, in comparison to the values obtained in the absence of inter-plate cylinders. Nevertheless, presence of these cylinders reduced the mortality rate from 67% to 20%.

We then tested the hypothesis that coating the cylinders with polyurea would reduce mortality even further by reducing both the maximal G force and the JERK. Polyurea is an elastomer commonly used in truck bed liners. Polyurea is compressible and rebounds following compression, resulting in an excellent ability to absorb energy in the form of acceleration [2]. The presence of five polyurea coated cylinders between the two aluminum plates resulted in a highly significant ($p<0.01$) 80% reduction in maximal acceleration and a 57% reduction in JERK. There were no deaths among 24 rats used in the experiments employing the polyurea-coated cylinders (Table 1).

Acceleration mitigation improves behavioral outcomes

The ability of different vehicle designs to mitigate blast-induced behavioral deficits was tested using the Y maze, for working memory, and the elevated plus maze, for anxiety, at different times up to four weeks following blast exposure (Fig.2). All animals were tested with the Y maze at one hr following exposure to the under-vehicle blast and again at 6, 13, and 27 days. In comparison to shams, at day zero, the percent spontaneous alteration among the three arms of the maze was substantially lower for rats that were exposed to the blasts using simulated vehicles that included uncoated cylinders (0.9 ± 0.7%; n=8) than the percent alteration for Shams (27 ± 12%; $p<0.001$; n=10) or for rats secured to the simulated vehicle that included polyurea-coated cylinders (40 ± 8%; $p<0.01$; n=16). By day 6, the percent spontaneous alternation for Shams rose to 68 ± 12%, which was significantly greater than the score for Shams at day zero ($p<0.001$). The score for animals used for the uncoated cylinder blast paradigm also rose significantly to 37 ± 7% in comparison to the score at day zero ($p<0.001$). Nevertheless, this score was still much lower than the score for either the Shams (68 ± 6; $p<0.01$) or for rats that were exposed to the blast in simulated vehicles equipped with polyurea-coated cylinders (58 ± 7; $p<0.005$). By days 13 and 27, there were no significant differences among the three animal groups.

Similar patterns of behavioral injury was observed among the three animal groups over 28 days post-blast using the elevated plus maze test for anxiety. There were no significant differences in the time spent in the open arms of the plus maze among the animal groups at one day following the blast, although there was a trend toward the

shortest time for rats used with the uncoated cylinder vehicle design. On day 8, the time in open arms (16 ± 8 sec) was much lower in these same rats compared to Shams (115 ± 22 sec; $p<0.001$) or to rats that were used with the uncoated cylinder vehicle (77 ± 9 sec; $p<0.05$). There were no significant differences among groups at day 14 following blasts; however, there was still a trend toward lower time for the rats used with the uncoated cylinder vehicles. At day 28 post-blast, the time spent in open arms by rats in the uncoated cylinder animal group (51 ± 22 sec) was significantly lower than that of Shams (130 ± 21 sec; $p<0.05$). The rats in the polyurea-coated cylinder animal groups expressed time in open arms of 100 ± 20 sec, which was not different from Shams.

These behavioral assays were also applied to the two rats that survived the blasts that generated 2850G, where no cylinders were present between the two platforms. Neither of these rats spent any time in the open arms of the plus maze on days 1 and 8 post-injury and just an average of 42 sec on day 28 (not shown). Moreover, neither rat exhibited any successful alternation between Y maze arms when tested an hour after blast and an average of only 38% on days 6 and 13 post-blast. However, these rats exhibited an average of 68% spontaneous alternations on day 27 compared to 69 ± 3% for sham rats.

Mitigation of acceleration reduces cerebrovascular damage caused by under-vehicle blasts

We recently reported that under-vehicle blasts generating either 1200G or 2400G acceleration force reduced the expression of tight junction proteins occludin and Zona occludin 1 (ZO-1) in the rat hippocampus and cortex [6]. This reduction in tight junction proteins was accompanied by increased expression of von Willebrand factor (vwf), a marker of cerebrovascular endothelial damage [6], suggesting a disruption of the blood brain barrier (BBB) integrity. In the current study, rat brain sections were immunostained for IgG at 24 h post-blast to detect extravasation from the vasculature into the parenchyma, indicative of compromised BBB (Fig. 3). The area of IgG immunostaining in the cortex was 140% greater for rats exposed to the blast paradigm with uncoated cylinders (5.7 ± 0.7%) compared to Sham animals (2.4 ± 0.2%; $p<0.01$; $n=5$-6) and 95% greater for rats exposed to the blast paradigm that incorporated polyurea-coated cylinders (3.1 ± 0.4%; $p<0.05$; Fig. 3A,B). In addition, exposure to an under-vehicle blast resulted in an increase in ICAM-1

immunoreactivity, which is a marker of leucocyte infiltration into the parenchyma (Fig. 4A,B) [13,14]The area of ICAM-1 immunoreactivity (6.7 ± 1.8%) in the cortex of rats after blasts using uncoated cylinders was significantly higher than that of Shams (0.9 ± 0.3%; ($p < 0.01$). ICAM-1 levels were partially reduced by blasts conducted under vehicles that included the polyurea-coated cylinders (3.0 ± 0.2%). The inserts in all images represent 4x magnification of the boxed area to provide a better view of the co-localized proteins.

Mitigation of acceleration reduces cellular inflammatory reactions

Inflammation is an important hallmark of brain injury in both animal models and TBI patients [6,15,16]. We observed that rats subjected to the lethal blast intensity in simulated vehicles that contained cylinders that were not coated with polyurea exhibited substantially higher iNOS and F4/80 co-expressing microglia/microphages covering 13.0 ± 3.4% of these animal brains compared to shams (1.5 ± 0.1%, $p < 0.01$; n=5-6). In contrast, the presence of polyurea-coated cylinders significantly prevented microglia/macrophages infiltration reducing populated brain area to 4.8 ± 1.0% ($p < 0.05$; n=5-6) (Fig.5.A,B).

Mitigation of acceleration reduces loss of hippocampal synaptic densities

A reduction in the levels of synaptic proteins has been demonstrated in animals and humans following impact and blast TBI [6,17,18]. Considering the important roles that the hippocampus plays in cognition and memory, we tested for the effects of blast-induced acceleration on the density of the pre-synaptic protein, bassoon, and the post-synaptic protein, homer-1 in the hippocampus dendate gyrus sub-granular layer (SGL) and in the cornu ammonis 2 (Ca2) sub-region. Rats exposed to the lethal blast paradigm which included included only non-coated cylinders in the frame design exhibited a 25% decrease in the SGL bassoon puncta ($p < 0.05$; n=5-6) (Fig. 6A,B) and a 46% reduction in homer-1 puncta ($p < 0.01$, Fig. 6B), resulting in a 44% reduced co-localized bassoon/homer-1 puncta ($p < 0.05$, Fig.6A,B), compared to sham animals. Overall, the interaction between pre-synaptic marker bassoon and post-synaptic marker homer-1 in the SGL gyrus indicated 26% greater bassoon puncta co-localization in the SGL of sham rats than in rats exposed to the lethal blast paradigm with non-coated cylinders. However, there was no significant change in the fraction of co-localized homer-1 between sham and blast rats following

experiments conducted in the presence of polyurea-coated cylinders, suggesting an overall loss of synapses in the hippocampus SGL (Fig. 6C). In addition to synaptic changes occurring in the dendate gyrus-SGL, we also observed that homer-1 puncta intensity in the Ca2 region of the hippocampus was reduced by 41% following experiments using non-coated cylinders compared to shams ($p < 0.01$, Fig.7B). No significant difference in bassoon puncta density was found between rats in those groups (Fig. 7.B). However, the decrease in homer-1 puncta was associated with 38% reduction in bassoon/homer-1 puncta co-localization in the Ca2 of rats subjected to blast with non-coated cylinders compared to shams ($p < 0.05$, Fig. 7.B) and 39% decreased in co-localized bassoon fraction, again suggesting an overall loss in synapses in the Ca2 of these blast animals (Fig.7.C).

The incorporation of polyurea-coated cylinders prevented the loss in bassoon and homer-1 puncta in the hippocampus SGL by 10% and 34% ($p < 0.05$, Fig. 6B), respectively, in comparison to the immunopositive puncta present in the SGL observed after blasts in the presence of non-coated cylinders. Moreover, this substantial protection of the post-synaptic marker homer-1 in the SGL of these rats resulted in a 42% increase in co-localized bassoon/homer-1 and 29% more co-localized bassoon fraction compared to rats exposed to blast with no coated cylinders ($p < 0.05$, Fig. 6B-C). In addition, the presence of polyurea-coated vehicles reduced the loss in homer-1 puncta in the Ca2 region by 12% versus rats exposed to blasts with non-coated cylinders. This protection of homer-1 puncta in the Ca2 region was associated with 28% increase in bassoon/homer-1 co-localized puncta and 11% higher co-localized bassoon puncta fraction in the same region (Fig. 7C). Taken together, these results indicate that the acceleration mitigation provided by the presence of polyurea-coated cylinders located between the two platforms prevented the loss of synapses both in the hippocampal SGL and Ca2 regions.

Mitigation of blast-induced acceleration reduces hippocampal neuronal apoptosis

We recently reported a blast intensity-dependent appearance of cleaved caspase 3 in the hippocampal neurons of rats exposed to blast intensity of 1200G and 2400G force [6]. In the current study, we observed a significant increase in cleaved caspase 3 immunopositive cells in the dendate gyrus (13.1 ± 2.7 cells/mm^2) and Ca2/Ca3 region (7.8

± 2.6 cells/mm^2) of rats exposed to blasts in the presence of non-coated cylinders, in comparison to shams in the dentate gyrus with 1.5 ± 0.3 cells/mm^2 ($p < 0.01$) and in the Ca2/Ca3 regions with 1.1 ± 0.2 cells/mm^2 ($p < 0.05$) (Fig. 8B). The polyurea coating mitigation system significantly reduced the presence of cleaved caspase 3 positive cells in the dentate gyrus with 6.3 ± 1.6 cells/mm^2 ($p<0.05$) and in the Ca2/Ca3 with 4.3 ± 1.0 cells/mm^2 ($p < 0.05$) (Fig. 8B; n=5-6).

Mitigation of acceleration with crushable cylinders partially protects against blast-induced ERK dephosphorylation and alpha ii spectrin proteolysis

Following the observation that exposure to high blast intensity increases hippocampal caspase 3 immunopositive cells, we examined the effect of blasts and mitigation of blast-induced acceleration on additional apoptosis-related proteins. Our results revealed a 60% decrease in ERK phosphorylation ($p < 0.01$; Fig 9A,C) and a dramatic 75% increase in alpha ii spectrin proteolytic breakdown products ($p < 0.001$; Fig 9 B,E) in rats subjected to under-vehicle blasts in the presence of non-coated cylinders compared to levels observed with sham rats. Importantly, the presence of polyurea coated cylinders reduced ERK phosphorylation by 50% ($p < 0.05$; Fig 9 A,C) and reduced alpha ii spectrin break down products by 60% ($p < 0.01$; Fig B,E) compared to levels in the hippocampus of rats exposed to blast with non-coated cylinders. However, the incorporation of polyurea-coated cylinders in the vehicle frame design did not protection against blast-induced reduction in the levels of Bcl-2, an important anti-apoptotic protein (Fig. 9 A,D).

Discussion

This study represents the first to provide neurochemical, histopathologic, and behavioral evidence that under-vehicle, blast-induced mortality and TBI in lab animals can be mitigated by vehicle design modifications that dramatically reduce the transmission of force from the bottom of the vehicle to where the animals are located. The scaling factor between these small-scale blasts and those full-scale explosions caused by land mines is approximately ten [19]. Thus, we estimate that the full-scale blast-induced acceleration of 280 would affect people similarly to that of 2850G on rats. The additional estimation that the G-forces transmitted to military vehicles by land mines range from 200 – 4000G

supports the relevance of the results we reported earlier using adult rats and our small-scale underbody blast model [4,6].

We previously demonstrated that 67% of animals exposed to blast-induced acceleration of 2850G die immediately after the blast exposure, apparently due to lung damage [6]. We therefore applied the settings used in these experiments to test the hypothesis that modifications of vehicle frame design can reduce the G-force experienced by the lab rats to an extent that increases survival. These settings included the stand-off distances from both the explosive and the water line to the bottom of the simulated vehicle and the weight of the PETN explosive that is used. Experiments performed in the absence of animals indicated that G-force mitigation could be detected with our system using aluminum cylinders placed between the top and bottom plates constituting the frame of a vehicle [2]. The first attempt at mitigating under-vehicle blast-induced mortality utilized the placement of five uncoated aluminum cylinders between the two plates. This modification resulted in a small but non-significant reduction in both the maximum G force and the JERK, i.e., the rate of change in acceleration (Table 1). Nevertheless, the presence of these collapsible structures resulted in a robust 80% reduction in mortality compared to the two thirds that died following blasts in the absence of any G-force mitigating vehicle design.

The next attempt at eliminating mortality employed cylinders of the same size except that they were coated with the compound polyurea, an elastomer with a high capacity for rapid compression and decompression in response to acceleration [2]. The incorporation of the polyurea-coated cylinders resulted in a reduction in the maximal acceleration to a level of 550G, which is only 19% of the load imparted in the absence of compressible cylinders and 23% of the load transmitted in the presence of un-coated cylinders. The mean JERK level of 0.76 meters sec^{-3} was also much less than that measured with no cylinders or uncoated cylinders. Most importantly, the presence of the polyurea-coated cylinders completely eliminated mortality (Table 1).

The mitigation of under-vehicle blast-induced G-force by the incorporation of polyurea-coated cylinders in the vehicle design was also associated with protection against

neurobehavioral alterations. The working memory deficits observed at day zero and at day 6 after blast exposure using uncoated cylinders were completely eliminated by substitution with polyurea-coated cylinders (Fig. 2A). More importantly, the anxiety-like behavior reflected by reduced time spent in the open arms of the Plus maze for up to at least 28 days post-blast was also fully attenuated by the presence of polyurea-coated cylinders (Fig. 2B). Mitigation by an elastomeric frame design of anxiety is particularly important since depression and anxiety are not uncommon among warfighters and civilians who are victims of blast TBI [20].

In addition to testing the effects of different frame designs on neurobehavioral alterations following under-vehicle blasts, we compared the ability of these modifications to mitigate the neuropathology and neurochemical alterations that occur in this under-vehicle blast TBI model. Cerebrovascular damage is a prominent feature in both impact-induced and open-field blast models of TBI [8,21,20,22]. In this study, we performed quantitative immunohistochemical measurements of markers commonly associated with vascular injury. For example, disruption of the blood brain barrier is accompanied by leakage of blood proteins through the vascular wall and into the brain parenchyma. In comparison to Shams, we observed a significant, two-fold increase in perivascular IgG immunoreactivity in the cortex of rats at 24 h following exposure to blast when uncoated cylinders were present within the frame of the model vehicle (Fig. 3). In contrast, the perivascular IgG immunoreactivity measured after blasts with polyurea coated cylinders was not significantly different than that expressed in Sham animals. In comparison with Shams, we also observed a greater than 5-fold increase in the cortical levels of ICAM-1 following blasts conducted in the presence of uncoated cylinders (Fig. 4). Increased ICAM-1 expression is often seen in other models of TBI and facilitates the transmigration of leucocytes from the blood into the brain parenchyma [13,14]. When polyurea-coated cylinders were substituted for uncoated cylinders, ICAM-1 levels were reduced by over 50%.

Based on changes in these biomarkers of vascular injury, we anticipated that additional indicators of neuroinflammation would be observed [15,16]. Brain tissue was therefore immunostained for F4/80, which is selective for activated microglia and

macrophages. As shown in Fig. 4, a ten-fold increase in the area of immunostaining for F4/80 was measured in the cortex after blasts employing uncoated cylinders, in comparison to Shams. The presence of polyurea-coated cylinders reduced the F4/80 immunoreactivity by 70%.

Neuroinflammation is often associated with neuronal death, which under some circumstances is preceded by the loss of neuronal synapses [23]. We detected a significant decrease in the pre-synaptic protein bassoon and the post-synaptic protein homer-1 in the hippocampal dentate gyrus and Ca2 regions following blasts that generated 2350G acceleration and included the presence of uncoated cylinders in the frame design (Fig. 7). These findings taken together with reductions in other synaptic proteins reported earlier for this under-vehicle blast model [6], provide evidence supporting the hypothesis that loss of synapses is an important contributor to blast TBI [24]. The reduction in homer and bassoon were associated with increased cell death in the same regions, as measured by the number of cells that were cleaved caspase-3 immunopositive (Fig 8) [6]. Proteolytic activation of caspase 3 is typically a marker of neuronal apoptosis following TBI [25]. Proteolysis of other proteins, e.g., alpha ii spectrin, is also observed following TBI [26,27]. For example, immunoblots revealed a four-fold increase in hippocampal alpha ii spectrin breakdown products at 24 h following the blasts that employed the uncoated cylinders in the vehicle frames (Fig 9). Alpha spectrin degradation is also implicated in the loss of synapses observed in Alzheimer's disease [28]. Thus, the substantial alpha ii spectrin breakdown observed following 2350G-associated blasts might contribute to the loss of synapses implicated by the loss of homer and bassoon immunoreactivity following these blasts. In contrast to the promotion of alpha spectrin hydrolysis, caspase 3 activation, and loss of synaptic proteins by exposure to blast-induced 2350G acceleration, all of these outcome measures were significantly reduced when the G-force was reduced to 550G by the use of the polyurea-coated aluminum cylinders.

We also performed immunoblots for phospho- and dephosph-ERK and Bcl-2, which are major regulators of cell survival [18,29,30,31]. Blasts that generated 2350G caused a significant reduction in the ratio of phospho-ERK to dephospho-ERK and a loss of Bcl-2 immunoreactivity. While lowering the G-force to 550G by the use of polyurea-coated

cylinders eliminated the drop in pERK/ERK, the loss of Bcl-2 was surprisingly not mitigated by this frame modification.

Conclusions

The maximum peak vertical acceleration that male Sprague-Dawley rats can survive in a small-scale under-vehicle blast model is approximately 2350G. This force is roughly equivalent to 230G in a full-scale under-vehicle blast scenario, which falls within the range generated when vehicles are targeted in theatre by land mines. Rats exposed to 2350G exhibit deficits in working memory for up to 6 days post-blast and anxiety-like behavior for at least 28 days post-blast. At one day following blast exposure, the brains display evidence for cerebrovascular injury, inflammation, neuronal death, and loss of synapses. However, when the vehicle frame design is modified by the use of polyurea-coated cylinders, the peak acceleration experienced by the rats is reduced by 77%, resulting in essentially complete protection against all neurobehavioral deficits and histologic evidence for brain injury. Work is in progress to further refine the elastomeric frame design with the goal of reducing under-vehicle blast-induced G-force by 90%. In addition to protecting against brain injury caused specifically by acceleration, these vehicle designs should also reduce the incidence or severity of brain injury caused by head impact within the vehicles.

ACKNOWLEDGMENTS

We thank Ashley Moore and Julie L. Proctor for their participation in the blast experiments.

Author Disclosure Statement

No competing financial interests exist.

References

1. Hopkinson, B. (1915). British ordnance board minutes 13565. The National Archives, Kew, UK 11.

2. Bonsmann, J., and Fourney, W. (2015). Mitigation of Accelerations Caused by Blast Loading Utilizing Polymeric-Coated Metallic Thin-Walled Cylinders. Journal of Dynamic Behavior of Materials 1, 259-274.

3. Tom, V. B. Pentagon: New MRAPs have been successful in saving troops' lives. USA Today

4. Proctor, J. L., Fourney, W. L., Leiste, U. H., and Fiskum, G. (2014). Rat model of brain injury caused by under-vehicle blast-induced hyperacceleration. Journal of Trauma & Acute Care Surgery 77, S83.

5. Proctor, J. L., Mello, K. T., Fang, R., Puche, A. C., Rosenthal, R. E., Fourney, W. L., Leiste, U. H., and Fiskum, G. (2017). Aeromedical evacuation-relevant hypobaria worsens axonal and neurologic injury in rats following underbody blast-induced hyperacceleration. J Trauma Acute Care Surg

6. Tchantchou, F., Fourney, W. L., Leiste, U. H., Vaughan, J., Rangghran, P., Puche, A., and Fiskum, G. (2017). Neuropathology and neurobehavioral alterations in a rat model of traumatic brain injury to occupants of vehicles targeted by underbody blasts. Exp Neurol 289, 9-20.

7. Zhao, X., Tiwari, V., Sutton, M. A., Deng, X., Fourney, W. L., Leiste, U., Tchantchou, F., and Zhang, Y. M. (2013). Scaling of the deformation histories for clamped circular plates subjected to blast loading by buried charges. Int J Impact Eng 54; 30, 31; 565-50; 579.

8. Tchantchou, F., and Zhang, Y. (2013). Selective Inhibition of Alpha/Beta-Hydrolase Domain 6 Attenuates Neurodegeneration, Alleviates Blood Brain Barrier Breakdown, and Improves Functional Recovery in a Mouse Model of Traumatic Brain Injury. J Neurotrauma 30, 565-579.

9. Budde, M. D., Shah, A., McCrea, M., Cullinan, W. E., Pintar, F. A., and Stemper, B. D. (2013). Primary blast traumatic brain injury in the rat: relating diffusion tensor imaging and behavior. Front Neurol 4, 154-154.

10. Tchantchou, F., Xu, Y. N., Wu, Y. J., Christen, Y., and Luo, Y. (2007). EGb 761 enhances adult hippocampal neurogenesis and phosphorylation of CREB in transgenic mouse model of Alzheimer's disease. FASEB JOURNAL 21, 2400-2408.

11. Ippolito, D. M., and Eroglu, C. (2010). Quantifying synapses: an immunocytochemistry-based assay to quantify synapse number. J Vis Exp

12. McKinstry, S. U., Karadeniz, Y. B., Worthington, A. K., Hayrapetyan, V. Y., Ozlu, M. I., Serafin-Molina, K., Risher, W. C., Ustunkaya, T., Dragatsis, I., Zeitlin, S., Yin, H. H., and Eroglu, C. (2014). Huntingtin Is Required for Normal Excitatory Synapse Development in Cortical and Striatal Circuits. J Neurosci 34, 9455-9472.

13. Di Lorenzo, A., Manes, T. D., Davalos, A., Wright, P. L., and Sessa, W. C. (2011). Endothelial reticulon-4B (Nogo-B) regulates ICAM-1-mediated leukocyte transmigration and acute inflammation. Blood 117, 2284-2295.

14. Liu, Y., Shaw, S. K., Ma, S., Yang, L., Luscinskas, F. W., Parkos, C. A., Di Lorenzo, A., Manes, T. D., Davalos, A., Wright, P. L., and Sessa, W. C. (2011). Regulation of leukocyte transmigration: Cell surface interactions and signaling events. Blood 172; 117, 7; 2284-13; 2295.

15. Corps, K. N., Roth, T. L., and McGavern, D. B. (2015). Inflammation and neuroprotection in traumatic brain injury. JAMA Neurol 72, 355-362.

16. Loane, D. J., and Byrnes, K. R. (2010). Review article: Role of Microglia in Neurotrauma. Neurotherapeutics 7, 366-377.

17. Gao, X., Deng, P., Zao, C. X., and Chen, J. (2011) Moderate traumatic brain injury causes acute dendritic and synaptic degeneration in the hippocampal dentate gyrus. PLoS ONE, Vol 6, Iss 9, p e24566 e24566.

18. Tchantchou, F., Tucker, L. B., Fu, A. H., Bluett, R. J., McCabe, J. T., Patel, S., and Zhang, Y. (2014). The fatty acid amide hydrolase inhibitor PF-3845 promotes neuronal survival, attenuates inflammation and improves functional recovery in mice with traumatic brain injury. Neuropharmacology 85, 427-439.

19. Chabai, A. J. (1965). On scaling dimensions of craters produced by buried explosives. Journal of Geophysical Research 70, 5075.

20. Agoston, D. V., and Kamnaksh, A. (2015). Modeling the Neurobehavioral Consequences of Blast-Induced Traumatic Brain Injury Spectrum Disorder and Identifying Related Biomarkers, in: *Brain Neurotrauma: Molecular, Neuropsychological, and Rehabilitation Aspects.* F. H. Kobeissy (ed), by Taylor & Francis Group, LLC: Boca Raton (FL),

21. Tanno, H., Nockels, R. P., Pitts, L. H., and Noble, L. J. (1992). Breakdown of the blood-brain barrier after fluid percussion brain injury in the rat: Part 2: Effect of hypoxia on permeability to plasma proteins. J Neurotrauma 9, 335-347.

22. Kabu, S., Jaffer, H., Petro, M., Dudzinski, D., Stewart, D., Courtney, A., Courtney, M., and Labhasetwar, V. (2015). Blast-associated shock waves result in increased brain vascular leakage and elevated ROS levels in a rat model of traumatic brain injury. PloS one 10, e0127971.

23. Kathryn, J. H., Cunningham, C., Richard, A. R., and V, H. P. (2013) Early Hippocampal Synaptic Loss Precedes Neuronal Loss and Associates with Early Behavioural Deficits in Three Distinct Strains of Prion Disease. PLoS ONE, Vol 8, Iss 6, p e68062 e68062.

24. Przekwas, A., Somayaji, M. R., and Gupta, R. K. (2016). Synaptic Mechanisms of Blast-Induced Brain Injury. Front Neurol 7, 2.

25. Clark, R. S. B., Kochanek, P. M., Watkins, S. C., Chen, M., Dixon, C. E., Seidberg, N. A., Melick, J., Loeffert, J. E., Nathaniel, P. D., Jin, K. L., and Graham, S. H. (2000). Caspase-3 Mediated Neuronal Death After Traumatic Brain Injury in Rats. J Neurochem 74, 740-753.

26. Schober, M. E., Requena, D. F., Davis, L. J., Metzger, R. R., Bennett, K. S., Morita, D., Niedzwecki, C., Yang, Z., and Wang, K. K. W. (2014). Research Report: Alpha II Spectrin breakdown products in immature Sprague Dawley rat hippocampus and cortex after traumatic brain injury. Brain Res 1574, 105-112.

27. Pike, B. R., Flint, J., Dutta, S., Johnson, E., Wang, K. K., and Hayes, R. L. (2001). Accumulation of non-erythroid alpha II-spectrin and calpain-cleaved alpha II-spectrin breakdown products in cerebrospinal fluid after traumatic brain injury in rats. J Neurochem 78, 1297-1306.

28. Kurbatskaya, K., Phillips, E. C., Croft, C. L., Dentoni, G., Hughes, M. M., Wade, M. A., Al-Sarraj, S., Troakes, C., O'Neill, M. J., and Perez-Nievas, B. G. (2016). Upregulation of calpain activity precedes tau phosphorylation and loss of synaptic proteins in Alzheimer's disease brain. Acta neuropathologica communications 4, 34.

29. Atkins, C. M., Falo, M. C., Alonso, O. F., Bramlett, H. M., and Dietrich, W. D. (2009). Deficits in ERK and CREB activation in the hippocampus after traumatic brain injury. Neurosci Lett 459, 52-56.

30. Kuo, J. R., Cheng, Y. H., Chen, Y. S., Chio, C. C., and Gean, P. W. (2013). Involvement of Extracellular Signal Regulated Kinases in Traumatic Brain Injury-Induced Depression in Rodents. J Neurotrauma 30, 1223-1231.

31. Subramanian, M., and Shaha, C. (2007). Up-regulation of Bcl-2 through ERK phosphorylation is associated with human macrophage survival in an estrogen microenvironment. J Immunol 179, 2330-2338.

Table 1:

Vehicle Design	G Force	JERK[1]	Mortality
No mitigation[2]	2851 ± 359*	1.77 ± 0.33	4/6 (67%)
Uncoated Cylinders	2331 ± 128	1.51 ± 0.27	4/20 (20%)
Polyurea-Coated Cylinders	536 ± 46	0.76 ± 0.11	0/24 (0%)

[1]JERK is the first derivative of acceleration (G force) and the second derivative of velocity and is expressed as $x10^{13}$ meter $^{-3}$.

[2]The acceleration data and survival outcomes obtained from experiments using simulated vehicles with no G force mitigation were published previously [6].

FIGURE LEGENDS

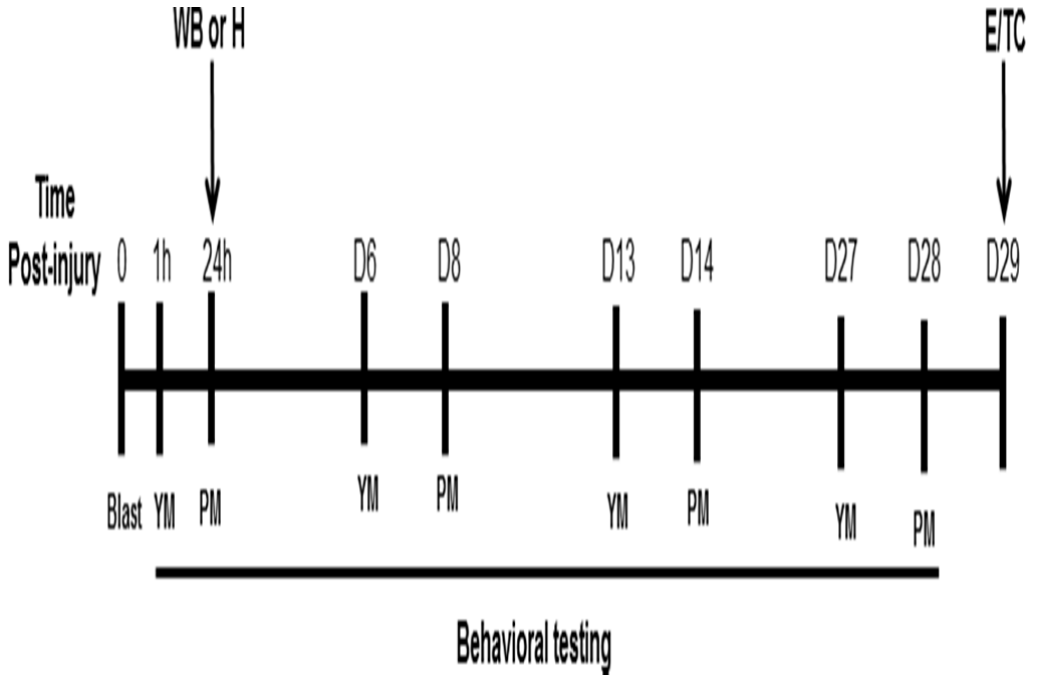

Figure 1: Experimental design. Detailed timeline of behavioral tests and end-points of experimental procedures starting on study day 0 (blast or sham blast exposure). YM, Y-maze test; PM, plus-maze test; H, histology; WB, western blots; E, euthanasia; TC, tissue collection.

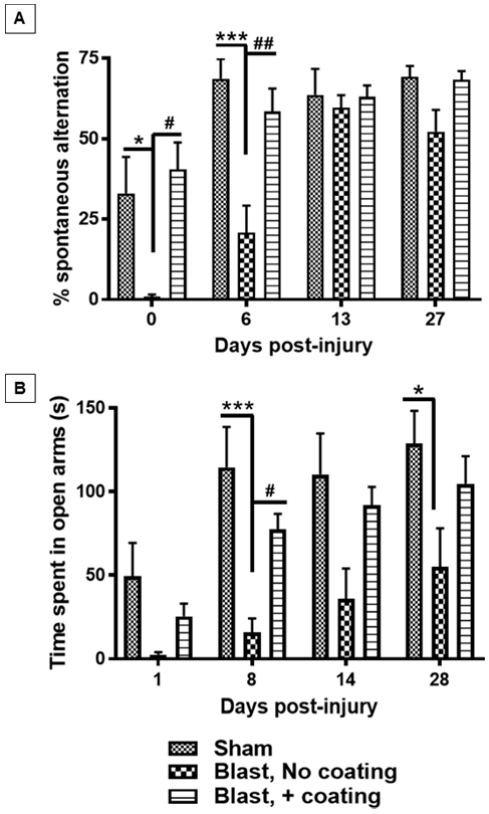

Figure 2: Coating of cylinders with polyurea is necessary for mitigation of behavioral deficits following under-vehicle blast. Rats were restrained on the top of a simulated vehicle that incorporated either uncoated or polyurea-coated aluminum cylinders, resulting in maximal acceleration of 2350G and 550G, respectively. A. Polyurea-coated cylinders protected rats from loss of spontaneous alternation in the Y maze at day zero ($^{*,\#}p < 0.05$, $^{\#\#}p < 0.01$; n=10 - 16) and at day 6 ($^{\#\#}p < 0.01$, $^{***}p < 0.001$). B. Polyurea-coated cylinders were also effective at protecting against anxiety behavior, which is inversely related to the time rats spend in the open arms of the elevated Plus maze. ($^{***}p < 0.001$, $^{\#}p < 0.05$, $^{*}p < 0.05$; n=10 - 16).

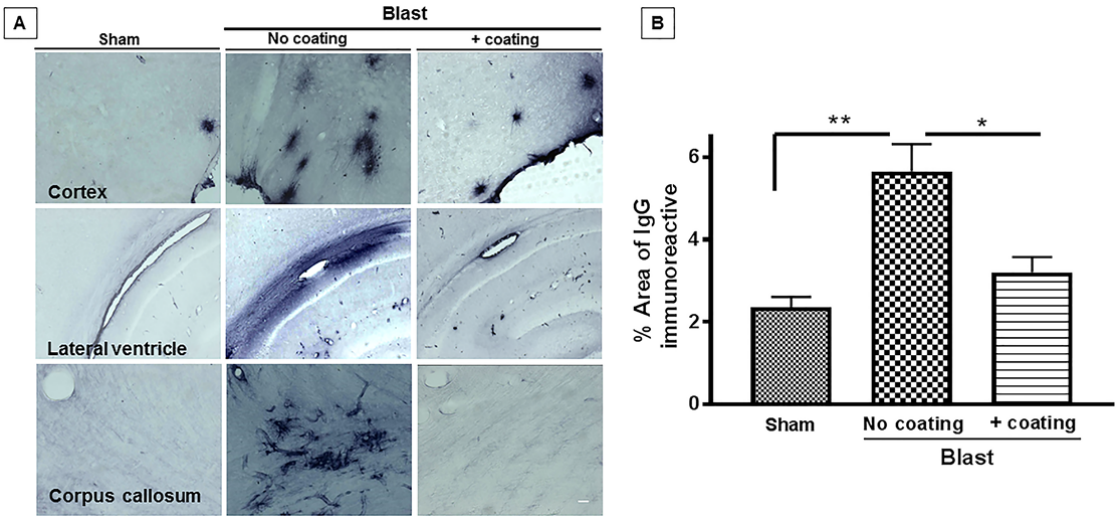

Figure 3: Increased perivascular immunoglobulin IgG effusion in the brain post-blast and by incorporation of polyurea-coated cylinders. A. Representative microscopic images exhibiting IgG immunoreactivity in different brain regions at 24 h post-blast or post-Sham blast. Scale bar is 50 µm. B. Quantification of the percentage of the cerebral cortex area that was immunopositive for IgG. There was a significant, 700% increase in rat cortical IgG immunostaining following blasts generating 2300G compared to sham animals ($^{**}p < 0.01$, n=5) and a 100% increase compared to the area present following blasts with vehicles that incorporated polyurea-coated cylinders ($^{*}p < 0.05$; n=6).

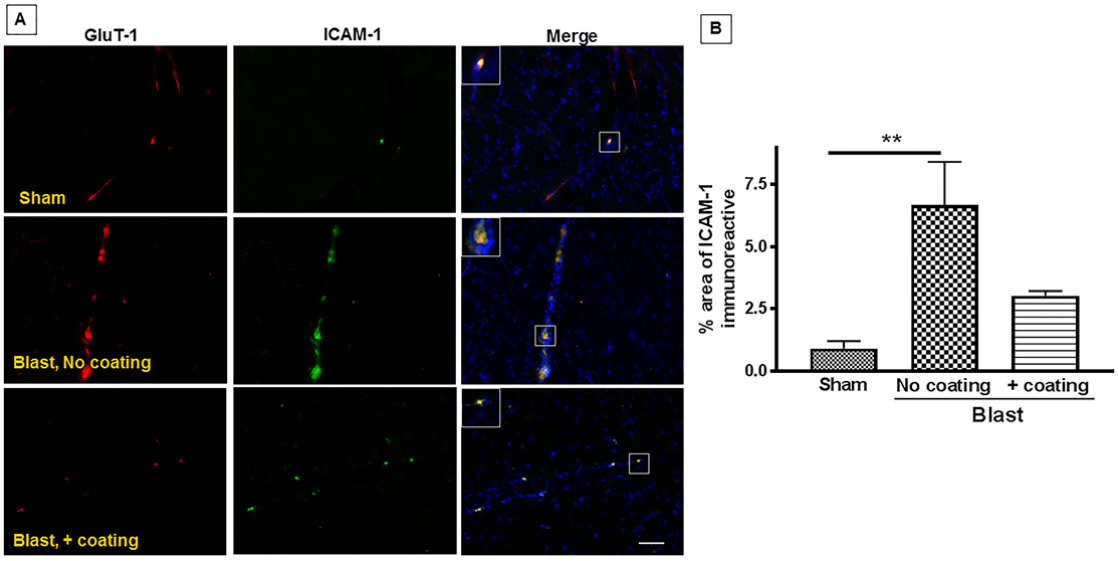

Figure 4: Increased ICAM-1 expression in the brain following under-vehicle blast and mitigation by incorporation of polyurea-coated cylinders. A. Representative microscopic images expression of ICAM-1(green) and GluT-1 (red) in immuno-stained rat brain sections at 24 h post-blast. Size bar is 100 µm. B. Quantification of the area of ICAM-1 immunoreactivity indicating significantly increased levels ICAM-1 in the brain (n = 5) of rats subjected to blast intensity with incorporation of uncoated cylinders compared to Shams ($^{**}p < 0.01$; n=6). ICAM-1 immunostaining was not significantly different between Shams and after blasts that incorporated the polyurea-coated cylinders.

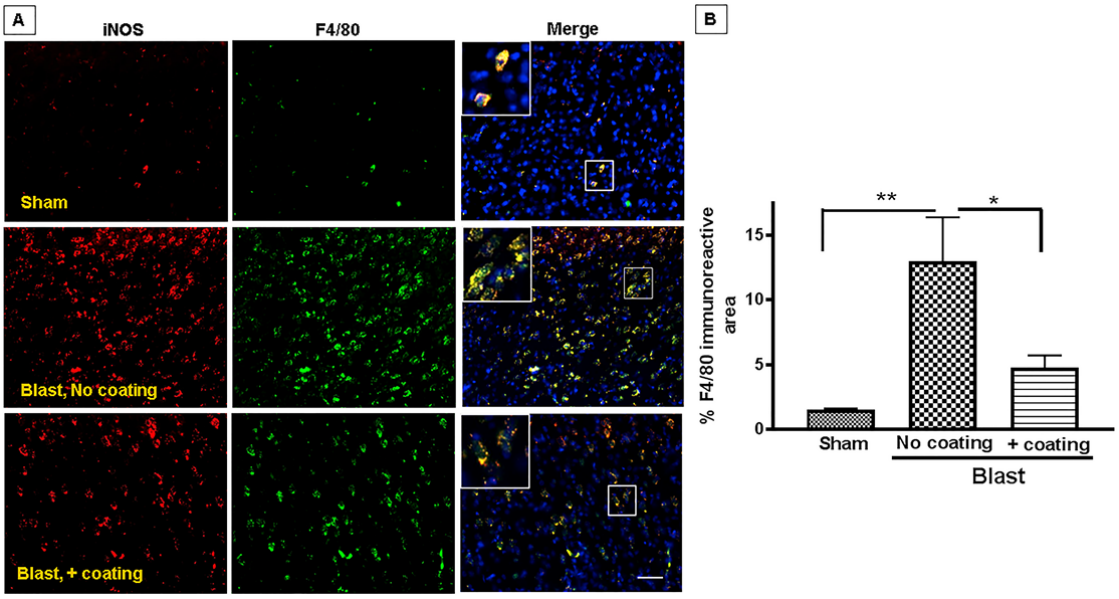

Figure 5: Activated microglia/microphages following under-vehicle blasts and mitigation by incorporation of poly-urea coated cylinders. A. Representative fluorescent images of F4/80 immuno-positive cells (green) showing overlap with iNOS immuno-positive cells (red) and Dapi as counterstain (blue). Scale bar is 100 µm. B. Quantification of F4/80 immunopositive area in the cortex suggests dramatic increase of activated microglia/microphages in the brain of rats subjected to lethal blast intensity with no P.U coating compared to sham rats (n = 5, **p < 0.01). Levels of activated microglia/microphages were significantly reduced (n = 6; #p < 0.05) in the brain of exposed to blast with P.U coating mitigation system.

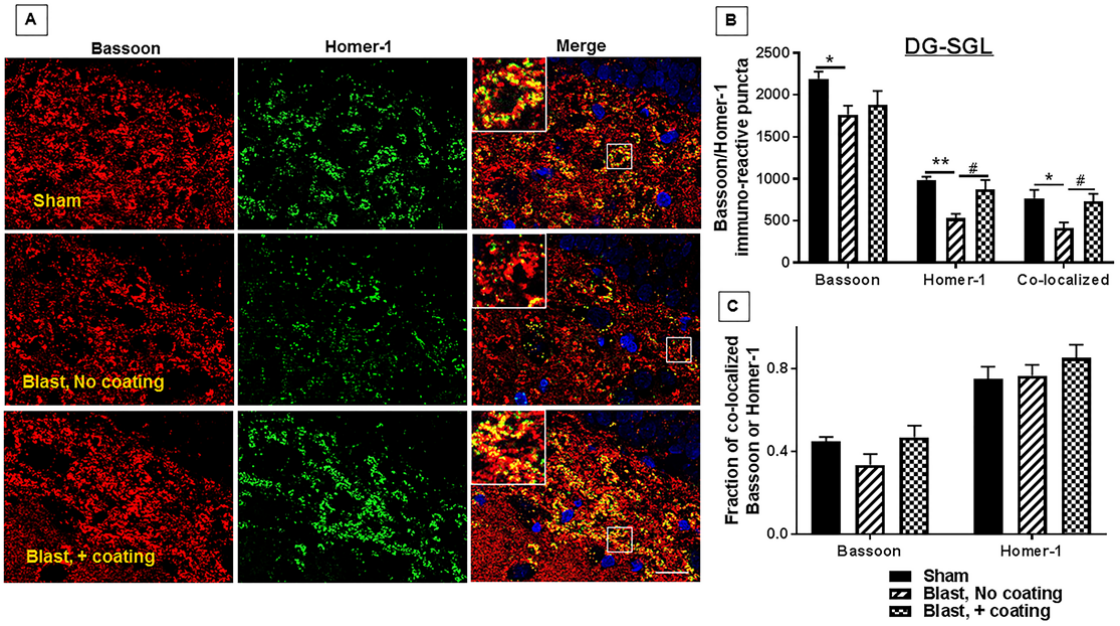

Figure 6: Synaptic protein density decreased in rat dendate gyrus-SGL 24 h post-injury, protection by the advanced hull design system A. Representative fluorescent images demonstrating the presence pre-synaptic protein bassoon (red) and post-synaptic protein Homer-1 (green) and Dapi stained nuclei in the dendate gyrus sub-granular layer (SGL) of the rat hippocampus. Scale bar is 100 µm. B. Quantitation of Bassoon, Homer-1 and Bassoon/Homer-1 co-colcalized puncta density indicated a significant decrease in Homer-1 and Bassoon/Homer-1 co-localized puncta in the SGL of rats exposed to lethal blast intensity with no P.U coating compared to sham (n = 5; *$p < 0.05$ and **$p < 0.01$). Blast-induced impairment in synaptic proteins expression was significantly prevented by the P.U coating mitigation system (n = 6; $^{\#}p < 0.05$).

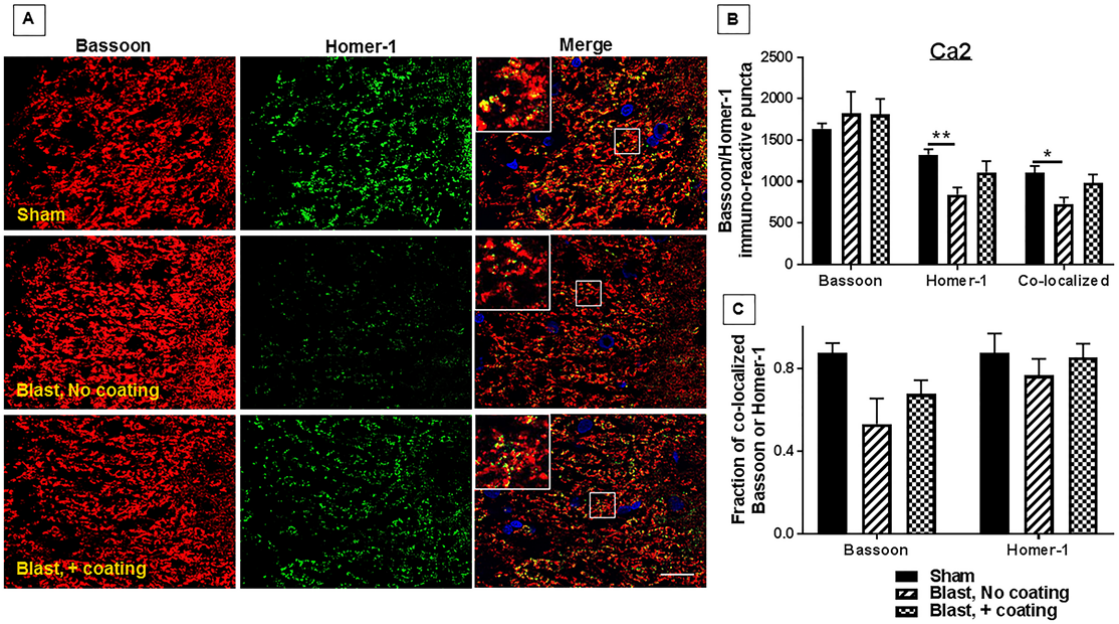

Figure 7: Synaptic protein density decreased in rat Ca2 region 24 h post-injury, protection by the advanced hull design system A. Representative fluorescent images demonstrating the presence pre-synaptic protein bassoon (red) and post-synaptic protein Homer-1 (green) and Dapi stained nuclei in the Cornu Ammonis 2 (Ca2) region of the rat hippocampus. Scale bar is 100 µm. B. Quantitation of Bassoon, Homer-1 and Bassoon/Homer-1 co-colcalized puncta density indicated a significant decrease in Homer-1 and Bassoon/Homer-1 co-localized puncta in the Ca2 region of rats exposed to lethal blast intensity with no P.U coating compared to sham (n = 5; *$p < 0.05$ and **$p < 0.01$). Blast-induced impairment in synaptic proteins expression was relatively prevented by the P.U coating mitigation system (n = 6).

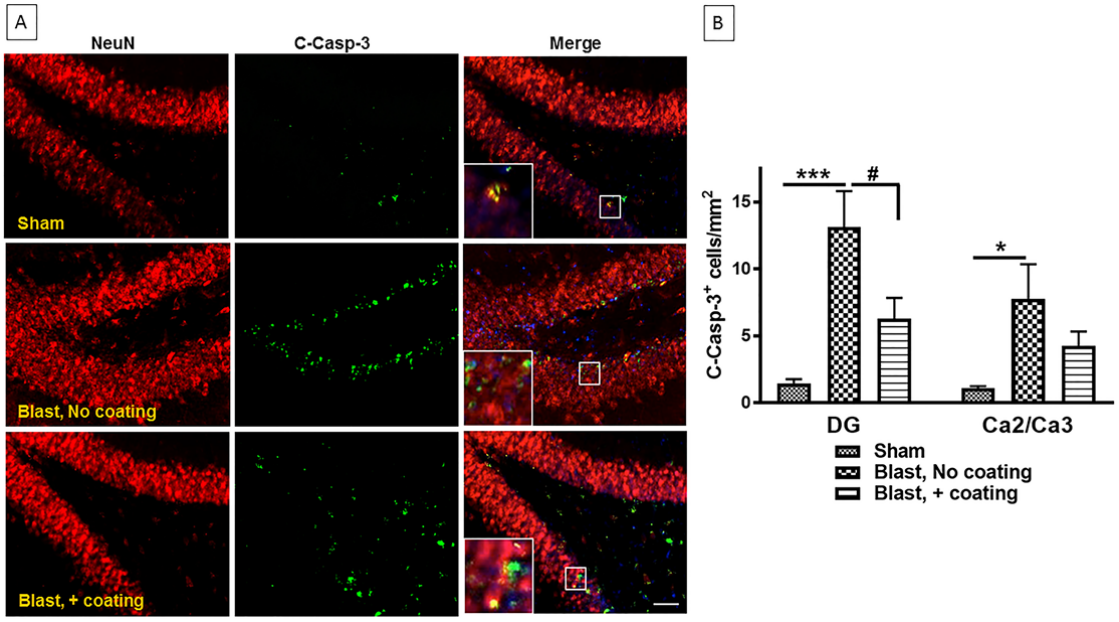

Figure 8: Cleaved caspase 3 immuno-positive cells present in rat hippocampus

A. Representative fluorescent images showing cleaved caspase 3 immuno-positive cells (green) overlapping mostly with NeuN immuno-reactive cells (red), and Dapi for nuclei counterstaining. Scale bar is 100 µm. B. Quantitation indicated significant increase in Cleaved caspase 3 immuno-reactive cells in the dendate gyrus and Ca2/3 region of rats subjected to blast with no P.U coating compared to sham animals ($n = 5$; $p < 0.05$ and $p < 0.001$). The advanced hull design significantly reduced the blast-initiated hippocampal apoptotic cell loss ($n = 6$; $^{\#}p < 0.05$).

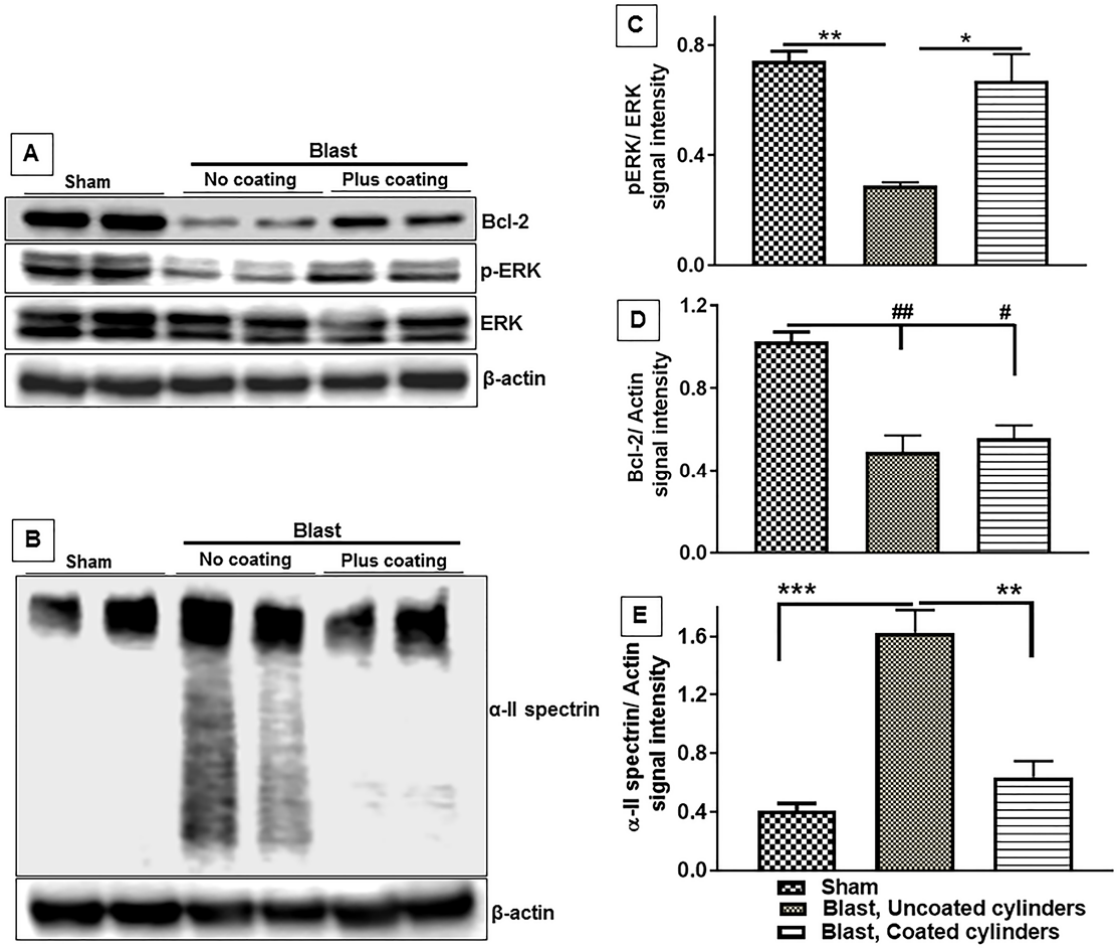

Figure 9: Decreased expression of cell survival promoting proteins and increased expression of pro-apoptotic protein in rat hippocampus 24 h post-blast and mitigation by the shock absorbing hull design system A-B. Representative immunoblots illustrating the expression of cell survival promoting protein phospho-ERK, anti-apoptotic protein Bcl-2 and pro-apoptotic marker α-II spectrin in rat hippocampus. C-E. Quantitation of protein band signal intensity showed compared to sham rats, a significant decrease in phosphor-ERK and Bcl-2 ($n = 6$, $p < 0.01$) a drastic increase in alpha ii spectrin ($n = 6$, $p < 0.001$) in the hippocampus of rats exposed to lethal blast intensity with no P.U coating compared to sham rats. However, the advanced hull mitigation design abrogated the deleterious effect of blast exposure on the expression phosphor-ERK and α-II spectrin ($n = 6$; *$p < 0.05$ and **$p < 0.01$ respectively).

APPENDIX 6

Mitigation of under-vehicle blast neurotrauma and death by advances in military vehicle designs. Dr. William Fourney, University of Maryland School of Engineering

Mitigation of under-vehicle blast neurotrauma and death by advances in military vehicle designs. Dr. William Fourney, University of Maryland School of Engineering

We have made very good progress on the development of devices for the mitigation of accelerations since the last progress report. Our original device was 15 inches in height for a full scale vehicle and was able to reduce the acceleration from around 140 g's to about 18 g's. It is felt that a human being can withstand rapidly applied accelerations of about 25 g's without major injury. For example a pilot who uses an ejection seat to bailout of a high speed jet fighter experiences about 25 g's and is allowed to eject twice before they are removed from flying status. Our aim is to develop our device such that the g levels experienced by occupants is on the order of 25 g's or less. The graph to the right shows the results obtained with our 1.5 inch tall device (which would be 15 inches in full scale). Notice that that device reduced the g level from about 3500 g's to something on the order of 200 g's. We are looking at not only making the devices as short as possible but also looking at geometry (height to diameter) of the

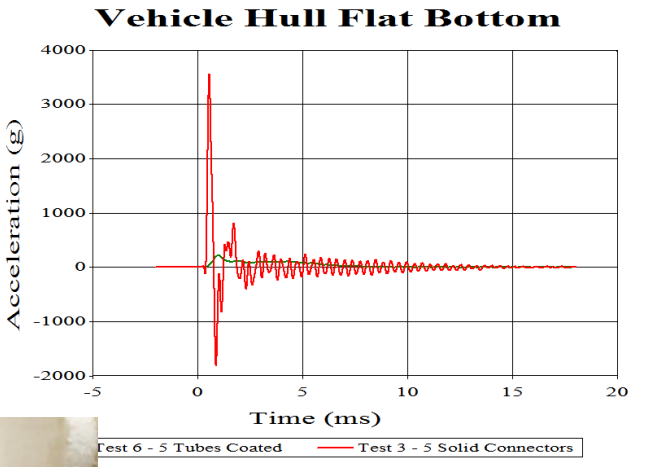

devices as well as looking at different material combinations necessary to optimize the devices. The picture to the left shows another one of our devices. In this case we have replaced the solid aluminum cylindrical carrier material to one that is a mesh. We have covered the mesh with a polyurea coating and have a foam material inserted into the center of the cylinder. This device was successful in reducing the accelerations to the desired level (25 g's or below) and was only 8.6 inches high. The foam material in the center was found to be necessary to further mitigate the accelerations when the loading becomes very large. When the loading is large the forces on the bottom of the vehicle load the mitigation devices and causes the polyurea coated cylinders to crumple. Without the foam the cylinders are completely collapsed and the hull strikes the frame of the vehicle causing accelerations that are larger than are acceptable. The foam material softens this slapping phenomen.

Our best result to date is shown to the left. These cylinders (shown after the loading was finished) were solid aluminum coated with polyurea and contained the foam material to prevent the hull slapping mentioned above. These cylinders in full scale would be 6 inches tall and the accelerations measured were 25 g's as shown in the graph below.

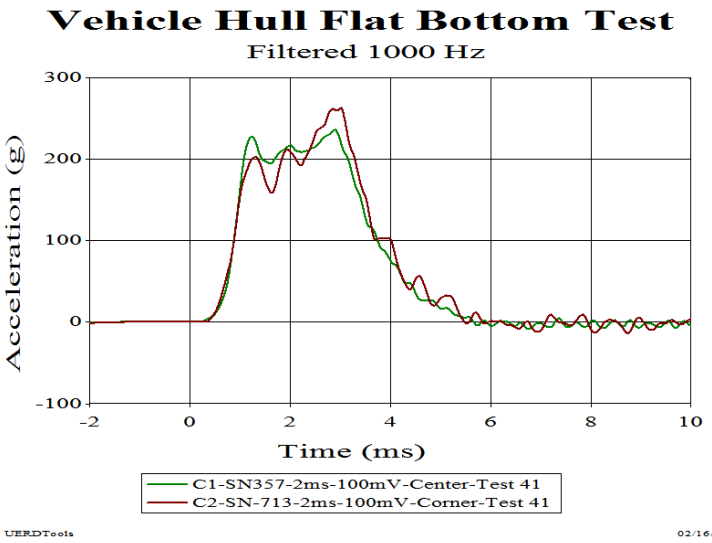

Future Plans:

We have achieved the results to date which are acceptable but by no means optimized. We want to look at other geometries. That is we want to vary the height to width ratios of these devices to determine the effects on acellerations. We also want to look at different materials for coating the cylinders. While we believe that polyurea is the best there are many different types of polyurea and we do not feel that the material we are currently using is the best. We also want to look at the effects that different materials for the cylinders (steels or even composities) might have on the results achieved. We are also looking at computational predictions for these devices but that work is laging behind the experimental testing.

APPENDIX 7

Effects of Under-vehicle blast exposure followed by impact TBI

Effects of Under-vehicle blast exposure followed by impact TBI

Behavioral changes have been observed following underbody blast 2400G acceleration in the absence and presence of secondary head impact using the projectile concussive impact (PCI) model developed by Dr. Frank Torella. In these experiments, we measured performance of rats on the Y maze (working memory) and Plus Maze (anxiety) for up to 29 days post-injury. The PCI model employs an impact by a 0.7 cm ball bearing on the top of the rat head, protected against skull fracture by a Kevlar helmet designed to fit the rat head. Our colleagues at Walter Reed Army Institute of Research have found that a single impact using PCI does not result in significant short or long term behavioral deficits; however, long-term alterations are observed following multiple impacts. We hypothesized that one PCI-mediated impact following blast-induced acceleration would cause greater brain injury than that observed with blast alone. The preliminary results obtained for the Y maze test are shown in the following figure for n=4-12 rats per group. The B-2400G rats were anesthetized with isoflurane in a box and then transferred to the restraints attached to the top hull of the "vehicle". Once the rats were fully conscious, the explosive located in the water under the vehicle was detonated, resulting in a peak acceleration force of 2400G, as measured with accelerometers. The B-2400G + PCI underwent the same procedure but were re-anesthetized with isoflurane at 2 min post-blast and subjected to PCI at an impact level of 100 psi. The Sham rats were isoflurane-anesthetized and placed in the restraints attached to the top of the top hull of the "vehicle", without subsequent exposure to blast. The "2- Iso" Shams underwent anesthetization, placement in restraints, and re-anesthetization, without exposure to either blast or PCI. On day zero, at approximately one hour post-injury or sham treatment, the 2400G blast rats exhibited very little spontaneous alteration among the three arms and the 2400G + PCI rats exhibited no spontaneous alternation. Note that n=12 for the Sham animals. All others, including the Sham – 2Iso animals currently were performed at an n=4 per group. On day 6 the 2400G rats still exhibited reduced spontaneous alternation. By days 13 or 27, this behavioral deficit appeared to be reversed.

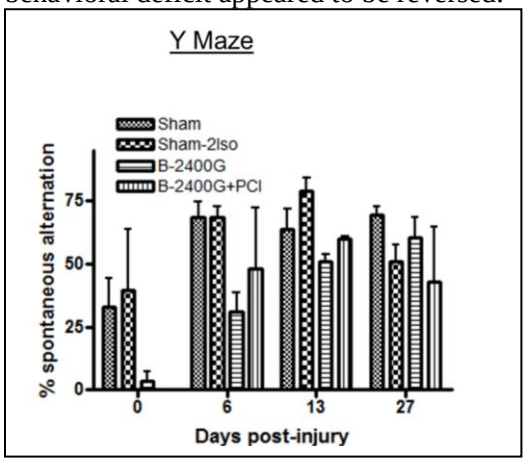

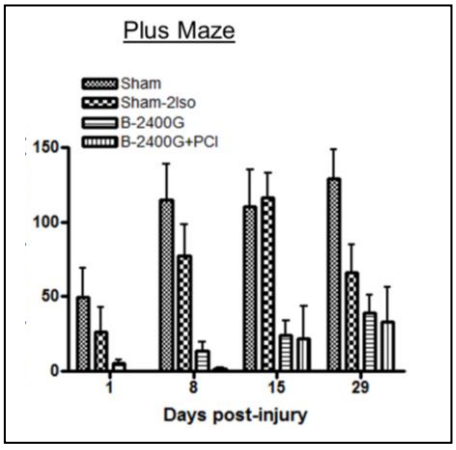

The results from the elevated Plus Maze test are shown. As seen previously, the time spent in open arms (inversely proportional to anxiety) was higher in the Sham groups at 8, 15, and 29 days compared to at 24 hr post-Sham treatment. The double isoflurane shams were also higher at days 8 and 15 than at day 1 but were actually similarly low at day 29. Time spent by 2400G and 2400G + PCI rats was very low at days 1, 8, and 15 post-injury, and still somewhat low at day 29 post-injury.

In addition to long-term neurobehavioral alterations, significant mortality was observed during these tests. For each of three blasts at 2400G that were followed by PCI, one of the two rats per blast died within 30 min. None of the four rats that experienced 2400G acceleration alone without subsequent PCI died. Therefore, these results support the hypothesis that the combination of blast-induced acceleration plus secondary impact results in greater mortality than either event alone.

APPENDIX 8

Quad Chart

Underbody Blast Models of TBI Caused by Hyper-Acceleration and Secondary Head Impact

PI: Gary Fiskum **Org: University of Maryland School of Medicine**

DMRDP

Problem, Hypothesis and Military Relevance

- *There is a high incidence of TBI among warfighter occupants of vehicles targeted by underbody blasts but little is known about the unique forces involved or the pathophysiology.*
- *We hypothesize:*
  - *Acceleration experienced during survivable underbody blasts produces dose-dependent TBI.*
  - *Underbody blast-induced acceleration combined with secondary head impact is also military relevant and can be modeled.*
  - *Neurologic outcome following underbody blast-induced TBI can be improved by force-modifying vehicle hull designs.*
- *We will expand our underbody blast animal model of TBI to establish full dose-response relationships and to model the combination of acceleration plus head impact. This research will promote development of engineering- and biomedical-based neuroprotective interventions translatable to warfighter TBI.*

Major Warfighter Health Problem

Underbody Blast Device

Underbody Blast Kinetics

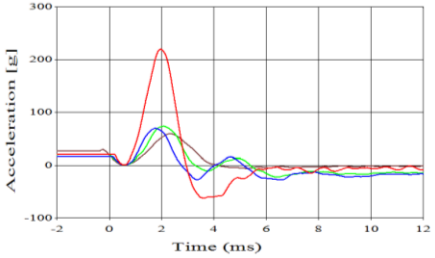

Diffuse Axonal Injury and Chronic Inflammation

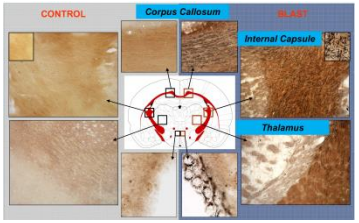

Proposed Solution

- *Anesthetized and awake animals will be used in experiments where the peak vertical acceleration elicited by an underbody blast will be varied between approximately 10 and 300 Gs. Anesthetized rats will be used in additional experiments where the top of the head is allowed to strike the surface of the cylinder (cockpit), which models a combined insult typical of underbody blasts.*
- *Comprehensive histopathology, multispectral magnetic resonance imaging, and behavioral tests will be performed at 2 hr to 30 days after these blasts to provide spatiotemporal quantification of diffuse axonal injury, cellular inflammatory responses, cell death, and neurologic outcome that are necessary for understanding and mitigating underbody blast TBI.*
- *Determine if TBI outcomes can be improved by modification to vehicle hull designs, including the use of hull geometries that reduce the rate and extent of blast-induced acceleration.*

Timeline and Cost

Activities FY	13	14	15	16
Establish minimum underbody blast-induced G-force that produces TBI and the maximum that is survivable				
Combine underbody blast-induced G-force with secondary head impact				
Test vehicle hull designs that lessen the extent and rate of blast-acceleration				
Estimated Budget ($K)	$276	$280	$284	$288
	DC			